



UNIVERSITAT POLITÈCNICA DE CATALUNYA
BARCELONATECH

Escola Politècnica Superior d'Enginyeria
de Manresa

OBJECT DETECTION WITH RADAR

PRESENT AND FUTURE AUTOMOTIVE TECHNOLOGY

Daniel Díaz Martínez

Automotive Engineering – UPC EPSEM | HTW Dresden

Prof. Toralf Trautmann

Jordi Vives Costa

2022



ABSTRACT

Radar-based object detection in cars is an integral part of autonomous driving systems. Radar sensors benefit from their excellent robustness in adverse weather conditions such as snow, fog or heavy rain.

Although machine learning-based object detection is traditionally a camera-based domain, great progress has been made in lidar sensors, and radar is also catching up.

Radar has been a key element of advanced automotive driver assistance systems for more than two decades.

As an inexpensive, all-weather, long-range sensor that simultaneously provides speed measurements, radar is expected to be indispensable for the future of autonomous driving.

Traditional radar signal processing techniques are often unable to distinguish reflections from objects of interest and are generally limited to detecting the peaks of the received signal.

These peak detection methods convert the radar signal as an image into a sparse point cloud.

Fully autonomous vehicles and the need to improve road safety have increased the reliability requirements of various advanced driver assistance systems (ADAS). Automotive radar is a key component of ADAS, as it adds safety and comfort features to vehicles.

One of the main challenges in developing automotive radar is to demonstrate its reliability, especially in the most difficult cases. Building and testing radar systems for specific cases is time-consuming, costly and impractical. Simulation is the only practical way to investigate the countless practical cases of automotive radar.

One interesting case is the reduction of radar returns due to sharp road curves. In particular, crucial targets with low radar cross sections (RCS), such as pedestrians, can become invisible to radar when driving on sharp curves.

This paper will implement a radar system for the simulation of object detection of a vehicle, and aims to show and analyse how reliable such systems can be, as well as their problems and more.

INDEX

INDEX.....	3
1 INTRODUCTION	6
1.1 PROJECT MOTIVATIONS	6
1.2 OBJECTIVES.....	7
2 BACKGROUND	7
2.1 INTRODUCTION TO RADAR SENSORS.....	7
2.1.1 WHAT IS RADAR?.....	7
2.1.2 HOW DOES RADAR DETECTION WORK?	7
2.1.3 WHAT ARE THE CHARACTERISTICS OF RADAR SENSORS?	8
2.1.4 WHAT ARE THE ADVANTAGES OF RADAR SENSORS?	8
2.1.5 WHAT DIFFERENTIATES RADAR FROM OTHER TYPES OF SENSORS?	9
2.1.6 PARAMETERS OF A RADAR.....	9
2.1.7 RADAR TECHNOLOGY CAPABILITIES.....	10
2.1.8 STRUCTURE OF A RADAR.....	15
2.2 RESEARCHES IN OBJECT DETECTION	16
2.3 GHOST OBJECTS & REFLECTIONS	17
3 RADAR BASICS	20
3.1 PHYSICAL FUNDAMENTALS OF THE RADAR PRINCIPLE.....	20
3.2 RADAR PRINCIPLE.....	21
3.2.1 BASIC DESIGN OF RADAR SYSTEM.....	21
3.3 PRINCIPLE OF MEASUREMENT.....	23
3.3.1 RANGE OR DISTANCE MEASUREMENT.....	23
3.3.2 DERIVATION OF THE EQUATION	24
3.3.3 DIRECT DETERMINATION	24
3.3.4 MAXIMUM UNAMBIGUOUS RANGE	24
3.3.5 MINIMAL MEASURING RANGE.....	25
3.3.6 RANGE RESOLUTION	26
3.3.7 RADAR USING INTRAPULSE-MODULATION.....	26
3.3.8 RADARS ACCURACY.....	26
3.3.9 ACCURACY IN RANGE DETERMINATION	27
3.3.10 ACCURACY IN ANGLE MEASUREMENT.....	28
3.3.11 HOW IS A MEASUREMENT PERFORMED?.....	29
3.4 RADAR TIMING PERFORMANCE.....	29
3.4.1 PULSE REPETITION FREQUENCY (PRF).....	29

3.4.2	RECEIVING TIME	30
3.4.3	DEAD TIME	30
3.4.4	BURST-MODE	31
3.4.5	PEAK- AND AVERAGE POWER	32
3.4.6	DUTY CYCLE	33
3.4.7	DWELL TIME AND HITS PER SCAN	33
3.4.8	TIME-DEPENDENCES IN RADAR.....	34
3.5	THE RADAR EQUATION.....	36
3.5.1	THE RADAR RANGE EQUATION	36
3.5.2	ARGUMENTATION/DERIVATION	36
3.5.3	RADAR CROSS-SECTION.....	39
3.5.4	NON-ISOTROPIC REFERENCE REFLECTOR.....	41
3.5.5	COMPUTATIONAL DETERMINATION OF THE REFLECTIVE AREA.....	41
3.5.6	RADAR CROSS SECTIONS FOR POINT-LIKE TARGETS	42
4	PROJECT METHODOLOGY.....	43
4.1	MEASUREMENTS SETUP.....	43
4.2	SHORT RANGE RADAR 20X /-2 /-2C /-21.....	49
4.2.1	DEVICE DATA	49
4.2.2	DEVICE SETTINGS.....	51
4.2.3	INSTALLATION	51
4.3	SIMULINK MODELS.....	55
4.3.1	CONFIGURATION.....	55
4.3.2	DISPLAY.....	56
4.3.3	LOG	58
4.3.4	REPLAY.....	60
4.4	MATLAB SCRIPTS	61
4.4.1	CAMERA VIDEO	61
4.4.2	TESTFIELD WEBCAM.....	61
4.4.3	RESULTS DISPLAY.....	62
5	STUDY CASES	70
5.1	FAMILIARIZATION.....	70
5.2	STATIC MEASUREMENTS.....	73
5.2.1	TRIPLE MIRROR.....	74
5.2.2	PEDESTRIAN.....	74
5.2.3	DUMMY	74



5.3	DYNAMIC MEASUREMENTS	74
5.3.1	PEDESTRIAN.....	75
5.3.2	BICYCLE.....	75
5.3.3	EXTRA MEASUREMENTS.....	75
6	ANALYSIS OF MEASUREMENTS AND RESULTS	76
6.1	STATIC MEASUREMENTS.....	76
6.1.1	REFLECTIONS PROBLEMS	76
6.1.2	DATA FILTER	94
6.2	DYNAMIC MEASUREMENTS	102
7	IMPACT OF THE TECNOLOGY	108
8	CONCLUSIONS	109
9	REFERENCES	110
10	ACKNOWLEDGEMENTS	113

1 INTRODUCTION

Automated vehicles are a major trend in today's automotive industry. Applications range from driver assistance to driver assistance to fully autonomous driving.

As advanced driver assistance systems (ADAS) and autonomous driving systems evolve, the range of in-car sensing solutions is also expanding and diversifying.

A variety of sensors have been used for detection, such as Lidar, short-range radar, long-range radar, RGB and infrared cameras and sonar. Camera and Lidar have high angular resolution and dense sensor scans. The most widespread sensor for providing detail-rich 3D information in automotive environments is Lidar.

On the other hand, automotive radar sensors have a good range capability. Thanks to their long wavelength, radar sensors are very resistant to adverse situations and weather conditions such as fog, snow, heavy rain or direct light impact.

Radar presents a low-cost alternative to Lidar as a range sensor. Currently, a typical automotive radar is considerably cheaper than Lidar due to the nature of its fundamental design. In addition, as discussed above, radar is resistant to different lighting and weather conditions compared to Lidar.

However, due to the specular nature of the electromagnetic reflection at the wavelengths employed by radar, the resulting signal is not as easy to interpret as that of Lidar or camera, so algorithm development is also more difficult. We will try to show all this in this work and analyse it in detail.

1.1 PROJECT MOTIVATIONS

Since I started my studies, I have always had the end of my degree in mind. And it has been inevitable not to think about what will become of me when I finish it. And thinking about the end of my studies also means thinking about my final project.

I think I speak for all students when I say that the final project scares us, or rather, imposes itself on us. You ask yourself questions like; "What subject will I do it on?", "Will I be sufficiently prepared to develop a project of this magnitude?", etc.

Well, when the time came to decide what to do the work on, it was clear to me that I wanted to do it on a current topic, rather thinking about the future. I know it would be risky because a current/future topic is never as developed as a topic from the past, for example steam engines.

When we talk about the automotive industry in present/future topics it is inevitable not to think about advanced driver assistance systems (ADAS) and autonomous driving. Also, it should be noted that in my period prior to the start of the development of this thesis I worked as an intern for a company in the ADAS department and this gave me a lot of perspective on the topic and helped me to "open my eyes".

Working on this topic in my thesis motivates me especially because I am aware that all the learning to be acquired will be very useful for me in the future because, as mentioned above, it is an area that will be worked on a lot in many of the companies in the sector in the future.

1.2 OBJECTIVES

From the first approach of this thesis, the main objective was clear. For a student finishing his degree, his desire is to get closer to the current situation of the sector and its future. To gradually start to enter the sector by acquiring useful and valuable knowledge.

On the other hand, as far as the thesis is concerned, the objective is to acquire knowledge about an important element of the current and future of the sector, radar sensors.

Knowing how they work, what they can provide, how much reliability they provide nowadays, how they should evolve, what they should improve... etc, are questions that the objective of the thesis is to have at least a minimum idea of the answer.

2 BACKGROUND

2.1 INTRODUCTION TO RADAR SENSORS

Radar sensors are one of the key technologies in the rapidly evolving automotive sector. In many areas, we are benefiting from innovative sensor solutions. But what is radar and how does this technology work?

In this thesis we want to give you an insight into the world of radar sensors, explaining in more detail the complexity of this technology.

2.1.1 WHAT IS RADAR?

RADAR stands for "Radio Detection And Ranging" and is an active method of transmission and reception in the GHz microwave range.

Radar sensors are used for non-contact detection, tracking and positioning of one or more objects by means of electromagnetic waves.

2.1.2 HOW DOES RADAR DETECTION WORK?

The radar antenna emits a signal in the form of radar waves, which move at the speed of light and are not detectable by humans. When the waves encounter objects, the signal changes and is reflected back to the sensor, similar to an echo.

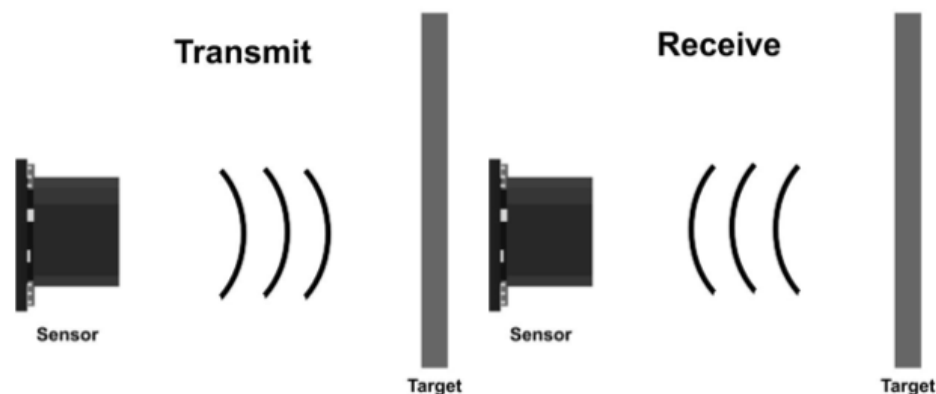


Fig. 1 - Signal transmitted and received by a radar

The signal arriving at the antenna contains information about the detected object. The received signal is processed to identify and position the object with the obtained data. In a second step, a pulse can be emitted to trigger a reaction.

2.1.3 WHAT ARE THE CHARACTERISTICS OF RADAR SENSORS?

Non-contact: The measurement method of radar detection does not involve any contact. The sensor does not have to be in direct contact with the material or object to be detected. Radar measures and detects even over long distances.

Anonymous: Radar sensors are used for industrial and automotive applications and do not produce images. They merely form a kind of point cloud that gives a rough idea of the outline of objects and the surrounding infrastructure. In contrast to a camera, people are not identifiable.

Complete data: Radar sensors detect movements and stationary objects. After signal processing, the data received via the reflection provides a wide range of information about the detected objects, vehicles, animals or people. Data such as direction of movement, speed, distance and angular position in relation to the sensor are available.

Multidimensional detection: Depending on its modulation, the radar obtains extensive data about its environment. This enables the sensors to detect the environment in three dimensions, just like the human eye.

Wide range variability: Radar waves propagate freely in space or in the air. Depending on the technical development of the sensor and its purpose, extreme ranges can be achieved if necessary.

In commercial applications, the range usually varies between one centimetre and a few hundred metres.

Material penetration: Electromagnetic waves from radar sensors penetrate various materials. Plastics, in particular, are well suited to cover or design a radome, a dome-shaped protective housing for the antenna. It allows sensors to be integrated unobtrusively into the design of a product.

2.1.4 WHAT ARE THE ADVANTAGES OF RADAR SENSORS?

Based on the properties of radar, the technology offers certain advantages for its respective application:

- ✓ It is independent of weather conditions
- ✓ Tolerates extreme heat and cold
- ✓ Works even in spite of overexposure and poor lighting conditions
- ✓ It works in the dark
- ✓ Maintenance-free
- ✓ Offers a wide range of functions
- ✓ Capable, for example, of measuring distance and speed, tracking, object positioning, ETA, object classification, and people counting
- ✓ Suitable for indoor and outdoor use
- ✓ Can be used for many applications

2.1.5 WHAT DIFFERENTIATES RADAR FROM OTHER TYPES OF SENSORS?

Different measurement methods have different strengths and weaknesses. Depending on the application, users should consider which sensor technology offers the greatest added value and addresses the respective tasks and objectives. The following table provides an overview:

FEATURES	PERFORMANCE LEVEL			
	RADAR	INFRARED	ULTRASONIC	LASER
Application flexibility	BEST	BAD	BAD	BAD
Resistance to moisture, dirt and temperature	BEST	BAD	BAD	BAD
Speed detection	BEST	BAD	GOOD	BEST
Accuracy sensitivity	BEST	BAD	BEST	BEST
Resolution (separability)	BEST	BAD	BEST	BEST
Direction capability	BEST	GOOD	GOOD	BAD
Distance measurement	BEST	GOOD	BAD	BEST
Penetration of materials	BEST	BAD	BAD	BAD
Size of solutions	BEST	BEST	BEST	BAD
Cost	GOOD	BEST	BEST	BAD

Fig. 2 - Comparison of different types of sensors by <https://www.innosent.de/en/radar/>

It is important to note that radars cannot detect the dimensions of objects.

2.1.6 PARAMETERS OF A RADAR

First of all, it should be noted that not all radars are the same. Sensors are often differentiated by their functions and properties. This is because, depending on the application, different configurations are required to perform the desired measurement. The differences between the various types of radar are defined by two basic parameters: the frequency band used and the modulation.

2.1.6.1 FREQUENCY BAND

The radar measurement method transmits and receives electromagnetic waves within a specific frequency range. Due to different physical properties, the range of radar sensors is divided into different gradations. And certain frequency ranges are labelled with letters designating the frequency band. This designation is defined by institutions such as IEEE and NATO and is recognised internationally.

Technical communication via radar waves is usually regulated by national authorities and international associations. These define power limits and the approval of frequency bands.

The typical range for commercial radar applications is between 10 and 120 GHz. Depending on the application, different frequency ranges are used due to their

respective technical characteristics. The choice of transmit and receive frequency also affects the performance and characteristics that the radar can achieve.

For example, 10 GHz radars penetrate even walls, while sensors in the 60 GHz or 77 GHz range support a higher resolution due to the higher bandwidth allowed. An advantage of 24 GHz sensors is their ability to be approved worldwide.

2.1.6.2 MODULATION

The type of radar is usually also defined by the specification of the radar method used. The radar signal is conditioned by the modulation of the transmitting frequency. The most common radar types are CW, FSK and FMCW.

CW stands for "continuous wave". In this method, the sensor transmits and receives the signal simultaneously and continuously (fixed transmission frequency). This type is also known as unmodulated continuous wave radar.

FSK stands for "frequency-shift keying". It is a special type of FMCW radar that alternately jumps between two frequencies.

FMCW stands for "frequency-modulated continuous wave". Frequency-modulated continuous wave radars do not use a fixed transmission frequency, but a time-varying frequency modulation (constant, cyclic and curved), also called chirp.

2.1.7 RADAR TECHNOLOGY CAPABILITIES

2.1.7.1 MEASURABLE RADAR INFORMATION AND ANALYSIS

Radar detection can be used to detect the presence or movement of objects or living beings. Depending on the modulation and antenna configuration, the following information can be obtained

- VELOCITY: exact data on the speed of an object
- DISTANCE: data on the distance of one or more objects
- DIRECTION OF MOTION: Direction of movement of an object
- ANGLE: Determination of the angle of incidence and angular resolution.

By analysing analogue and digital signals, further information can also be obtained from these base values. For example, intelligent algorithms can be used to create groups of radars, which then record the motion history. And it is also possible to classify these objects. From the signal analysis, the radar uses the raw data, such as the radar cross section (RCS), to detect whether a certain object is a person or a vehicle. If reference values are available, this also makes it possible to determine limit values, filling quantities or arrival times.

2.1.7.2 ACCURACY OF MEASUREMENTS

Misunderstandings often occur in relation to radar resolution. While resolution describes the ability of a radar to distinguish objects, its accuracy refers to the smallest measurable difference in the measured variable. It describes the accuracy with which parameters such as speed, distance or angular position are measured. It takes into account a plus/minus tolerance, indicated as the rate of deviation.

The accuracy of the measurement depends on the time in which the measurement is made. The longer the object detection time, the more readings the radar receives. The more data available for analysis, the more meaningful and reliable the detection will be.

In practice, a compromise often has to be found between detection time and accuracy. Because if the information is to be available as quickly as possible, the measurement time must be reduced.

2.1.7.3 ANTENNA DESIGN

The antenna design defines the range of the sensor. By varying the antenna layout, the emission of the radar waves is directed. The antenna pattern shows in which direction the antenna emits the most energy. With directional antennas, the shape and range are designed to achieve the highest possible antenna gain. This allows the energy to be concentrated at the desired viewing angle and reduces energy waste and side lobes.

The detection area can be narrow and elongated, but can also be wide. The design depends on the downstream application. A new method is advanced MIMO technology, which combines the use of several transmit and receive antennas.

2.1.7.4 RADAR WAVES AND MATERIALS

Radar waves propagate freely in space in the air. When they hit an object, the signal is influenced by the composition of the object. And different materials have different impacts on radar waves. They absorb or reflect them completely or partially. Radar beams also penetrate different substances.

In general, the following statements can be made about 24 GHz radars:

MATERIAL	ABSORPTION	REFLECTION	WAVE
Metal	None	Straight-on incidence: complete; Diagonal angle of incidence: Refraction and partial reflection possible	Virtually impossible, only millimetre fractions penetrate into the surface (skin effect)
Wood (depending on humidity)	Medium to high	Low	Low
Water	Very high	Depending on the angle of incidence: Partial or complete reflection possible	None, due to absorption
Foams (e.g. polystyrene, Roofmate)	Low	None	Very good
Plastics	Low to high (depending on material and thickness)	Low to high (depending on material, thickness, and distance)	Low to high (depending on material, thickness, and distance)

Fig.3 - Detection of different materials by 24 GHz radar by <https://www.innosent.de/en/radar/>

2.1.7.5 RANGE

The range of radar can vary widely, from a few centimetres to hundreds or thousands of metres. The distance a radar can measure depends on several factors.

In general, the further away an object is, the more difficult it is to detect it. Objects with a low RCS (radar cross-section) are also more difficult to detect at a distance. After all, the signal has to travel a long communication path back and forth. This results in signal losses, for instance due to environmental influences or interference factors. The higher the transmitting and receiving power, the better the signal after a long reflection path.

The radar range is always limited by the selected frequency band, which determines the available wavelength and its frequency, and the transmitting power is also restricted by regulations. At the same time, the receiving power is defined by the gain of the antenna and its design. If the directionality of the antenna is designed (for example, with a strong focus) and several antennas are integrated, a high sensitivity is achieved. However, this leads to an increase in noise, which must be suppressed by additional technical work.

In the development of a radar, an optimal ratio between range, range area and resolution have to be achieved for the respective application and technical work has to be done to minimise unwanted side effects.

2.1.7.6 OBJECT CLASSIFICATION

An advanced feature of radar is object classification, which requires extensive information about an object. This can be achieved with a high resolution, as more measurement points of an object can be detected. The classification is then performed by intelligent signal processing algorithms. For example, in traffic-related applications, it is possible to identify the object as a specific class of vehicle based on the length of the object (how far the object extends in space).

However, measures such as RCS, speed or information about movement patterns also help to assign objects to a specific type. For example, a person has a different RCS value than a vehicle. From the available data and appropriate programming, statements can be made about the classification of the object, for example in terms of the categories "person, vehicle, animal or other".

2.1.7.7 RESOLUTION

Radar resolution is the ability of radar sensors and systems to distinguish targets from each other (differentiability). The following overview shows the different radar solutions.

1D-RADAR (CW): CW (continuous wave) radars

CW (continuous wave) radars are widely used in many motion detection applications. FSK (frequency-shift keying) radars also separate objects according to their speed, but also offer the advantage of measuring distance.

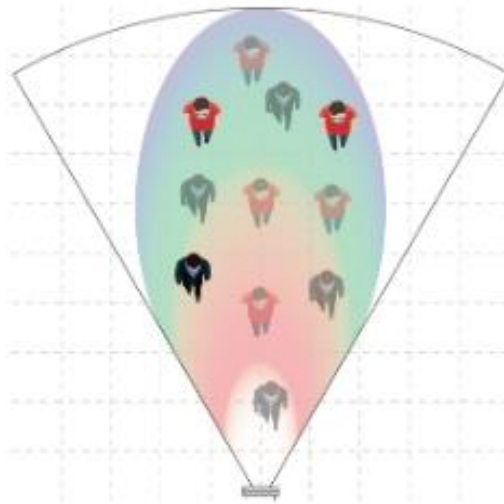


Fig. 4 – 1D RADAR CW resolution

Separation of objects by: **Speed**

There is no separation of objects with the same speed (localisation of objects is not possible). In the upper part of Fig. 4 we can see that there are two people in red in parallel and this means that they are going at the same speed. In this case the radar is not able to distinguish the objects, so it detects both as one object, just as it would if the people were located at all positions of the people in red that appear as shadows.

On the other hand, at the bottom we can see a person in black moving at a higher speed than the people in red above, in this case the radar is able to distinguish the "red" object from the "black" object, and would do the same if the person in black were located in all the positions of the people in black who appear as shadows.

2D-RADAR (FSK)

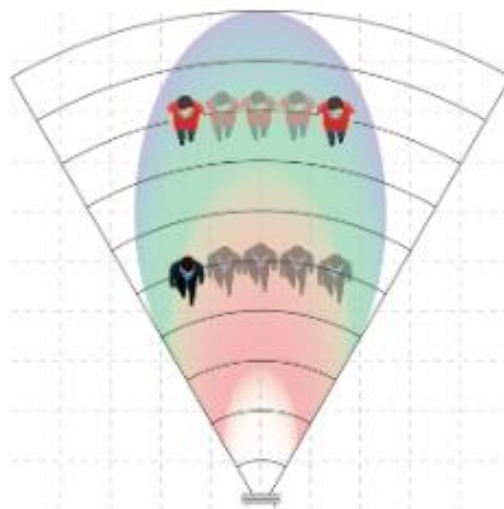


Fig. 5 – 2D-RADAR (FSK) resolution

Separation of objects by: **Speed and distance**

No separation of objects with the same speed and distance (localisation of objects in a one-dimensional environment, no angle information). In the upper part of Fig. 5 we can see that there are two people in red in parallel, they are at the same distance from the radar and they are going at the same speed. In this case the radar is not able to distinguish the objects, so it detects both as a single object, just as it would if the people were located in all the positions of the people in red that appear as shadows.

On the other hand, at the bottom we can see a black person moving at a different speed from the red ones above and closer to the radar (different distance), in this case the radar is able to distinguish the "red" object from the "black" one, and it would do the same if the black person was located in all the positions of the black people appearing as shadows.

FMCW (Frequency Modulated Continuous Wave)

Radars are used when speed measurement alone is not sufficient. If the radar device has only one transmit and one receive channel, the distance to the object can be measured, but the angular displacement cannot be measured.

3D-RADAR (FMCW MIMO): These radars have multiple transmitting and receiving antennas. Each transmitted signal can be received by any antenna. The special arrangement of multiple antennas improves spatial resolution and reduces susceptibility to interference.

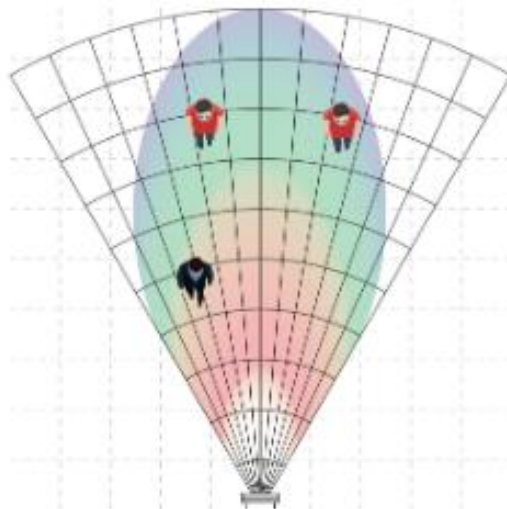


Fig. 6 – 3D-RADAR (FMCW MIMO) resolution

Separation of objects by: **Speed, distance and angle.**

Objects with the same speed, distance and angular position can be separated (possibility to locate objects in a two-dimensional environment).

4D-RADAR (FMCW MIMO): Compared to 3D radar, a 4D radar also has several antennas offset in elevation and can thus separate detections in elevation angle. This enables localisation in a 3D environment.



Fig. 7 – 4D-RADAR (FMCW MIMO) resolution

Separation of objects by: **Speed, distance and angle (horizontal, vertical).**

Objects with the same speed, distance and angular position can be separated (possibility to locate objects in a three-dimensional environment).

2.1.8 STRUCTURE OF A RADAR

In addition to its front end (microwave component with antenna structure), a complete radar sensor consists of signal conditioning and processing units. These elementary components can also be completed by a radome, a housing, a lens and a component carrier.

Throughout the antenna design, the front end plays a key role, as it constitutes the sensor itself and sets the parameters for the downstream functions. Signal conditioning and signal processing analyse and interpret the signals provided by the front end. This is necessary to give the individual, raw radar detections an understandable meaning for users by assigning units of measurement and references.



Fig. 8 – Radar Structure

The radar front-end transmits and receives the electromagnetic microwaves. These received signals are sent to the signal processing component. To protect the antenna and the electronic components, the radar is usually equipped with a housing. Technicians call the antenna housing the radome. In addition to protecting the front part, it also serves to secure the antenna. Some radars also have a special lens that serves to focus the radar beam. Another component of a radar is the interface necessary for the radar information to be output and transmitted to other technical products.

2.2 RESEARCHES IN OBJECT DETECTION

Radars are capable of estimating a relative velocity (Doppler velocity*) with a single scan of the sensor or, more recently, of measuring polarimetric* information. In the radar community, the most common approach to using Doppler values is to separate the sensing task for stationary and moving objects.

**Polarimetric: Pertaining to or relating to polarimetry, which is the measurement of the direction and extent of the rotational power of a body over polarised light.*

**Doppler velocity: The doppler effect is the apparent frequency change of a wave produced by the relative motion of the source relative to its observer. The velocity of the Doppler effect is the speed at which the object emitting the waves is moving, which is comparable to the propagation speed of those waves.*

In the static world, radar data can be accumulated over long-time frames, as moving objects can be filtered through their Doppler signature, thus alleviating the problem of data sparsity. Due to their dynamic nature, moving objects require smaller time frames, typically a few hundred milliseconds.

Most detection and classification methods require an accumulation of several measurement cycles to increase the density of the point cloud, as shown in Fig. 9. However, the accumulation can be implemented as a sliding window, allowing updates for each sensor cycle. So far, most of the research in the field of automotive radar is concerned only with classification or instance detection.

Fewer papers are available for multi-class object detection problems in dynamic road users. As the new field of automotive radar-based object detection is just emerging, many of the existing methods still use limited data sets or lack a comparison with other methods.

In Fig. 9 we can see a camera image as a reference, and below we have the point cloud from the detections that a radar would obtain. With a good programming of an object classification model, we could be able to identify objects through data processing with the number of detection points in the cloud. It should be noted that this is a complex programming and many parameters have to be taken into account.

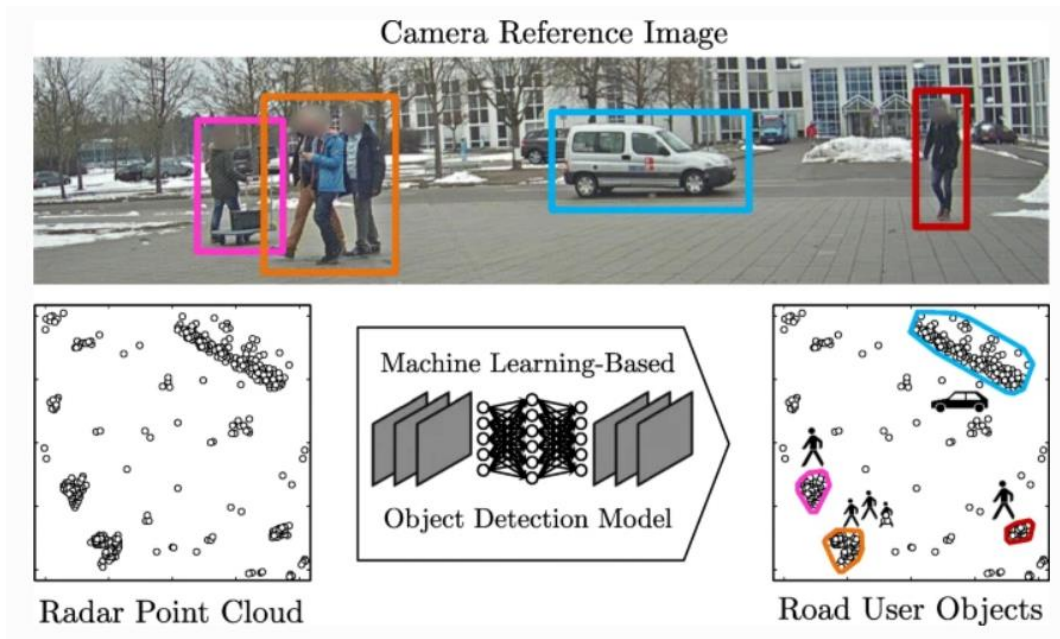


Fig. 9 – Processing of a point cloud of a detection compared to a camera image

To carry out this programming, we could calculate an average number of points in the cloud per object, that is to say if a certain number of points appear in the cloud during the detection of a person, make a series of measurements that allow you to calculate an average number of points and assign that average with a tolerance to that object for identification in the following measurements of the same object.

The classification and/or identification of objects is one of the biggest challenges for radar sensors in the industry, as their programming for data processing is very complex due to the variability of the data. The better the programming and characterisation of the radar, the better and easier its subsequent programming and data processing will be due to the reduction of variability of the data obtained.

2.3 GHOST OBJECTS & REFLECTIONS

In real situations, a radar sensor produces imaginary targets (so-called ghost objects). Ghost objects are objects that appear at erroneous locations in the radar data and are caused by the presence of multiple indirect reflections between the target and the sensor. They have nothing in common with real objects, such as vehicles or pedestrians, but are due to multipath propagation of a transmitted radar wave or interference from other radar sensors.

A radar sensor emits a signal and part of the signal is reflected and returned as an echo when it hits a target. From the echo, the distance (range) to the detected target can be calculated based on the time of flight, and the angle of arrival (azimuth angle*) is calculated by having several receiving antennas with a known distance and calculating the echo reception delay at each antenna. The relative radial velocity (Doppler velocity) of the target is measured using the frequency shift between the incident and reflected waves.

*Azimuthal angle: the direction of the compass that indicates where the sunlight comes from. (See Fig.10).

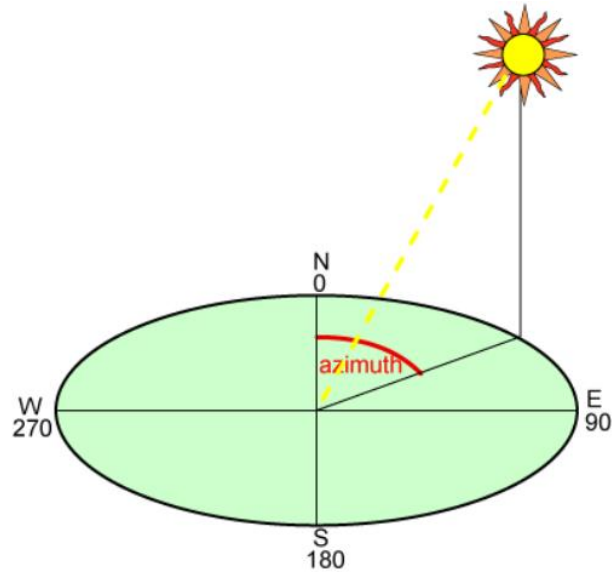


Fig. 10 - Azimuth angle

Since a radar sensor usually emits waves in all directions within its field of view, and the location of the target is calculated based on the angle of arrival of the echoes, the possibility arises that the reflected signal takes an indirect path between the sensor and the target. This indirect reflection path results in detections at erroneous positions, either with a different range or azimuth, or both. These detections are referred to as ghost targets or multipath reflections.

Detection of ghost targets is essential to ensure reliable and robust performance of automotive radars. Fig. 11 shows an example where radar waves reflect off the target vehicle towards the ego vehicle above the crash barrier, resulting in the detection of a ghost object on the opposite side of the barrier.

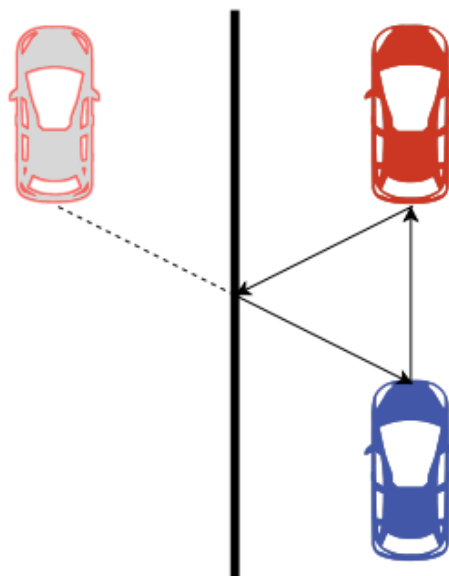


Fig. 11 – Ghost object reflected

In Fig. 11 the ego vehicle equipped with the radar sensor (blue) detects a ghost target (weak red) on the wrong side of the guardrail due to the indirect reflection of the radar signals on the target vehicle (red).

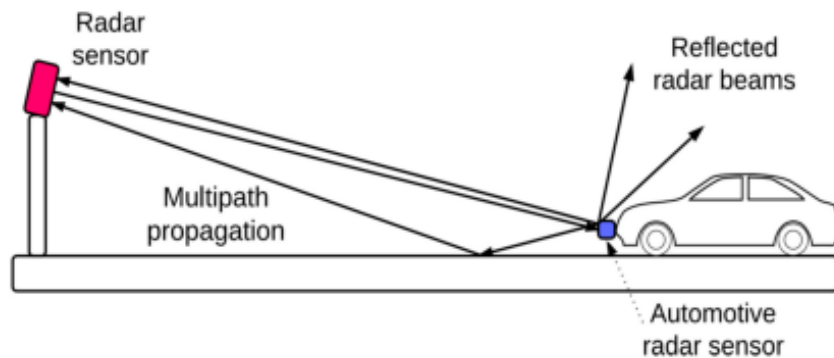


Fig. 12 - Propagation of radar signals

Fig. 12 illustrates a situation where radar signals echo from the same position through multiple paths. If the radar signal echoes from its destination to the sensor via the shortest path, there will be no problem in obtaining information about the target, but in real situations, radar signals do not do that.

Fig. 13 is another example of specular reflection and multipath propagation in radar detection.

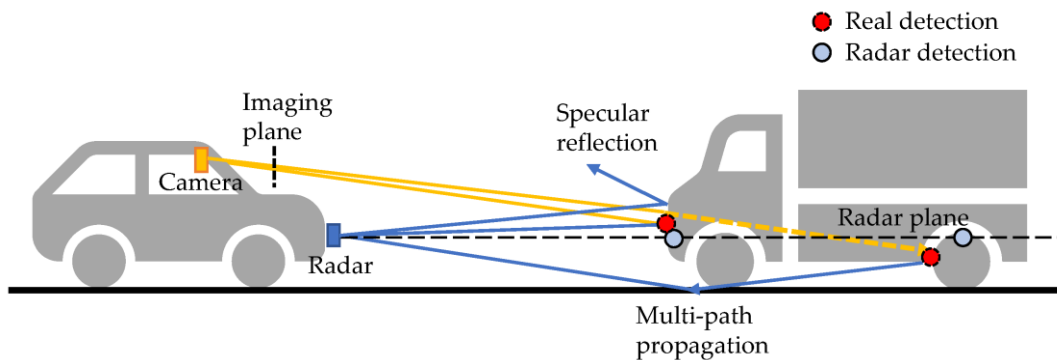


Fig. 13 - Propagation of radar signals

Even radar signals from other radar sensors can interfere with the transmitted radar signals as graphically depicted in a real-life situation in Fig. 14.

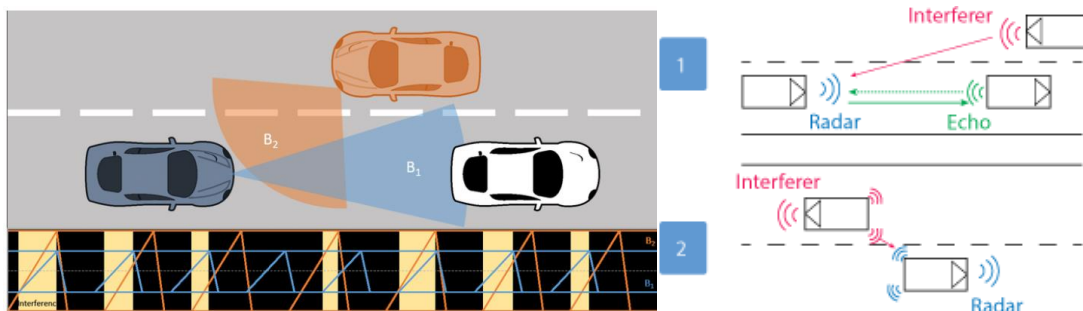


Fig. 14 - Interferences between two radar sensors

These are all causes of ghost objects. The presence of ghost objects in radar data reduces the reliability of sensors and the robustness of their detections. Robust radar detection is essential for the safe operation of autonomous and highly automated vehicles.

The unpredictability of modern driving scenarios makes the problem of ghost targets complex, especially in urban environments where there are numerous unknown reflective surfaces. This has made it extremely difficult to solve the phantom object problem using conventional model-based methods that require the model of the target or the environment, as is done in through-wall radar imaging.

In addition, classifying radar data for ghost targets is a difficult task because many surfaces can reflect electromagnetic waves and can become more complicated and error-prone the more complex the scenario and the denser the acquired data.

3 RADAR BASICS

Following the introduction in the previous section, this section aims to go into more detail on the explanation of the radars and how they work.

3.1 PHYSICAL FUNDAMENTALS OF THE RADAR PRINCIPLE

The basic principle of basic radar operation is simple to understand. However, the theory can be quite complex. Understanding the theory is essential to be able to specify and operate primary radar systems correctly. The implementation and operation of primary radar systems involves a wide range of disciplines, such as construction works, heavy mechanical and electrical engineering, high-power microwave engineering, and advanced signal and high-speed data processing techniques. Some laws of nature are of major importance here.

Radar measurement of range, or distance, is made possible by the properties of radiated electromagnetic energy.

- Reflection of electromagnetic waves

The electromagnetic waves are reflected if they meet an electrically leading surface. If these reflected waves are received again at the place of their origin, then that means an obstacle is in the propagation direction.

- Electromagnetic energy travels through air at a constant speed, at approximately the speed of light,
 - 300,000 kilometers per second or:
 - 186,000 statute miles per second or:
 - 162,000 nautical miles per second

This constant speed allows the determination of the distance between the reflecting objects and the radar site by measuring the running time of the transmitted pulses.

- This energy normally travels through space in a straight line, and will vary only slightly because of atmospheric and weather conditions. By using of special radar antennas this energy can be focused into a desired direction. Thus the direction (in azimuth and elevation) of the reflecting objects can be measured.

These principles can basically be implemented in radar system, and allow the determination of the distance, the direction and the height of the reflecting object.

3.2 RADAR PRINCIPLE

The electronic principle on which radar operates is very similar to the principle of sound-wave reflection. If you shout in the direction of a sound-reflecting object (like a rocky canyon or cave), you will hear an echo. If you know the speed of sound in air, you can then estimate the distance and general direction of the object. The time required for an echo to return can be roughly converted to distance if the speed of sound is known.

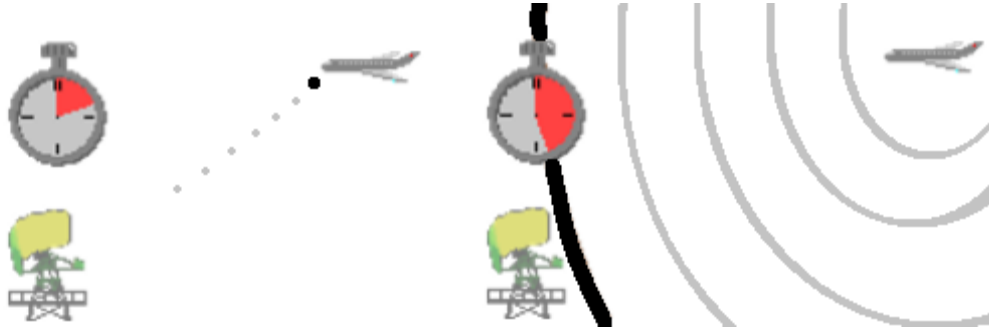


Fig. 15 – Radar principle

Radar uses electromagnetic energy pulses in much the same way, as shown in Fig. 15. The radio-frequency (rf) energy is transmitted to and reflected from the reflecting object. A small portion of the reflected energy returns to the radar set. This returned energy is called an ECHO, just as it is in sound terminology. Radar sets use the echo to determine the direction and distance of the reflecting object.

3.2.1 BASIC DESIGN OF RADAR SYSTEM

The following figure shows the operating principle of a primary radar set. The radar antenna illuminates the target with a microwave signal, which is then reflected and picked up by a receiving device. The electrical signal picked up by the receiving antenna is called echo or return. The radar signal is generated by a powerful transmitter and received by a highly sensitive receiver.

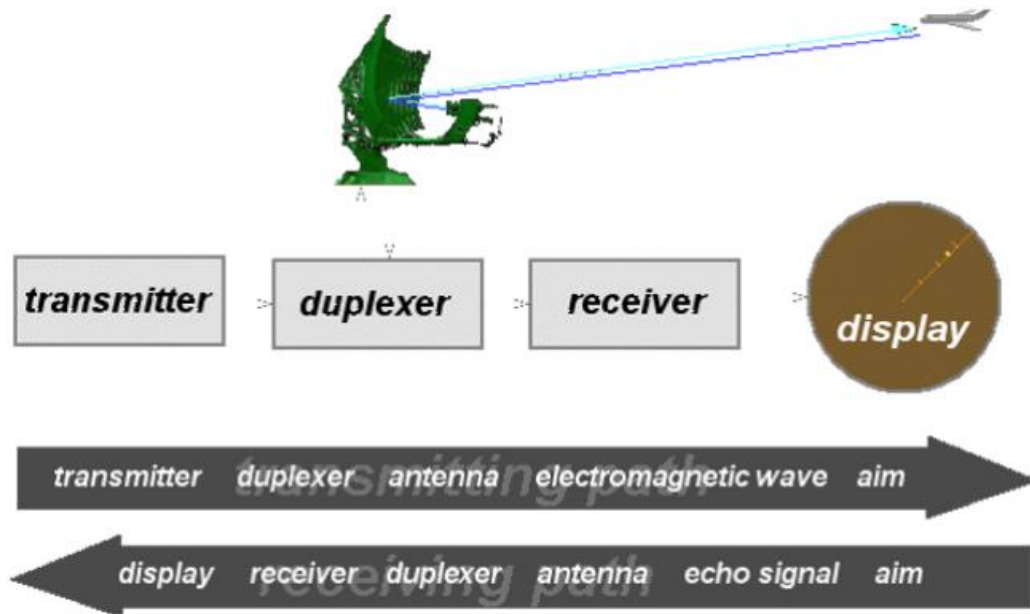


Fig. 16 – Block diagram of a primary radar

All targets produce a diffuse reflection i.e., it is reflected in a wide number of directions. The reflected signal is also-called scattering. Backscatter is the term given to reflections in the opposite direction to the incident rays.

Radar signals can be displayed on the traditional plan position indicator (PPI) or other more advanced radar display systems. A PPI has a rotating vector with the radar at the origin, which indicates the pointing direction of the antenna and hence the bearing of targets.

- **Transmitter:** The radar transmitter produces the short duration high-power rf pulses of energy that are into space by the antenna.
- **Duplexer:** The duplexer alternately switches the antenna between the transmitter and receiver so that only one antenna need be used. This switching is necessary because the high-power pulses of the transmitter would destroy the receiver if energy were allowed to enter the receiver.
- **Receiver:** The receivers amplify and demodulate the received RF-signals. The receiver provides video signals on the output.
- **Radar Antenna:** The Antenna transfers the transmitter energy to signals in space with the required distribution and efficiency. This process is applied in an identical way on reception.
- **Indicator:** The indicator should present to the observer a continuous, easily understandable, graphic picture of the relative position of radar targets. The radar screen (in this case a PPI-scope) displays the produced from the echo signals bright blibs. The longer the pulses were delayed by the runtime, the further away from the centre of this radar scope they are displayed. The direction of the deflection on this screen is that in which the antenna is currently pointing.

3.3 PRINCIPLE OF MEASUREMENT

3.3.1 RANGE OR DISTANCE MEASUREMENT

The radar transmits a short radio pulse with very high pulse power. This pulse is focused in one direction only by the directivity of the antenna, and propagates in this given direction with the speed of light.

If in this direction is an obstacle, then a part of the energy of the pulse is scattered in all directions. A very small portion is also reflected back to the radar. The radar antenna receives this energy and the radar evaluates the contained information.

The distance we can measure with a simple oscilloscope. On the oscilloscope moves synchronously with the transmitted pulse a luminous point and leaves a trail. The deflection starts with the transmitter pulse. The luminescent spot moves to scale on the oscilloscope with the radio wave. At this moment, in which the antenna receives the echo pulse, this pulse is also shown on the oscilloscope. The distance between the two shown pulses on the oscilloscope is a measure of the distance of the obstacle.

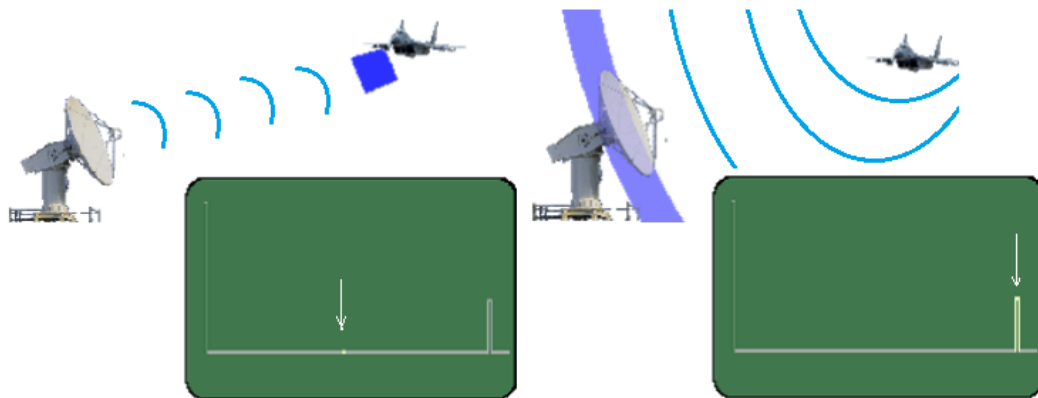


Fig. 17 – Runtime measurement by radar

Since the propagation of radio waves happens at constant speed (the speed of light c_0) this distance is determined from the runtime of the high-frequency transmitted signal. The actual range of a target from the radar is known as slant range. Slant range is the line of sight distance between the radar and the object illuminated. While ground range is the horizontal distance between the emitter and its target and its calculation requires knowledge of the target's elevation. Since the waves travel to a target and back, the round trip time is dividing by two in order to obtain the time the wave took to reach the target. Therefore, the following formula arises for the slant range:

$$R = \frac{c_0 \cdot t}{2} \quad (1)$$

c_0 = speed of light = $3 \cdot 10^8$ m/s

t = measured runtime [s]

R = slant range antenna - aim [m]

3.3.2 DERIVATION OF THE EQUATION

Range is the distance from the radar site to the target measured along the line of sight.

$$v = \frac{s}{t} \quad (2)$$

$$c_0 = \frac{2R}{t} \quad (3)$$

The factor of two in the equation comes from the observation that the radar pulse must travel to the target and back before detection, or twice the range.

$$R = \frac{c_0 \cdot t}{2} \quad (4)$$

Where $c_0 = 3 \cdot 10^8 \text{ m/s}$, is the speed of light at which all electromagnetic waves propagate.

If the respective running time t is known, then the distance R between a target and the radar set can be calculated by using this equation.

3.3.3 DIRECT DETERMINATION

The angular determination of the target is determined by the directivity of the antenna. Directivity, sometimes known as the directive gain, is the ability of the antenna to concentrate the transmitted energy in a particular direction. An antenna with high directivity is also-called a directive antenna. By measuring the direction in which the antenna is pointing when the echo is received, both the azimuth and elevation angles from the radar to the object or target can be determined. The accuracy of angular measurement is determined by the directivity, which is a function of the size of the antenna.

Radar units usually work with very high frequencies. Reasons for this are:

- quasi-optically propagation of these waves.
- High resolution (the smaller the wavelength, the smaller the objects the radar is able to detect).
- Higher the frequency, smaller the antenna size at the same gain.

3.3.4 MAXIMUM UNAMBIGUOUS RANGE

The maximum unambiguous range (R_{max}) is the longest range to which a transmitted pulse can travel out to and back again between consecutive transmitted pulses. In other words, R_{max} is the maximum distance radar energy can travel round trip between pulses and still produce reliable information.

The relationship between the PRF or their reciprocal value interpulse period T (PRT) and R_{max} determines the unambiguous range of the radar. Suppose the radar emits a pulse that strikes a target and returns to the radar in round trip time t :

- If $t < T$ then the return signal arrives before the next pulse has been emitted.

- If $t = T$ then the return signal arrives exactly when the next pulse has been emitted.
- If $t > T$ then the return signal arrives after the next pulse has been emitted and there is an ambiguity, i.e. the radar cannot tell whether the return signal has come from the first or second pulse.

Therefore, maximum unambiguous range R_{max} is the maximum range for which $t < T$.

$$R = \frac{c_0 \cdot (T - t)}{2} \quad (1)$$

R_{max} = unambiguous Range in [m]

c_0 = speed of light [$3 \cdot 10^8$ m/s]

T = Pulse Repetition Time (PRT) [s]

τ = length of the transmitted pulse [s]

The factor of 2 in the formula accounts for the pulse traveling to the target and then back to the radar. The length of the transmitted pulse (pulse width τ) in this formula indicates that the complete echo impulse must be received. Often, the entire pulse length must first be processed to detect a target. If the transmitted pulse is very short in relation to the pulse period, it can be ignored. Ignoring pulse length, the maximum unambiguous range of any pulse radar can be computed with the formula:

$$R_{max} = \frac{c_0 \cdot T}{2} = \frac{c_0}{2 \cdot f_p} \quad (2)$$

f_p = Pulse Repetition Frequency (PRF) [Hz or s^{-1}]

The greater the pulse repetition frequency f_p (in pulses per second), the shorter the pulse repetition time T (interpulse period) and the shorter the maximum unambiguous range R_{max} of the radar. R_{max} must be larger than the Maximum Display Range (so-called: instrumented range).

The pulse repetition time (PRT) of the radar is important when determining the maximum range because target return-times that exceed the PRT of the radar system appear at incorrect locations (ranges) on the radar screen. Returns that appear at these incorrect ranges are referred as ambiguous returns, second-sweep echoes or second time around echos.

3.3.5 MINIMAL MEASURING RANGE

Monostatic pulse radar sets use the same antenna for transmitting and receiving. During the transmitting time the radar cannot receive: the radar receiver is switched off using an electronic switch, called duplexer. The minimal measuring range R_{min} ("blind range") is the minimum distance which the target must have to be detected. Therein, it is necessary that the transmitting pulse leaves the antenna completely and the radar unit must switch on the receiver. The transmitting time τ and the recovery time $t_{recovery}$ should be as short as possible, if targets shall be detected in the local area.

$$R_{min} = \frac{c_0 \cdot (\tau + t_{recovery})}{2} \quad (1)$$

Targets at a range equivalent to the pulse width from the radar are not detected. A typical value of 1 μ s pulse width of a short range radar corresponds to a minimum range of about 150 m, which is generally acceptable. However, radars with longer waveforms suffer a relatively large minimum range, notably pulse compression radars, which can use pulse lengths of the order of tens or even hundreds of microseconds. Targets at ranges closer than this minimum are said to be eclipsed.

3.3.6 RANGE RESOLUTION

The target resolution of radar is its ability to distinguish between targets that are very close in either range or bearing. Resolution is usually divided into two categories; range resolution and bearing resolution.

Range resolution is the ability of radar system to distinguish between two or more targets on the same bearing but at different ranges. The degree of range resolution depends on the width of the transmitted pulse, the types and sizes of targets, and the efficiency of the receiver and indicator. Pulse width is the primary factor in range resolution. A well-designed radar system, with all other factors at maximum efficiency, should be able to distinguish targets separated by one-half the pulse width time τ . Therefore, the theoretical range resolution cell of radar system can be calculated from the following equation:

$$S_r \geq \frac{c_0 \cdot \tau}{2} \quad (1)$$

3.3.7 RADAR USING INTRAPULSE-MODULATION

In a pulse compression system, the range-resolution of the radar is given by the length of the pulse at the output-jack of the pulse compressing stage. The ability to compress the pulse depends on the *bandwidth* of the transmitted pulse (BW_{tx}) not by its *pulse width*. As a matter of course the receiver needs at least the same bandwidth to process the full spectrum of the echo signals.

$$S_r \geq \frac{c_0}{2BW_{tx}} \quad (2)$$

This allows very high-resolution (and a small radar range resolution cell) to be obtained with long pulses, thus with a higher average power.

3.3.8 RADARS ACCURACY

Accuracy is the degree of conformance between the estimated or measured position and/or the velocity of a platform at a given time and its true position or velocity.

The stated value of required accuracy represents the uncertainty of the reported value with respect to the true value and indicates the interval in which the true value lies with a stated probability. The recommended probability level is 95 percent, which corresponds to 2 standard deviations of the mean for a normal (Gaussian) distribution of the variable. The assumption that all known correction is taken into account implies that the errors in the reported values will have a mean value close to zero.

Any residual bias should be small compared with the stated accuracy requirement. The true value is that value which, under operational conditions, characterizes perfectly the variable to be measured/observed over the representative time, area and/or volume interval required, taking into account siting and exposure.

3.3.9 ACCURACY IN RANGE DETERMINATION

The theoretical maximum accuracy with which a distance can be measured depends on the accuracy of the runtime measurement.

RANDOM MEASUREMENT ERROR

A random error occurs with a pulse radar when the rising edge of the echo signal is distorted by noise. Since the pulse is always superimposed with noise during measurement and the pulse plus the noise is measured as amplitude, the pulse is also displayed larger than it is in reality. This shifts the pulse edge and causes a measurement error in the run-time measurement.

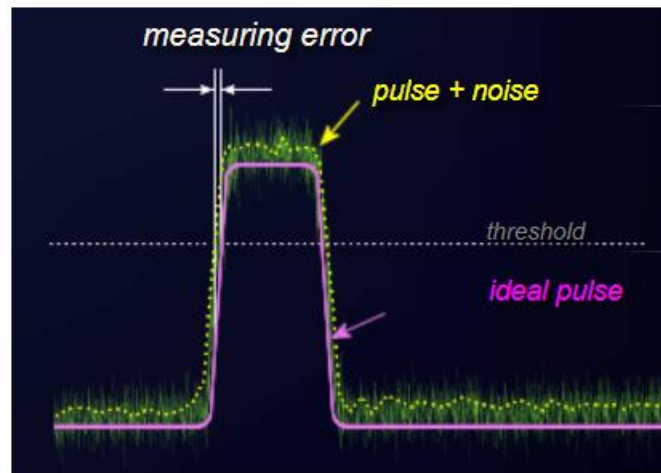


Fig. 18 - Falsification of the pulse edge due to superimposition of noise

Fig. 18 shows the influence of noise on the detectable edge of the echo pulse. The solid line (magenta) shows an almost ideal trapezoidal impulse with quite steep edges. This pulse cannot become quite rectangular because this would require an infinite bandwidth. The time is measured at a point determined by a threshold value, usually at 0.707 of the maximum voltage. However, this pulse is superimposed with the noise level (green). Only a voltage can be measured, which is formed by the sum of the instantaneous voltage of the pulse and the noise (dotted yellow line). This voltage exceeds the threshold value at an earlier time than the clean pulse. The difference is the random measurement error caused by the noise.

If the duration of the pulse is known (which cannot be the case with primary radar but with secondary radar), then this random error can be reduced mathematically by simultaneous evaluation of the front and rear edges of the pulse.

MATHEMATICAL CONTEXT

The accuracy of the distance measurement depends essentially on the noise or better: the size of the noise in relation to the impulse. This quantity is described by the Signal-to-Noise Ratio (SNR). The size of the noise itself also depends on the bandwidth. The slope of the pulse edge also depends on the bandwidth. For a signal-to-noise ratio of considerably higher than 1, the following relationship exists between these variables:

$$\delta R \cong \frac{c_0}{2B\sqrt{2SNR}} \quad (1)$$

δR = measuring error

c_0 = speed of light

B = bandwidth

SNR = signal-to-noise ratio

However, the bandwidth is also significant for the radars range resolution $S_r = c_0 / 2B$. Thus, the maximum achievable accuracy can also be represented as a function of the radars range resolution:

$$\delta R \cong S_r \cdot \frac{1}{\sqrt{2SNR}} \quad (2)$$

From this, it can be seen that the maximum achievable accuracy in range determination must be considerably better than the range resolution.

SYSTEMATIC MEASUREMENT ERRORS

With a pulse radar, the run time is generally measured from the rising edge of the transmit pulse to the rising edge of the echo signal. The accuracy of this measurement depends on the magnitude of the clock frequency for this time measurement. Measurement results between the cycles are not possible and generate a systematic measurement error. Practically, the accuracy depends on the size of the individual range-cells in signal processing.

With a CW radar, the measurement of the phase shift of the received signal relative to the current phase of the transmitter may contain (albeit ambiguous) distance information.

The accuracy of an FMCW radar also depends on the transmitter, especially on the slope and linearity of the frequency drift.

3.3.10 ACCURACY IN ANGLE MEASUREMENT

The accuracy of the angle measurement depends both on internal signal processing methods and on external conditions. Anomalous propagation conditions, which frequently occur due to changes in air pressure in height angle measurements, can in principle also occur in side angles and form a random error. However, more frequent systematic error sources occur internally.

For example, the angle determination by the sliding window is a rather inaccurate procedure. In practice, the half-width of the antenna is only divided by the number of quantizations of the method (e.g., 8 or 16 pulse periods) and thus results in a systematic error of the order of magnitude of up to one degree. Other correlation methods can also interpolate intermediate values and are therefore much more accurate. The best accuracy is currently achieved with the conical scan and the monopulse method.

3.3.11 HOW IS A MEASUREMENT PERFORMED?

The measurement is performed exactly as the measurement result is defined: the position measured by the radar is compared with the actual position of the target.

Statistical methods are also used for the calculation. Obvious erroneous measurements are excluded from the calculation because the systematic error of the radar unit is to be calculated. This does not mean, however, that many hits are necessary (perhaps to achieve a good value). If the radar uses monopulse technology, then a value is also determined for each pulse. If the radar determines the position using the Sliding Window method, then the respective value is determined according to the concrete number of hits required.

For good accuracy in distance determination, a stable and steep edge of the radar pulse is required. This steep pulse edge is often not visible when intrapulse modulation is used. But here it has to be said that the distance can only be measured after the pulse compression. At this point, the (now compressed) impulse is present again with a very good edge steepness.

The only condition for the measurement is that the radar operates in an interference-free environment. Interference-free means: the received echo signal is not superimposed by external interference signals. This also includes the noise level. A useful measurement is therefore only possible if the signal strength of the measured echo signal of the aircraft is much higher than the noise level. Finally, a flight calibration should detect possible additional systematic errors and not random errors.

3.4 RADAR TIMING PERFORMANCE

3.4.1 PULSE REPETITION FREQUENCY (PRF)

Pulse Repetition Frequency (PRF) of the radar system is the number of pulses that are transmitted per second.

Radar systems radiate each pulse at the carrier frequency during transmit time (or Pulse Width PW), wait for returning echoes during listening or rest time, and then radiate the next pulse. The time between the beginning of one pulse and the start of the next pulse is called *pulse-repetition time* (PRT) and is equal to the reciprocal of PRF as follows:

$$PRT = \frac{1}{PRF} \quad (1)$$

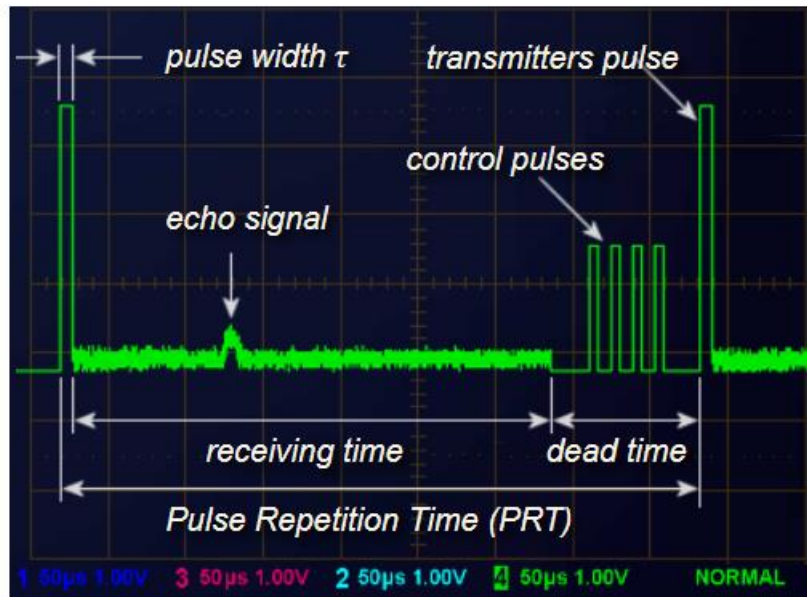


Fig. 19 – Radar pulse relationships

3.4.2 RECEIVING TIME

Generally, the *receiving time* is the time between the transmitters pulses. The receiving time is always smaller than the difference between the pulse repetition period and the length of the transmitter's pulse. It is sometimes also limited by a so-called *dead time*, in which the receiver is already switched off just before the next transmitting pulse.

In some radars between the transmitting pulse and the receiving time, there is a short recovery time of the duplexer. This recovery time occurs when the duplexer must switch off the receiver response to the high transmitting power. At very low transmitting power, however, can already be received during the transmit pulse also. The receiving time includes transmission time then.

3.4.3 DEAD TIME

If the receiving time ends before the next transmitting pulse, the result is a *dead time*. During the dead time are carried out system test loops in modern radars generally. Radars that use a phased-array antenna, urgently need such a dead time. For within this time, the phase shifters of the antenna must be reprogrammed to prepare the antenna for the next direction of the antennas beam. This can take up to 200 microseconds, why then the dead time takes quite large values compared with the receive time.

In this dead time, the receiver is already switched off because during the reprogramming the antenna cannot provide received signals. Because during this time, no real data can be processed in any case, this time is used to perform internal testing procedures in the modules of the receive path. This is done in order to verify the operational readiness of certain electronic circuits and to adjust them, if necessary. For this purpose, signals are generated with known size. These signals are fed into the receive paths and their processing in the individual modules is monitored. However, the video processor switches off these pulses, so that they do not appear on the screen. If necessary, as a

result of the tests the modules can be automatically reconfigured and it can be written a detailed error message.

3.4.4 BURST-MODE

The distribution of the dead time does not have to be uniform. It can be also be transmitted a number of pulses in rapid succession one after the other with each a short receive time before dead time appears. For example, if several pulse periods are orientated in the same direction (as like necessary for pulse pair processing and moving target detection), then a dead time is not needed. This has advantages for the time budget of the radar. A random unwanted change in the phase angle of the generator is not likely after a shorter time. Therefore, the radar will be more accurate in the distance measurement. Simultaneously, the pulse repetition frequency changes in this short period of time: it is very higher than the average. The higher the pulse repetition frequency, the better is the unambiguous measurement of the velocity.

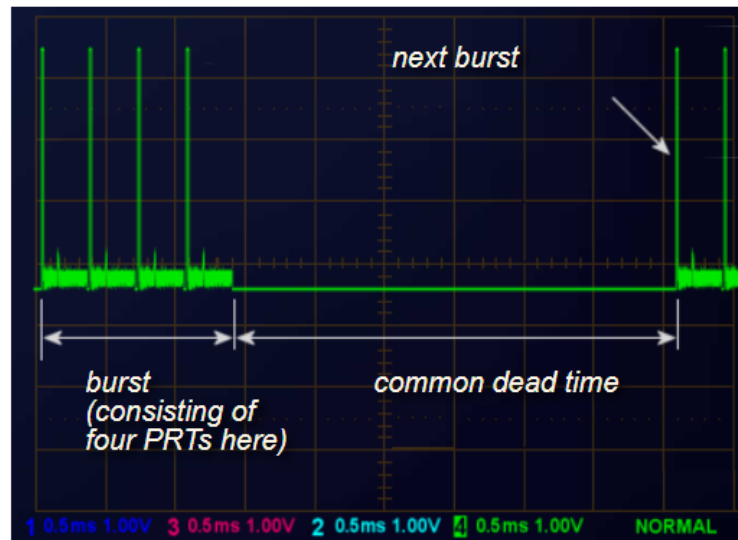


Fig. 20 – Burst mode of a pulse radar

DOPPLER DILEMMA (DOPPLER AMBIGUITY)

In pulse radar, the modulation of the carrier frequency is a periodic sequence of rectangular pulses. The frequency spectrum of the transmitted signal is a comb-shaped line spectrum. The line spacing of the spectrum is equal to the Pulse Repetition Frequency f_{PRF} or PRF. These lines cannot be separated by a simple amplitude comparison. The received frequency spectrum (subject to the Doppler Effect) can only be used for unambiguous velocity measurements when the displacement of the received spectrum is smaller than the line spacing in the spectrum i.e., the Doppler frequency must be lower than the PRF, or the PRF must be higher.

While the electromagnetic waves travel with the speed of light, the pulse radar needs a given receiving time to detect far away objects. If the interpulse period is long enough that isn't a problem. When the interpulse period is shortened, the time to the last previous pulse is shorter than the actual time it took, giving a false (ambiguous) shorter

range. Long range radars operate with a low PRF. Doppler radars capable of measuring a large range of velocities unambiguously operate at high PRF therefore.

The DOPPLER Dilemma: A good choice of PRF to achieve a large unambiguous range will be a poor choice to achieve a large unambiguous velocity and vice versa.

Using the general equation for Doppler Frequency, we can calculate the range of the unambiguous radial speed v_r :

$$f_{PRF} > |f_D| = \frac{2 \cdot v_r \cdot f_{tx}}{c_0} \quad (1)$$

$$v_r < \frac{c_0 \cdot f_{PRF}}{2 f_{tx}} \quad (2)$$

This equation is valid, if the direction of the Doppler shift is known, i.e., it is known, that the aim is moving toward or away from the radar site. If this direction is unknown, the unambiguous value of the velocity is halved again:

$$v_r < \frac{c_0 \cdot f_{PRF}}{4 f_{tx}} \quad (3)$$

The pulse repetition frequency is a measure of the unambiguous range too. If the transmitter's pulse width is much smaller than the pulse period, then the value of the pulse repetition frequency f_{PRF} can be substituted by the relation $c_0 / 2 \cdot R_{max}$:

$$R_{max} \cdot v_r < \frac{c_0^2}{8 f_{tx}} \quad (4)$$

Now you can see, that the radars ability to measure an unambiguous range and an unambiguous Doppler frequency (i.e. the aims radial speed) depends on the transmitter's carrier frequency only.

3.4.5 PEAK- AND AVERAGE POWER

The energy content of a continuous-wave radar transmission may be easily figured because the transmitter operates continuously. However, pulsed radar transmitters are switched on and off to provide range timing information with each pulse. The amount of energy in this waveform is important because maximum range is directly related to transmitter output power. The more energy the radar system transmits, the greater the target detection range will be. The energy content of the pulse is equal to the peak (maximum) power level of the pulse multiplied by the pulse width. However, meters used to measure power in radar system do so over a period of time that is longer than the pulse width. For this reason, pulse-repetition time is included in the power calculations for transmitters. Power measured over such a period of time is referred to as average power.

$$D = \frac{\bar{P}}{P_i} = \frac{\tau}{T} \quad (1)$$

\bar{P} = average power

P_i = pulsed power

τ = pulse width

T = pulse-repetition time PRT

Peak power must be calculated more often than average power. This is because most measurement instruments measure average power directly. Transposing the upper equation gives us a common way for calculating peak power/average power.

Since the storage of the energy in the modulator, the power supply must make plant for the transmitter available a little more than the average power only.

3.4.6 DUTY CYCLE

The product of pulse width (τ) and pulse-repetition frequency (prf) as the reciprocal of the pulse period (T) in the above formula is called the duty cycle of radar system. Duty cycle is the fraction of time that a system is in an "active" state. In particular, it is used in the following contexts: Duty cycle is the proportion of time during which a component, device, or system is operated. Suppose a transmitter operates for 1 microsecond, and is shut off for 99 microseconds, then is run for 1 microsecond again, and so on. The transmitter runs for one out of 100 microseconds, or 1/100 of the time, and its duty cycle is therefore 1/100, or 1 percent. The duty cycle is used to calculate both the peak power and average power of radar system.

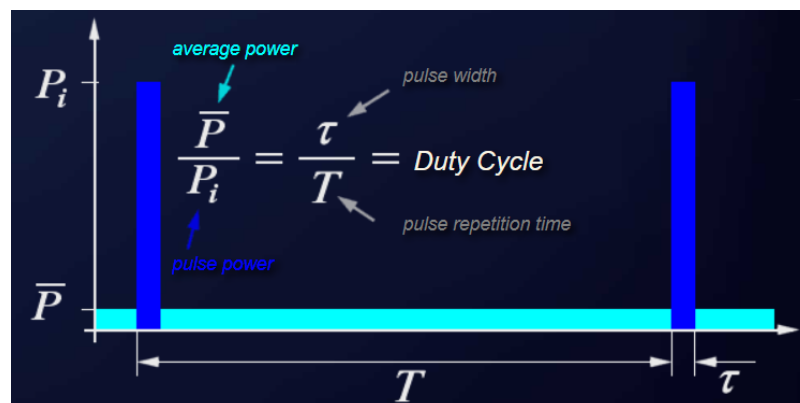


Fig. 21 – Duty cycle, peak- and average power

3.4.7 DWELL TIME AND HITS PER SCAN

Most processes in pulsed radar are time-dependent. Thus, some terms like Dwell Time and Hits per Scan have been established to describe this time-dependence.

DWELL TIME

The time that an antenna beam spends on a target is called dwell time T_D . The dwell time of a 2D-search radar depends predominantly on:

- the antennas horizontally beamwidth θ_{AZ} and
- the speed of rotation n of the antenna (rotations per minute).

The dwell time can be calculated using the following equation:

$$T_D = \frac{\theta_{AZ} \cdot 60}{360^\circ \cdot n} \quad (1)$$

HITS PER SCAN

The value of hits per scan m says how many echo signals *per single target* during every antenna rotation are received. The hit number stands e.g. for a search radar with a rotating antenna for the number of the received echo pulses of a single target per antenna turn. The dwell time T_D and the pulse repetition time PRT determine the value of hits per scan.

$$m = \frac{T_D}{PRT} = \frac{\theta_{AZ} \cdot 60}{360^\circ \cdot n \cdot PRT} \quad (2)$$

In order to evaluate the target position in radar systems with sufficient accuracy, hit numbers from 1 to 20 are necessary (depending on the working principle of the radar system). The greater the number of hits per scan, the more accurate will be the angle measurement and the better the MTI performance.

For analog displays, the size and brightness of the target character on the screen is also determined by how many hits per scan the target has received. A measurement of the accurate azimuth of the target is still defined herein in the center of the blip on the screen. (The distance is measured at the front edge of this blip.)

Many radars use pulse integration in the radar signal processing to distinguish the target signals from noise and interference pulses. If the number of hits per scan is too small, this target can be suppressed by the increased threshold values because of these disturbances.

In the case of a digital plot extractor, which uses the method of sliding window to determine the azimuth, a predetermined number of hits per scan must also be achieved. A radar with a monopulse antenna requires only one pulse for the accurate azimuth measurement. However, monopulse radars also often require two, three, or more pulses for moving target indication.

3.4.8 TIME-DEPENDENCES IN RADAR

Radar parameters such as antenna rotations per minute, dwell time, maximum unambiguous range, pulse repetition frequency (PRF), the maximum number of hits per target are strongly interdependent.

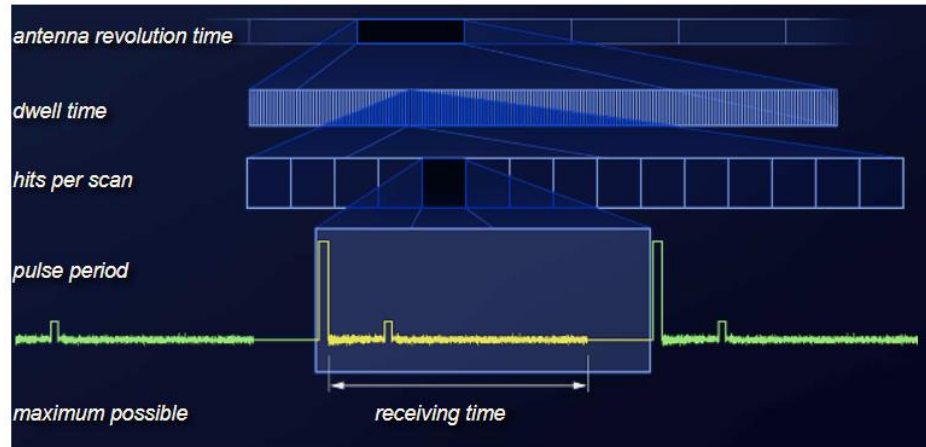


Fig. 22 – Time-dependences in Radar

Finally, also all other radar characteristics such as range and azimuth resolution, blind speed, etc could be derived from these basic timing considerations. A classic radar (i.e. radar, not using monopulse technology) operating as an ATC-Radar needs a data renewal time of fewer than 5 seconds. This requirement limits the receiving time and the maximum unambiguous range as following:

Since the radar processing in this surveillance radar is still in real-time (with relatively low but constant delay), the data renewal time depends on the antenna revolution time. To direct in the same azimuth angle after 5 seconds, so that the radar can measure the coordinates again, the antenna must turn with 12 revolutions per minute at least.

The dwell time, the time that an antenna beam spends on a target, depends predominantly on the antennas horizontally beamwidth and the turn speed of the antenna. If we assume, that a well designed parabolic antenna got a beamwidth of 1.6 degrees, the full circle of 360 degrees is divided by $360^\circ/1.6^\circ = 225$ different directions. 5 seconds divided by the number of 225 gives a dwell time of $5 \text{ s} / 225 = 22.22$ milliseconds.

These radar sets need a given number of hits per scan. This is necessary, to integrate the signals (see pulse integration) of different pulse periods for a better distinction of wanted signals from unwanted noise, as well as to measure a correct angular direction. Assumed a necessary number of 20 hits per scan, the maximum pulse period takes a time of 1 millisecond, therefore. Assuming a receiving time less than 1 millisecond, the maximum unambiguous range of the ATC-radar is smaller than 150 kilometers. If the radar uses a staggered pulse repetition frequency to avoid blind speeds in radar signal processing, then the smallest period gives the base to the range calculation. So we must calculate with a period of about 0.8 ms instead of 1 ms. The maximum unambiguous range of this given ATC-radar is 120 kilometers or 65 nautical miles, therefore.

So we can see, that the time scheduling of radar is very important. Most of the parameters are fixed and the maximum range of given radar set is time-dependent predetermined. Additional measuring of an elevation angle is not possible often. To promise a higher range demands fundamental changes in the radar signal processing as like as monopulse technology and/or digital beamforming. Even small changes in the needed number of hits per scan (as a possible alternative to increase the receiving time

to achieve a better unambiguous range) have a negative influence on the radars' probability of detection.

3.5 THE RADAR EQUATION

3.5.1 THE RADAR RANGE EQUATION

The radar range equation represents the physical dependences of the transmit power, which is the wave propagation up to the receiving of the echo signals. The power P_e returning to the receiving antenna is given by the radar equation, depending on the transmitted power P_s , the slant range R , and the reflecting characteristics of the aim (described as the radar cross-section σ). At the known sensibility of the radar receiver, the radar equation determines the achieved by a given radar theoretically maximum range. Furthermore, one can assess the performance of the radar set with the radar range equation (or shorter: *the radar equation*).

3.5.2 ARGUMENTATION/DERIVATION

First, we assume, that electromagnetic waves propagate under ideal conditions, i.e. without dispersion.

If high-frequency energy is emitted by an isotropic radiator then the energy propagates uniformly in all directions. Areas with the same power density, therefore, form spheres ($A=4\pi R^2$) around the radiator. The same amount of energy spreads out on an incremented spherical surface at an incremented spherical radius. That means: the power density on the surface of a sphere is inversely proportional to the square of the radius of the sphere.

So, we get the equation to calculate the Non-directional Power Density S_u

$$S_u = \frac{P_s}{4\pi R_1^2} \quad (1)$$

P_s = transmitted power [W]

S_u = nondirectional power density

R_1 = range from transmitter antenna to the aim [m]

Since a spherical segment emits equal radiation in all direction (at constant transmit power) if the power radiated is redistributed to provide more radiation in one direction, then this results in an increase of the power density in direction of the radiation. This effect is called antenna gain. This gain is obtained by directional radiation of the power. So, from the definition, the directional power density is:

$$S_g = S_u \cdot G = \frac{P_s}{4\pi R_1^2} \cdot G \quad (2)$$

S_g = directional power density

S_u = nondirectional power density

G = antenna gain

Of course, in reality, radar antennas are not “partially radiating” isotropic radiators. Radar antennas must have a small beamwidth and an antenna gain up to 30 or 40 dB (e.g. parabolic dish antenna or phased array antenna).

The target detection isn't only dependent on the power density at the target position, but also on how much power is reflected in the direction of the radar. In order to determine the useful reflected power, it is necessary to know the radar cross-section σ . This quantity depends on several factors. But it is true to say that a bigger area reflects more power than a smaller area. That means:

An Airbus offers more radar cross-section than a sporting aircraft at the same flight situation. Beyond this the reflecting area depends on the design, surface composition and materials used.

If the previously mentioned is summarized, the reflected power P_r (at the destination, i.e., the radar receiver) results from the power density S_u , the antenna gain G , and the very variable reflection area σ :

$$P_r = \frac{P_s}{4\pi R_1^2} \cdot G \cdot \sigma \quad (3)$$

P_r = reflected power [W]

σ = radar cross-section [m²]

R_1 = range, distance antenna - aim [m]

Simplified a target can be regarded as a radiator in turn due to the reflected power. In this case, the reflected power P_r is the emitted power.

Since the echoes encounter the same conditions as the transmitted power, the power density yielded at the receiver S_e is given by:

$$S_e = \frac{P_r}{4\pi R_2^2} \quad (4)$$

S_e = power density at receiving place

P_r = reflected power [W]

R_2 = range aim - receiving antenna [m]

At the radar antenna, the received power P_e is dependent on the power density at the receiving site S_e and the effective antenna aperture A_w .

$$P_e = S_e \cdot A_w \quad (5)$$

P_e = received power [W]

A_w = effective antenna aperture [m²]

The effective antenna aperture arises from the fact that an antenna suffers from losses, therefore, the received power at the antenna is not equal to the input power. As a rule, the efficiency of the antenna is around 0.6 to 0.7 (Efficiency K_a).

Applied to the geometric antenna area, the effective antenna aperture is:

$$A_w = A \cdot K_a \quad (6)$$

$$A_W = \text{effective antenna aperture [m}^2\text{]}$$

$$A = \text{geometric antenna area [m}^2\text{]}$$

$$K_a = \text{efficiency}$$

The power received P_e is then calculated:

$$P_e = S_e \cdot A_W \quad (5)$$

$$A_W = A \cdot K_a \quad (6)$$

$$P_e = S_e \cdot A \cdot K_a \quad (7)$$

$$S_e = \frac{P_r}{4\pi R_2^2} \quad (4)$$

$$P_e = \frac{P_r}{4\pi R_2^2} \cdot A \cdot K_a \quad (8)$$

The transmitted and reflected waves have been seen separately. The next step is to consider both transmitted and reflected power: Since R_2 (aim - antenna) is equal to the distance R_1 (antenna - aim) then:

$$P_e = \frac{P_r}{4\pi R_2^2} \cdot A \cdot K_a \quad (8) \quad P_r = \frac{P_s}{4\pi R_1^2} \cdot G \cdot \sigma \quad (3)$$

$$P_e = \frac{\frac{P_s \cdot G \cdot \sigma}{4 \cdot \pi \cdot R_1^2}}{4 \cdot \pi \cdot R_2^2} \cdot A \cdot K_a$$

$$P_e = \frac{P_s \cdot G \cdot \sigma}{(4 \cdot \pi)^2 \cdot R_2^2 \cdot R_1^2} \cdot A \cdot K_a$$

$$R_2 = R_1$$

$$P_e = \frac{P_s \cdot G \cdot \sigma}{(4 \cdot \pi)^2 \cdot R^4} \cdot A \cdot K_a$$

Another equation, which will not be derived here, describes the antenna gain G in terms of the wavelength λ .

$$G = \frac{4\pi AK}{\lambda^2} \quad (10)$$

Solving for A , antenna area, and replacing A into equation 9; after simplification it yields:

$$P_e = \frac{P_s G^2 \sigma \lambda^2}{(4\pi)^3 \cdot R^4} \quad (11)$$

Solving for range R , we obtain the classic radar equation:

$$R = \sqrt{\frac{P_s G^2 \sigma \lambda^2}{P_e (4\pi)^3}} \quad (12)$$

All quantities that influence the wave propagation of radar signals were taken into account at this equation. Before we attempt to use the radar equation in the practice for example to determine the efficiency of radar sets, some further considerations are necessary.

For given radar equipment most sizes (P_s , G , λ) can be regarded as constant since they are only variable parameters in very small ranges. The radar cross-section, on the other hand, varies heavily but for practical purposes, we will assume 1 m^2 .

The smallest received power that can be detected by the radar is called P_{Emin} . Smaller powers than P_{Emin} aren't usable since they are lost in the noise of the receiver. The minimum power is detected at the maximum range R_{max} as seen from the equation.

$$R_{max} = \sqrt[4]{\frac{P_s G^2 \sigma \lambda^2}{P_{e_{min}} (4\pi)^3}} \quad (13)$$

An application of this radar equation is to easily visualize how the performance of the radar sets influences the achieved range.

3.5.3 RADAR CROSS-SECTION

The Radar Cross Section σ (RCS) is an aircraft-specific quantity that depends on many factors. The computational determination of the RCS is only possible for simple bodies. The RCS of simple geometric bodies depends on the ratio of the structural dimensions of the body to the wavelength.

Practically, the RCS of a target depends on:

- the physical geometry and exterior features of the target
- the direction of the illuminating radar
- the radar transmitters frequency
- the electrical properties of the target's surface

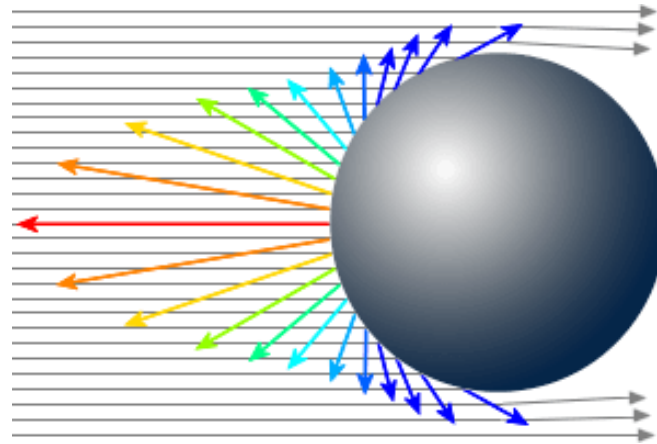


Fig. 23 - The reference for the radar cross section: a metallic sphere, which in the view offers a (projected) circle with an area of 1 m^2

WHAT DOES RCS MEAN FOR RADAR?

The RCS of any reflector can be seen as a ratio to an idealized reference reflector. The projected area of an equivalent isotropic reflector (that is: reflecting equally in all directions) has an RCS of exactly one square meter. Reflecting equally in all directions means: in practice, this is only performed by a spherical reflector with an ideally conducting surface. From a large distance, you cannot see the spherical shape, you can only see a circular area: the so-called projection, both with the same diameter. The diameter of this sphere must be approximately 1.128 m to be the size of one square meter. Such an equivalent isotropic reflector delivers the same power per unit measure of solid angle back to the radar, regardless of the aspect angle (i.e., regardless of the direction of the radar). Isotropic reflective does not mean that this sphere would distribute the power arriving from one direction equally in all directions. The shape and size of the distribution are different, but always the same relative to the aspect angle of the illuminating radar, regardless of the angle from which the radar illuminates this sphere. However, the reference reflector can re-radiate only the power it has received:

$$\frac{\sigma S_t}{4\pi} = S_r \cdot r^2 \quad (1)$$

S_t : power density of the transmitter at the radar target in $[\text{W}/\text{m}^2]$

S_r : scattered power density at the receiving site in $[\text{W}/\text{m}^2]$

σS_t : is the power received and re-radiated by the radar target (in watts)

$\sigma S_t/4\pi$; is this power per solid angle, i.e., divided by 4π steradian (in watts per steradian)

r : radius of the sphere

This equation (1) expresses only a power balance: only the power that arrives at this reflecting object can be reflected, and this power is radiated in many directions. From this power, however, the radar can only receive a small part again. This part depends on the effective antenna area, the antenna aperture.

Since the power density generated by the radar transmitter and arriving at the reflection point is put into a ratio with the reflected power density arriving at the radar, all other influences, such as free space attenuation and distance to the radar, are eliminated. It

is assumed that for a monostatic radar, the propagation conditions are the same on the outbound and return paths.

Let S_r be the power density at the receiving point of the radar, which we now see from the perspective of the reflecting object. This power density has the unit of measurement watts per unit area: W/m^2 . The receiving antenna of the radar has only one effective antenna aperture A_r (this is an area and a part of the surface of a sphere). The received power of the radar antenna is then $S_r \cdot A_r$, which is the power density at the antenna multiplied by its effective aperture.

However, this antenna can receive only a very small portion of the power reflected from the object in all directions, because it occupies only a small part of the surface of the sphere. This area is proportional to the solid angle Ω occupied by the total reflected power distributed on a spherical surface:

$$\Omega = \frac{A_r}{r^2} \quad (2)$$

Thus, a power density (power per solid angle) of $S_r \cdot A_r / \Omega$ arrives at the receiving antenna. The solid angle can be replaced with the expression from equation (2) and leads to:

$$\frac{S_r \cdot A_r}{\Omega} = \frac{S_r \cdot A_r}{\frac{A_r}{r^2}} = S_r \cdot r^2 \quad (3)$$

The expression $S_r \cdot r^2$ thus stands for the received power per unit solid angle (in watts per steradian) and corresponds to equation (1) above. This can then be rearranged to the equation (4) used below.

3.5.4 NON-ISOTROPIC REFERENCE REFLECTOR

In contrast to the isotropic radiator mentioned in the antenna technology, such an isotropic reference reflector can very well be constructed in reality. It would only be very unwieldy because of its dimensions. Since the direction to the radar is known in a measurement setup, a calibrated corner reflector can also be used. As usual in antenna technology, this has a gain G compared to the isotropic reflector, which, however, can be calculated out of the measurement result later.

3.5.5 COMPUTATIONAL DETERMINATION OF THE REFLECTIVE AREA

In the following formula, the radar cross section indicates an effective area that captures the incoming wave and re-radiates it into space. Thus, only a power density caused by the surface of the sphere ($4\pi r^2$) arrives at the receiving antenna of the radar. The radar cross section σ is defined as:

$$\sigma = 4\pi r^2 \cdot \frac{S_r}{S_t} \quad (4)$$

σ : apparent area in [m^2], measure of the backscattering ability.

S_t : power density of the transmitter at the radar target in [W/m^2]

S_r : scattered power density at the receiving location in [W/m^2]

The following formulas for calculation of the radar cross section are valid under the condition of optical, i.e., frequency-independent reflection at bodies that are much further away from the radar than the wavelength and which are much larger than the used wavelength of the radar.

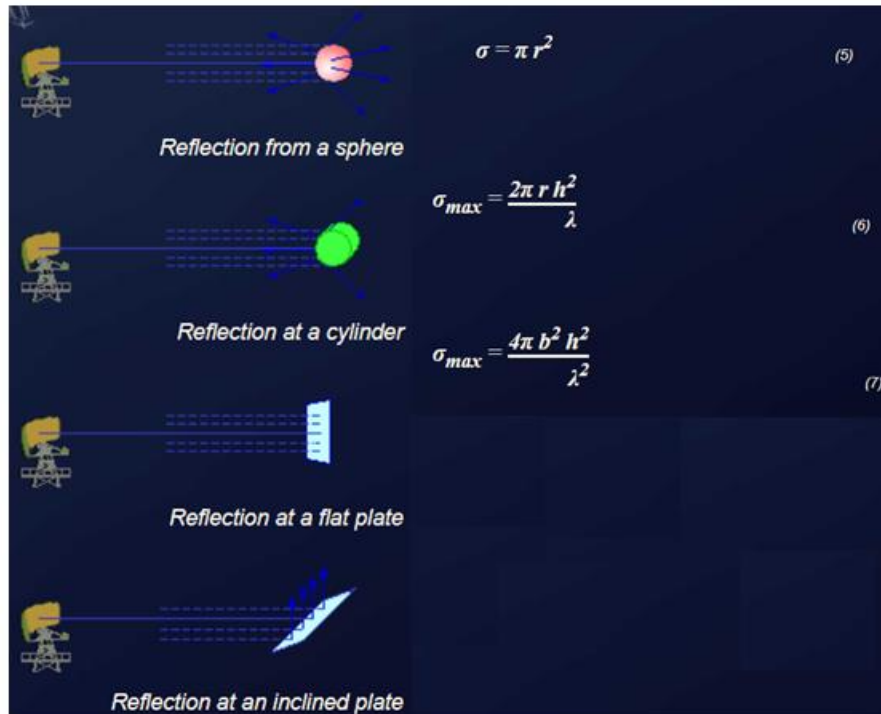


Fig. 24 – Reflection from geometric objects

3.5.6 RADAR CROSS SECTIONS FOR POINT-LIKE TARGETS

In radar technology, point-like targets are targets whose geometric dimensions are smaller than the pulse volume of the radar set. In contrast to volumetric targets (occurring mainly in weather radar), they do not completely fill the pulse volume. In radar signal processing they occupy one resolution cell (maximum two if they are exactly on the boundary).

In reality, the radar cross section is composed of the sum of many small partial powers, which are located at different points of the reflecting object. Depending on the angle from which this object is illuminated, these partial areas have more or less influence, they may be obscured or their distance to the radar may differ by several multiples of half the wavelength so that they overlap partly constructively and partly destructively (see interference).

<i>Targets</i>	<i>RCS [m²]</i>	<i>RCS [dB]</i>
<i>bird</i>	0.01	-20
<i>man</i>	1	0
<i>cabin cruiser</i>	10	10
<i>automobile</i>	100	20
<i>truck</i>	200	23
<i>corner reflector</i>	20379	43.1

Fig. 25 – RCS for Point-Like Targets

The RCS is thus strongly dependent on the aspect angle and can no longer be easily calculated geometrically. It is usually a result of extensive practical measurements either on the original or with a model scaled down to the wavelength currently used in the measurement.

Some targets mentioned as examples have according to their geometrical extension a very large amount of the RCS and reflect therefore a rather large amount of the transmitted energy. The table on the right gives some examples of reflective surfaces in the X-band.

4 PROJECT METHODOLOGY

In this section we will show and explain all the tools used to carry out the experimental part of the thesis.

4.1 MEASUREMENTS SETUP

First of all, it is worth mentioning that the measurements will be carried out on the HTW Mechlab circuit. The circuit has two lanes and a guardrail to simulate a real situation on a conventional road (see Fig. 26 and Fig. 27), a perfect scenario to give a dose of reality to the work.



Fig. 26 – HTW Meclab circuit



Fig. 27 – HTW Meclab circuit

In order to carry out the radar measurements, we set up a setup with different components, which we will show below.

For a correct positioning of the objects to be detected, we created a grid, as follows:

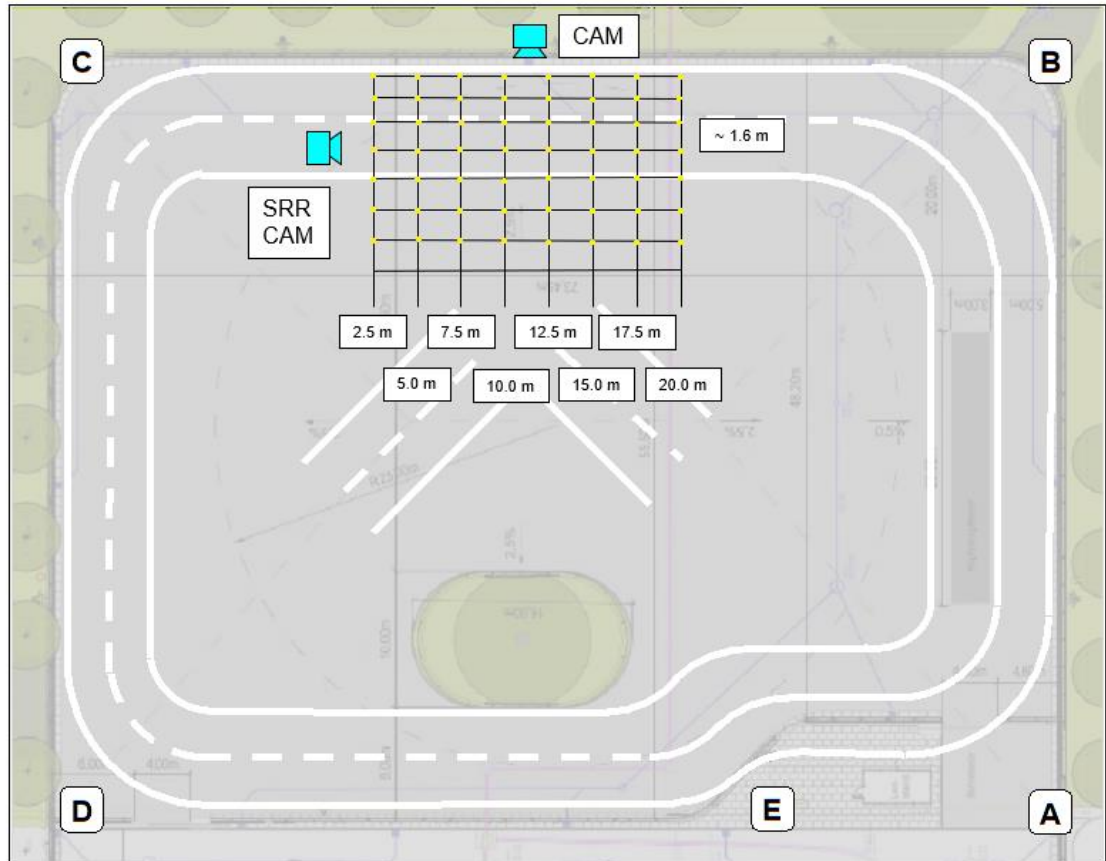


Fig. 28 – Grid draft

After having created a grid for a more precise and correct positioning of the objects to be detected, the next step is to paint it on the floor of the circuit. For this we create a template in the shape of a thin cross, and with different metres we place the template on the yellow dots shown in the draft. To paint we use a yellow spray paint (see Fig. 29).



Fig. 29 – Painting the grid

An important component of the setup is the camera, it's a BASLER a2A1920 camera. Its function is to display an image to support the radar detections, to facilitate the identification and position of objects in order to later make a comparison between what

the radar detects and the reality shown by the camera. Initially we made a support that we later had to change, as the camera was in a very low position with respect to the ground and did not have enough ball and socket joints to always show the target on the display. In that case the camera only had the ball joint in the anchor that allowed a 180° rotation vertically, but it could not rotate horizontally (see in Fig. 30).



Fig. 30 – First camera support

The final mount is in a much higher position for a better perspective (in the highest part of the setup) and has a ball joint in its base to rotate 180° horizontally, and another ball joint in the anchorage to the base to rotate 180° vertically (see in Fig. 31 and Fig. 32). In this way we can orientate the camera to centre the lens and always show it on the display.



Fig. 31 – Camera for radar image support



Fig. 32 – Definitive camera support

The camera is connected to the computer via a USB cable, as is the Vector CANCase XL.

The Vector CANCase XL combines two products in one device: A professional CAN/LIN/J1708 bus interface with USB 2.0 interface and a logger for easy recording of bus traffic during test drives or in the test lab.

MATLAB Vehicle Network Toolbox™ supports Vector CAN interface hardware. With Vector CAN interface support, you can perform the following tasks in MATLAB or Simulink:

- Transmit and receive CAN and XCP messages
- Pack and unpack CAN messages to simplify decoding and encoding
- Filter, log and replay CAN messages
- Use .dbc database and A2L description files
- Searching and displaying CAN interface device configuration
- In MATLAB and Simulink, you can transmit and receive CAN messages using the CAN FD standard if the CAN interface hardware supports CAN FD



Fig. 33 – Vector CANcaseXL

The Vector CANcaseXL is also connected to the radar via a VGA cable and to a power supply with a positive and negative cable (see Appendix).

The webcam is a feature of the circuit which is great for providing extra image support for the radar detection display. With the camera we have an image of what the front of the car or the radar itself would see, and with the webcam we have a bird's eye view which together shows more easily the position of the object to be detected and also makes it easier to compare simulation - reality. The position of the webcam on the circuit can also be seen in Fig. 28.



Fig. 34 – Webcam and its position

The last component of the setup that remains to be explained is the radar, which will be discussed in more detail in section 3.2 *SHORT RANGE RADAR 20X /-2 /-2C /-21*.



Fig. 35 – Radar

Once all the components have been shown and explained, the setup is as follows:



Fig. 36 – Radar measurements setup

4.2 SHORT RANGE RADAR 20X /-2 /-2C /-21

The full description of the radar can be found in the folder at the following path:

DanielDiaz_FinalThesis\Radar_description\Short-Description_2017_05_31-01_SRR20X_-
 2_-2C_-21_en_V1.09

For the development of this thesis, a Continental radar sensor has been used, the SRR 20X
 24 GHz short-range radar sensor manufactured by A.D.C. GmbH.

It should be noted that the technical description of the radar can be found with the
 following path in the thesis folder:

DanielDiaz_FinalThesis\Radar_description\Short-Description_2017_05_31-01_SRR20X_-
 2_-2C_-21_en_V1.09

This section is intended to give an overview of the radar used.



Fig. 37 – SRR 20X 24 GHz short-range radar sensor manufactured by A.D.C. GmbH

4.2.1 DEVICE DATA

The SRR 20X is a 24 GHz short-range radar sensor (operating in the ISM band*) which has been specially designed by A.D.C. GmbH for use in automotive applications. Its purpose is the non-contact measurement of distance, speed and position by means of digitally formed beams with a F.o.V. (field of view) of up to $\pm 75^\circ$ at medium distances. The SRR 20X is normally mounted behind a plastic secondary surface (radome).

**ISM band: The industrial, scientific, and medical radio band (ISM band) refers to a group of radio bands or parts of the radio spectrum that are internationally reserved for the use of radio frequency (RF) energy intended for scientific, medical and industrial requirements rather than for communications. ISM bands are generally open frequency bands, which vary according to different regions and permits.*

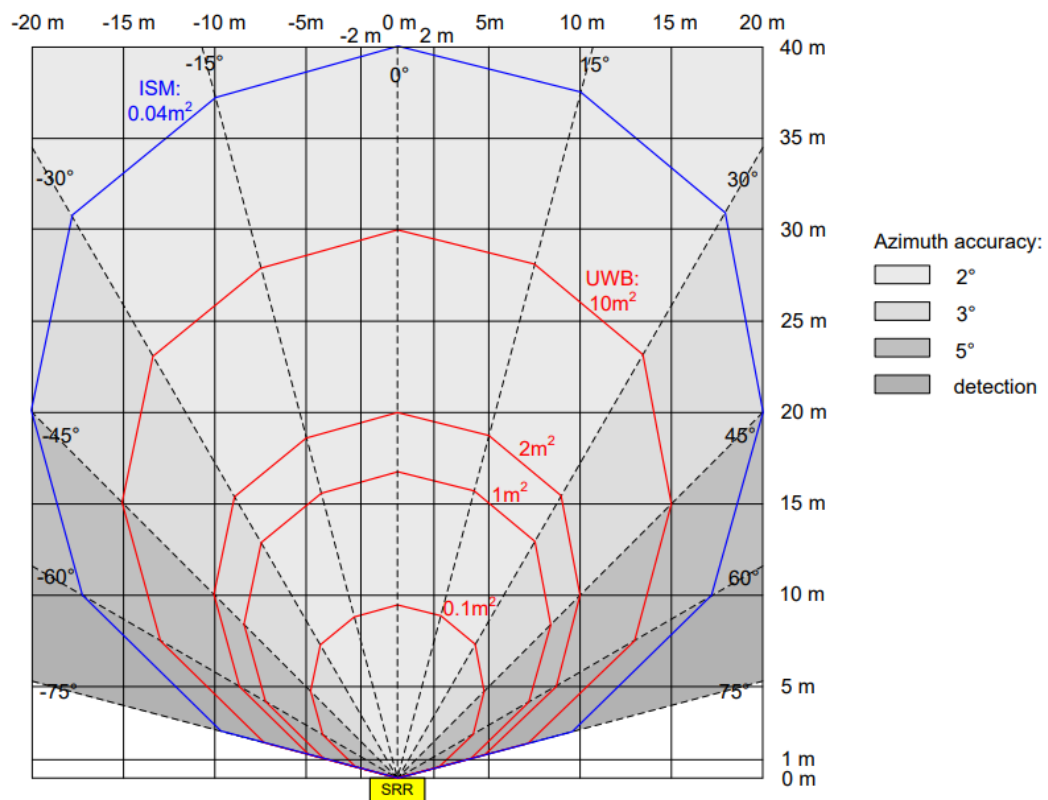


Fig. 38 - Field of View from SRR 20X with ISM band

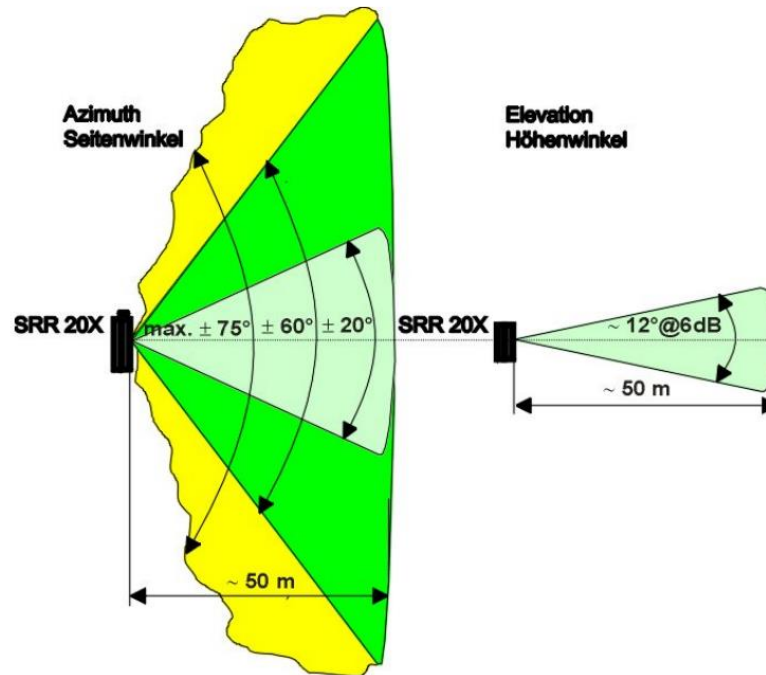


Fig. 39 - F.o.V. Field of View SRR 20X with azimuth and elevation exposure

4.2.2 DEVICE SETTINGS

4.2.2.1 CONNECTION

In order to check the SRR 20X or put it into operation, the SRR 20X must be connected to a power supply. The SRR 20X must also be connected to a PC or notebook via CAN bus and a separate and suitable interface converter CAN/USB – by example PCAN from company PeakSystems or CanAnalyzer from company Vector.

4.2.2.2 CONFIGURATION

Having connected the SRR 20X, the device needs to be configured by taking the data protocol as described in the separate Technical Documentation SRR 20X for the CAN protocol.

4.2.3 INSTALLATION

4.2.3.1 PLACE OF INSTALLATION

The SRR 20X sensor can be mounted in any direction in a vertical mounting window of 500 mm up to 1200 mm to the ground.

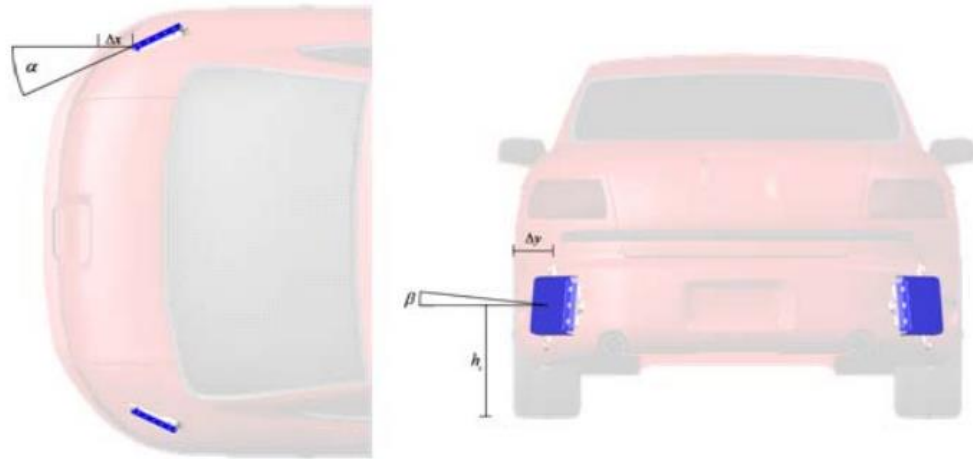


Fig. 40 - SRR 20X mounted behind a secondary surface (bumper) of a car

The mounting window is depending on the function which realized with the SRR 20X sensor. In addition to these mounting windows from Fig. 42 the function has additional requirements which are given in this section.

	Min	Nominal	Max
α	20°	25°	30°
β	-1°	0°	1°
Δx	100 mm	300 mm	500 mm
Δy	50 mm	100 mm	150 mm
h_z	500 mm	600 mm	1200 mm

Fig. 41 - SRR 20X mounting orientation requirements

Note: Reference point is center of module.

The sensor shall be protected from direct impact of water / mud / snow.

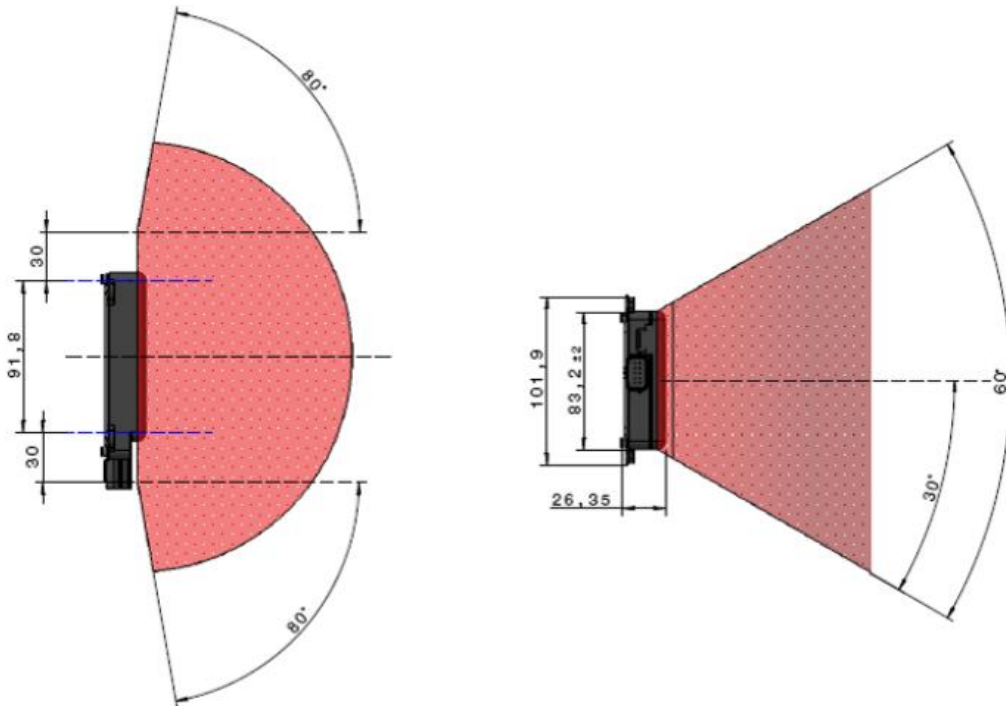


Fig. 42 - Mounting windows SRR 20X for azimuth and elevation exposure

4.2.3.2 KEEP OUT AND INTERFERENCE ZONES

For a proper SRR 20X performance the area in front of the SRR 20X sensor field of view (F.o.V.) needs to be kept free of any materials or objects that may disturb the millimeter wave emission characteristics.

Although a free space with a radius of app. 5 cm to 10 cm in front of the sensor can be assumed, detailed information needs to be agreed upon on a case by case basis.

Radar signal disturbing material should not be located within the keep out zone described in the following:

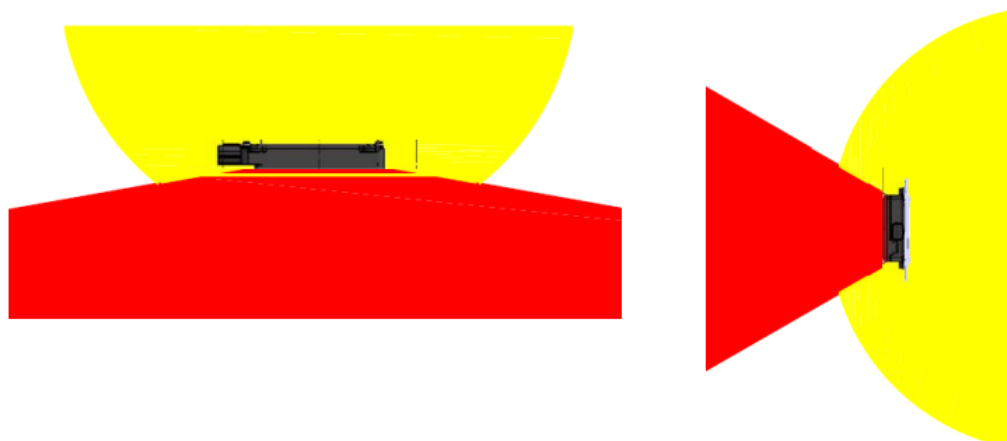


Fig. 43 - Keep out zones of SRR 20X for azimuth and elevation exposure

Legend for Details of keep out zone:

- Red Zone = "Must" Keep Out Zone

- Yellow Zone = "Want" Keep Out Zone
- Metal / strong reflection objects have to be:
 - Minimum 5 cm in front of the sensor
 - Minimum 15 cm to the right and the left of the sensor
 - Minimum 10 cm upper and under the sensor
- If metal / strong reflection objects are within the interference zone, evaluation driving tests have to be carried out to evaluate influence on sensor performance and warning efficiency.

Comments for SRR 20X sensor interference zones:

- Metal/strong reflecting objects have to be outside the interference (red) zone.
- Metal/strong reflecting objects have to be minimum 5 cm in front of the sensor, minimum 15 cm to the right and the left of the sensor and minimum 10 cm upper and under the sensor.
- If metal/strong reflecting objects are within the interference zone, evaluation driving tests have to be carried out to evaluate influence on sensor performance and warning efficiency.

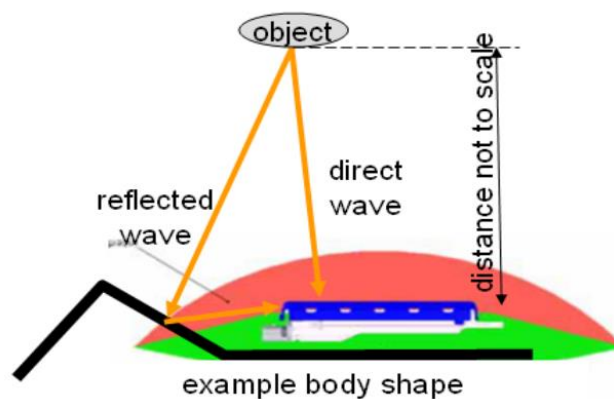


Fig. 44 - Mounting boundary conditions of SRR 20X

Comment for Mounting Boundary Conditions:

Metal shapes that might reflect waves should be avoided as much as possible.

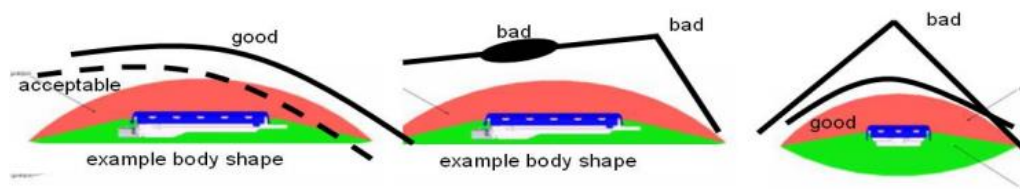


Fig. 45 - Guideline for secondary surface or bumper design of SRR 20X

4.2.3.3 CABLE CONNECTION AND FUSE PROTECTION

The connecting cable for the SRR 20X can be ordered separately with cable plug connector (without CAN termination) in a standard cable length of 5 m. It is also possible to order only a connector with pins and sealing. The cable has a pre-assembled cable plug connector (female) for plugging into the device, with a 9 pin SUB-

D connector (female) for CAN and two pin plugs (banana plugs) for Power Supply at the other end.

4.2.3.4 CAN BUS

The CAN interface allows the communication between a Notebook or PC and the device via separately converter CAN to USB. The CAN bus must have a terminal resistance of respectively 120Ω between CAN H and CAN L at the first and last subscriber to avoid reflections. Further details about the CAN interface can be found in Chapter 6 "Interfaces".

4.3 SIMULINK MODELS

Once we have the radar and the setup, we need to create Simulink models to be able to display what the radar shows and to be able to log the data.

All the designed models that are going to be shown below can be found in the thesis folder with the following path:

DanielDiaz_FinalThesis\conti_radar_SRR

4.3.1 CONFIGURATION

You can find the file in the folder here:

DanielDiaz_FinalThesis\conti_radar_SRR\matlab2021b_SRR_Conti_CAN_configuration

First, we create a Simulink model to configure the rest of the models according to the radar's operating mode. The radar has two operating modes, Track mode and Cluster mode, so the configuration model has two possible configurations.

Clusters are radar reflections with information like position, velocity and signal strength. They are newly evaluated every cycle. In contrast to this, objects have a history and dimension.

Tracking refers to a radar following the position of one or multiple targets in space. Before the tracking process, the radar has to detect targets and find their range, angular location, and sometimes velocity. The requirements on the accuracy of angle measurement for a tracking radar are stricter than those for a search radar.

The principle of tracking radar is to use the error signal to adjust the antenna's pointing direction. The difference between the target direction and the reference direction, usually the axis of the antenna, is defined as the angular error. The tracking radar attempts to position the antenna with zero angular error (i.e., to locate the target along the reference direction).

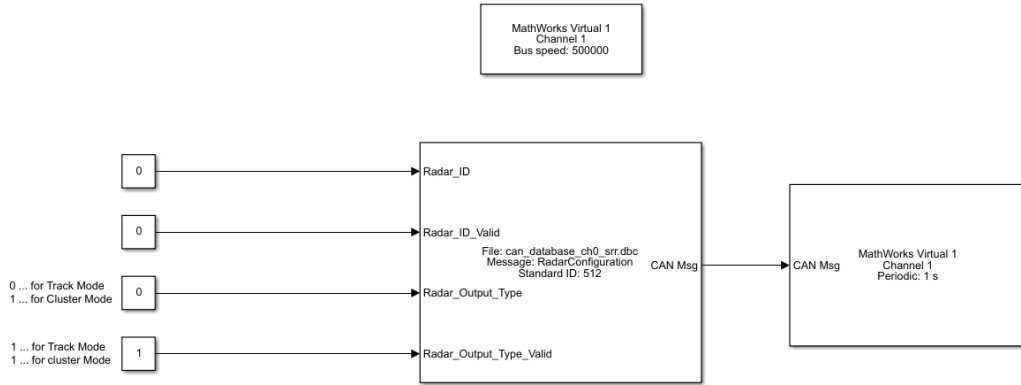


Fig. 46 – Radar configuration Simulink model

As we can see, in the input data we have two variables which are the two numbers below. To configure the radar in Track mode, a 0 must be set in the first input variable, and a 1 in the second. On the other hand, to configure the radar in Cluster mode, a 1 must be set in the first input variable, and a 1 also in the second one.

4.3.2 DISPLAY

TRACK MODE – DISPLAY DATA

You can find the file in the folder here:

DanielDiaz_FinalThesis\conti_radar_SRR\matlab2021b_SRR_Conti_CAN_Track

What is shown in Fig. 47 is the model created in Simulink for the live radar data display in Track Mode.

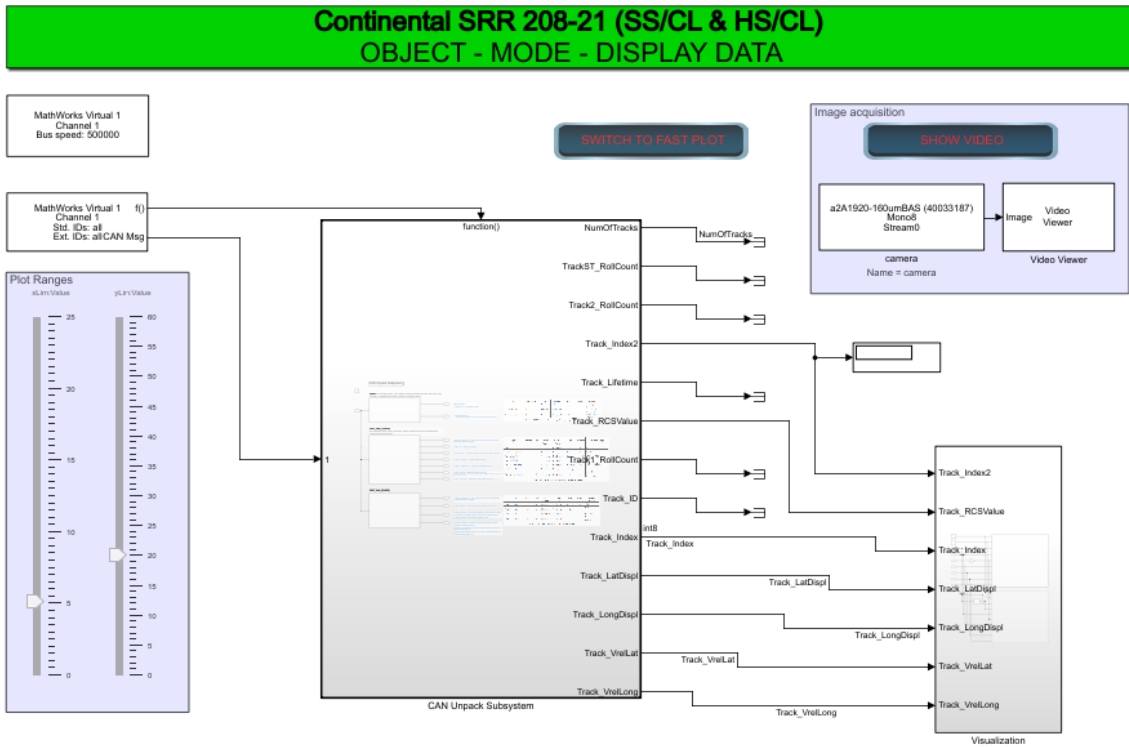


Fig. 47 – Track mode – Display Data Simulink model

For correct operation, we must change the input channels and choose the Vector CANcase XL channels.

Below these channels is the plot range, where we can modify the horizontal and vertical range of the display.

In the centre of the model is the CAN Unpack Subsystem block, which is responsible for unpacking a CAN message into signal data using the output parameters specified in each time step. The data is output as individual signals.

From this CAN block output variables form the display block, which represents the display of the data.

The square at the top of the model with Image Acquisition is used to activate or deactivate the radar support camera. In case of activation, the live camera image will appear in a different window than the data display.

Once everything is correct in the model, it is ready to be executed.

CLUSTER MODE – DISPLAY DATA

You can find the file in the folder here:

DanielDiaz_FinalThesis\conti_radar_SRR\matlab2021b_SRR_Conti_CAN_Cluster

What we can see in Fig. 48 in this case is the model created in Simulink for the visualisation of the live radar data in Cluster mode.

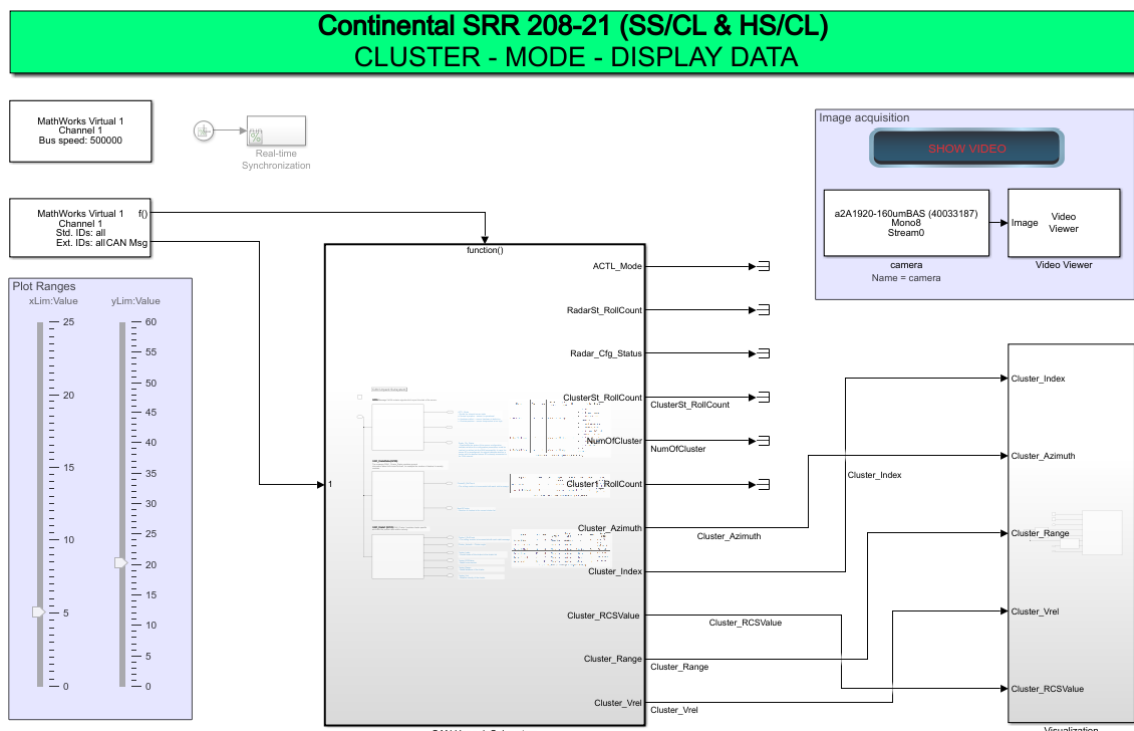


Fig. 48 – Cluster mode – Display Data Simulink model

We know that the operation of the radar in Cluster and Track mode is different. But as far as the Simulink model is concerned, its configuration is similar.

First of all, we have the input channels, which we must change and choose the Vector CANcase XL channels.

Below these channels is also the plotting range, where we can change the horizontal and vertical range of the display.

In the centre of the model is, as in Track mode, the CAN Unpack Subsystem block, which is responsible for unpacking a CAN message into signal data using the output parameters specified in each time step. The data are output as individual signals.

From this CAN block, different output variables are also generated, but they form the display block, which represents the visualisation of the data.

The square at the top of the model with Image Acquisition is used to activate or deactivate the radar support camera. In case of activation, the live camera image will appear in a different window than the data display.

Once everything is correct in the model, the model is ready to be run.

One thing to mention is that the development of the thesis has been carried out only with the radar in Track mode.

4.3.3 LOG

TRACK MODE – LOG DATA

You can find the file in the folder here:

DanielDiaz_FinalThesis\conti_radar_SRR\matlab2021b_SRR_Conti_CAN_log_to_ws

For data analysis we need to be able to save the data. For this purpose, Fig. 49 shows the Simulink model in Track mode for data logging.

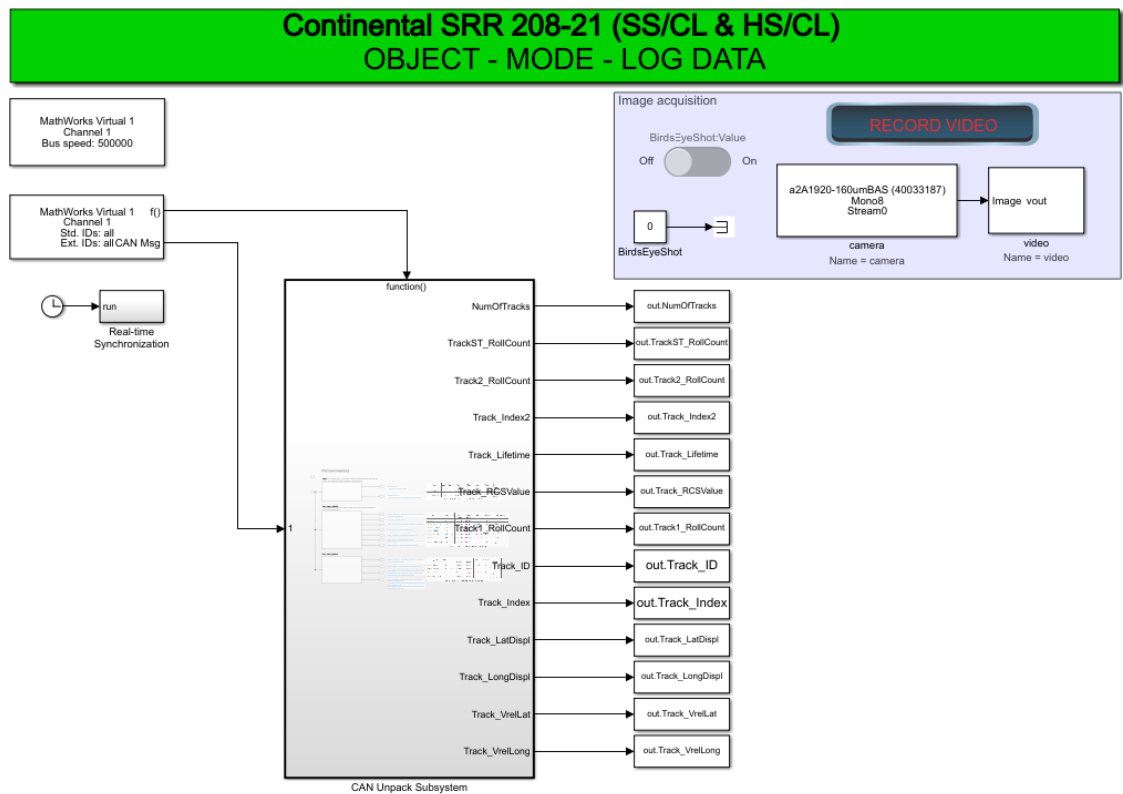


Fig. 49 – Track mode – Log Data Simulink model

First of all, we must also check that the input channels are both set to Vector CANcase XL.

Then, at the top right we see the Image Acquisition square in which we have the options of:

- ✓ “Record video” which, if activated, will take an image capture from the Basler camera.
- ✓ “BirdEyeShotValue” which, if activated, will take an image capture from the circuit's webcam.

As far as the rest of the model is concerned, the Unpack Subsystem works in a similar way to the rest by creating output variables. However, this logging model is able to save three possible variables in a folder (the destination folder can be modified by the user). The folder in this case is the following:

DanielDiaz_FinalThesis\conti_radar_SRR\records

The three possible variables that the model can store are:

- ✓ 2022-05-03_123331_SRR-IMG-BirdEye: when this variable is imported into MATLAB it appears as **img**. The variable **img** corresponds to the image capture from the webcam.

- ✓ 2022-05-03_123356_SRR-Data: when this variable is imported into MATLAB it appears as **in**. The **in** variable corresponds to the data obtained by the radar, i.e., the detections.
- ✓ 2022-05-03-03_123356_SRR-Video: when this variable is imported into MATLAB it appears as **vout**. The **vout** variable corresponds to the image capture from the Basler camera.

Furthermore, as we can see, the log model stores the variables in the following way:

year-month-day_hourminutessecond_SRR-variablename

The date and time are the time at which the model is run, SRR is the name of the radar (Short Range Radar) and the last name corresponds to the saved variable, either IMG-BirdEye, Data or Video (img, in and vout respectively).

CLUSTER MODE – LOG DATA

(See Appendix).

4.3.4 REPLAY

TRACK MODE – REPLAY DATA

You can find the file in the folder here:

DanielDiaz_FinalThesis\conti_radar_SRR\ matlab2021b_SRR_Conti_CAN_Track_Replay

Once we have the display and data log models, we create the data replay model in order to simulate what would be a live radar display but with stored data. The data replay model can be seen in Fig. 50.

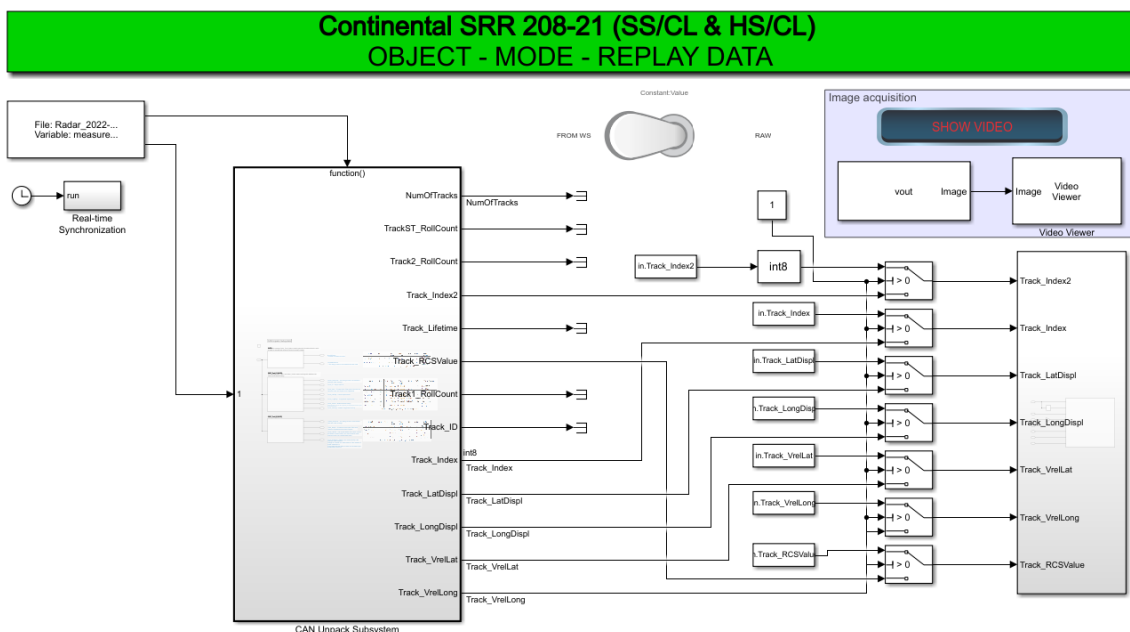


Fig. 50 – Track mode – Replay Data Simulink model

To execute the replay model, we must load an input variable, which in this case corresponds to the variable in, which refers to the data.

On the other hand, in the Image Acquisition square, if we want to reload the video or the image of the Basler camera from the moment in which the data of the input variable in was obtained, we have to load in the input variable the variable vout, it is important to take into account that it corresponds to the variable that goes hand in hand with the variable in.

Also, it is important to note that the data to be loaded into the input variables must be stored data from a Track mode model. If we enter input variables that are data stored by a Cluster mode model into the replay model in Track mode, logically, we will have to load the input variables from a Cluster mode model.

Once the input variables are already entered, we can execute and we will see the radar data display during the log time with which the model has been executed.

CLUSTER MODE – REPLAY DATA

(See Appendix).

4.4 MATLAB SCRIPTS

In this section, the different Matlab scripts created during the development of the thesis and some of their evolution will be shown.

These scripts can be found in the folder at the following path:

DanielDiaz_FinalThesis\conti_radar_SRR\scripts

4.4.1 CAMERA VIDEO

This script can be found in the folder with the following path:

DanielDiaz_FinalThesis\conti_radar_SRR\scripts\fx_createVideo

The following script is used to record a video with the Basler camera of the size that we want, depending on the variables that we enter. The script description is coloured green on the second and third lines.

```
function fx_createVideo(imgAry, fps)
% Creates a .avi-Video file from all images within the array imgAry.
% The speed of the video will be in the fps-size of the input

sz = size(imgAry);
writerObj = VideoWriter('myVideo.avi');
writerObj.FrameRate = fps;
open(writerObj);
for u=1:sz(end)
    writeVideo(writerObj, imgAry(:,:,u));
end
close(writerObj);
end
```

4.4.2 TESTFIELD WEBCAM

This script can be found in the folder with the following path:

DanielDiaz_FinalThesis\conti_radar_SRR\scripts\webcam_testarea

The following script displays the live webcam image of the HTW Mechlab circuit when executed (see Fig. 51). The description of the scripts is green, it corresponds to the first two lines.

```
% here you see a little test script
% for testing the connection to the ipcam at the test area of HTW

cam = ipcam('rtsp://141.56.12.38:554/s0','mechlab','mechlab');
preview(cam);
pause(30);
closepreview;
clear cam;
```

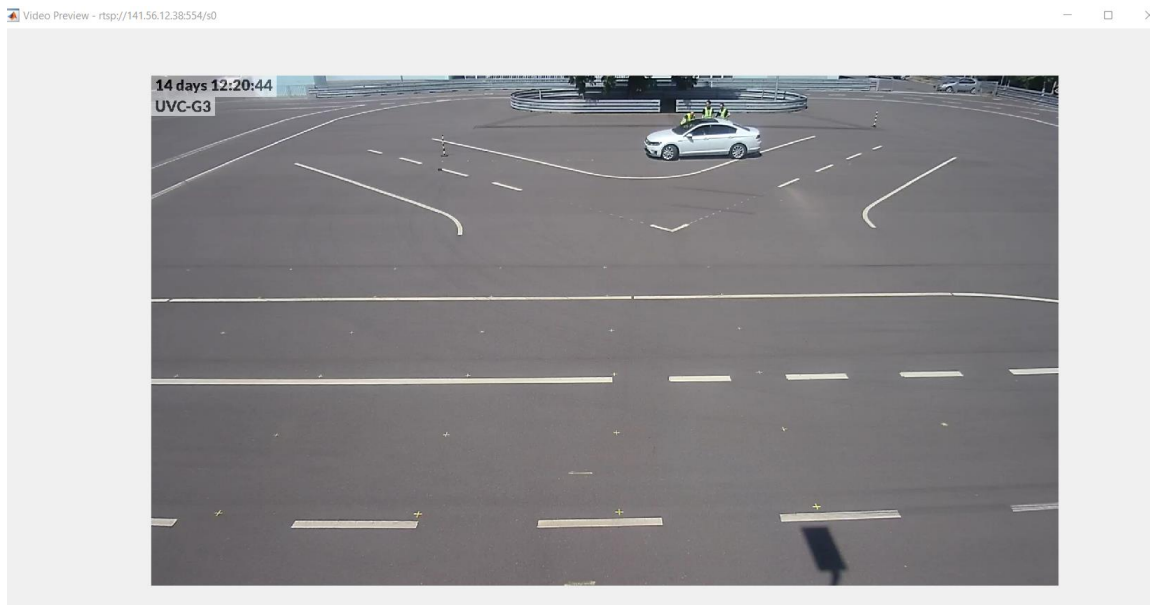


Fig. 51 - Live webcam image of the HTW Mechlab circuit

4.4.3 RESULTS DISPLAY

In this section, the different scripts created for the display of results will be shown, that is, the detections, and the evolution of these scripts can also be appreciated.

First way to display results

The first way to display the results were a few command lines, which we can see below:

```
hfig = figure(); hax1 = axes(hfig,'Position', ...
    [.1 .1 .3 .8], 'xlim', [-5 5], 'ylim', ...
    [0 20]); hax2 = axes(hfig, 'Position', ...
    [.5 .5 .5 .5]); hax3 = axes(hfig, 'Position', ...
    [.5 0 .5 .5]); line(hax1, -in.Track_LatDispl.Data, ...
    in.Track_LongDispl.Data, 'LineStyle', 'none', 'Marker', ...
    '*'); grid(hax1, 'on'); imshow(img, 'Parent', ...
    hax2); imshow(vout(:,:,1), 'Parent', hax3);
```

What these command lines show is the following:

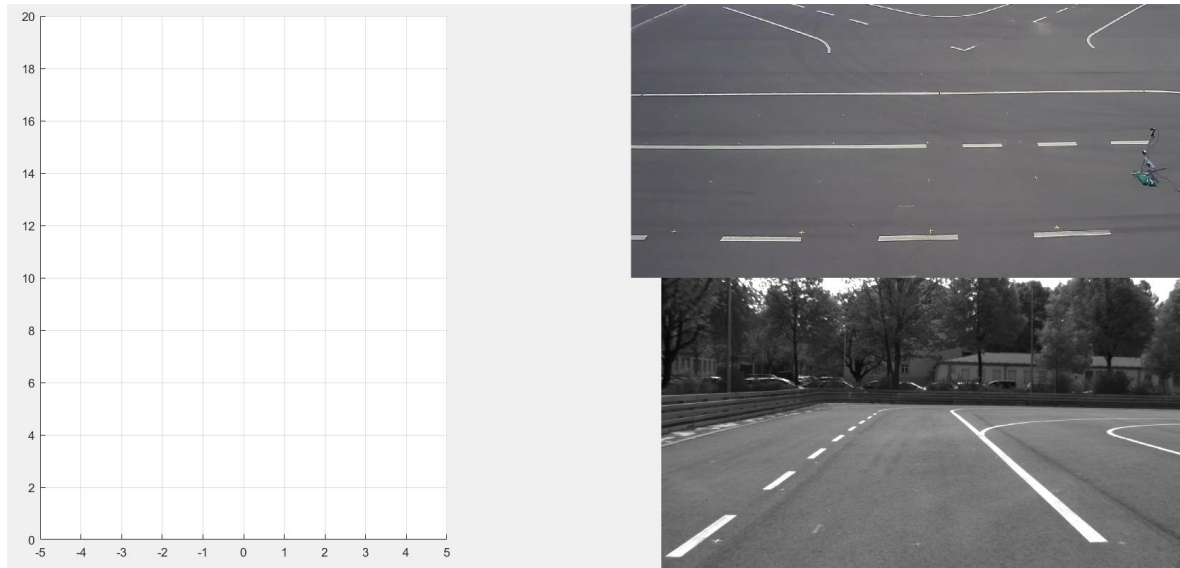


Fig. 52 - First way to display results through some command lines

This way of displaying the results was created for quick familiarization with the radar. Once we became familiar with the radar, we began to create functions more developed than these command lines.

First function for the results display

This script can be found in the folder with the following path:

DanielDiaz_FinalThesis\conti_radar_SRR\scripts\fx_evalResults

This function was the first for the results display. As we can see, the function is well structured, the command blocks have a title to know what they refer to.

In the first command block (INIT) the separation of X and Y between points is described, in addition to the horizontal and vertical display limits.

In the following command block (FIGURE) the grids for the display of the image of the Basler camera and the webcam are created (see Fig. 53).

In the last command block (PLOT) the background grid is created (which simulates the grid painted on the circuit, see Fig. 29). Next, the detections and rcs are marked, respectively, in the background grid. Finally, the legend of the background grid and of the different grids is created.

```
function fx_evalResults(in,img,vout)
%FX_EVALRESULTS

%% INIT
xSep = 1.6; % [m]
ySep = 2.5; % [m]
xlim = [-3*xSep,5*xSep];
ylim = [0 ,9*ySep];

%% FIGURE
% check existing plot window
h = findobj('Tag','SRR_Results_plot');
```

```

if ishandle(h)
    close(h)
end
% create new plot window
hfig = figure('Color',[1 1 1],'Tag','SRR_Results_plot');
hpanel1 = uipanel(hfig,'Position',[.01 .01 .48 .98],...
    'Title','Measurement Plot', ...
    'BackgroundColor',[1 1 1]);
hax1 = axes(hpanel1,'Position',[.1 .1 .8 .8],...
    'xlim',xlim,'ylim',ylim, ...
    'XTick',(min(xlim):xSep:max(xlim)), ...
    'YTick',(min(ylim):ySep:max(ylim)));
hold(hax1,"on")
hpanel2 = uipanel(hfig,'Position',[.51 .51 .48 .48],...
    'Title','sky cam',...
    'BackgroundColor',[1 1 1]);
hax2 = axes(hpanel2,'Position',[.01 .01 .98 .98]);
hold(hax2,'on');
hpanel3 = uipanel(hfig,'Position',[.51 .01 .48 .48],...
    'Title','basler cam',...
    'BackgroundColor',[1 1 1]);
hax3 = axes(hpanel3,'Position',[.01 .01 .98 .98]);
hold(hax3,'on');

% create Coordinates Array of position grid
cols = 8; % grid number of x-direction
rows = 10; % grid number of y-direction
M = zeros(cols*rows,2);
i = 1;
for n = -(3*xSep):xSep:((cols-3)*xSep)
    for m = 0:ySep:(rows*ySep)
        M(i,1) = n;
        M(i,2) = m;
        i = i + 1;
    end
end

%% PLOT
% background grid
line(hax1,M(:,1),M(:,2),'LineStyle','none','Marker','+','Color',[.5 0
1]);

% detections
line(hax1,-in.Track_LatDispl.Data,
in.Track_LongDispl.Data,'LineStyle', ...
    'none','Marker','*','Color',[0 0 .5]);

% rcs
for i = 1:length(in.Track_RCSValue.Data)
    line(hax1,-in.Track_LatDispl.Data(i),in.Track_LongDispl.Data(i),
    ...
    'marker','o','MarkerSize',(in.Track_RCSValue.Data(i)+51),'Color','c');
end

xlabel(hax1,'lateral displacement [m]');
ylabel(hax1,'longitudinal displacement [m]');

```



```

legend(hax1,'measurement grid','detection','rcs
intensity','Location','northoutside');
grid(hax1,'on');
imshow(img,'Parent',hax2);
imshow(vout(:,:,1),'Parent',hax3);
end

```

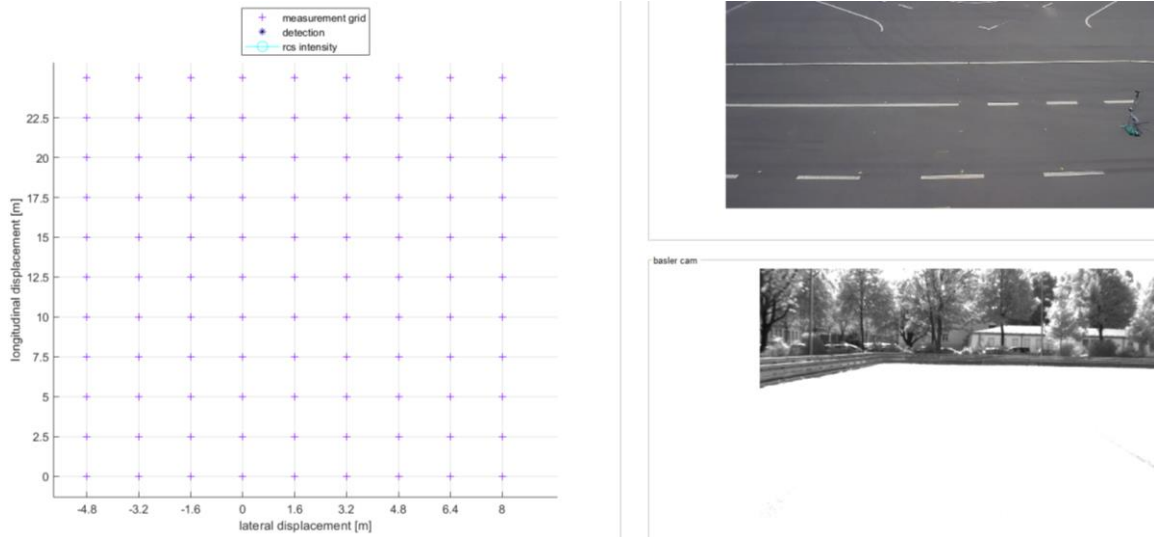


Fig. 53 - Display of the function without detections

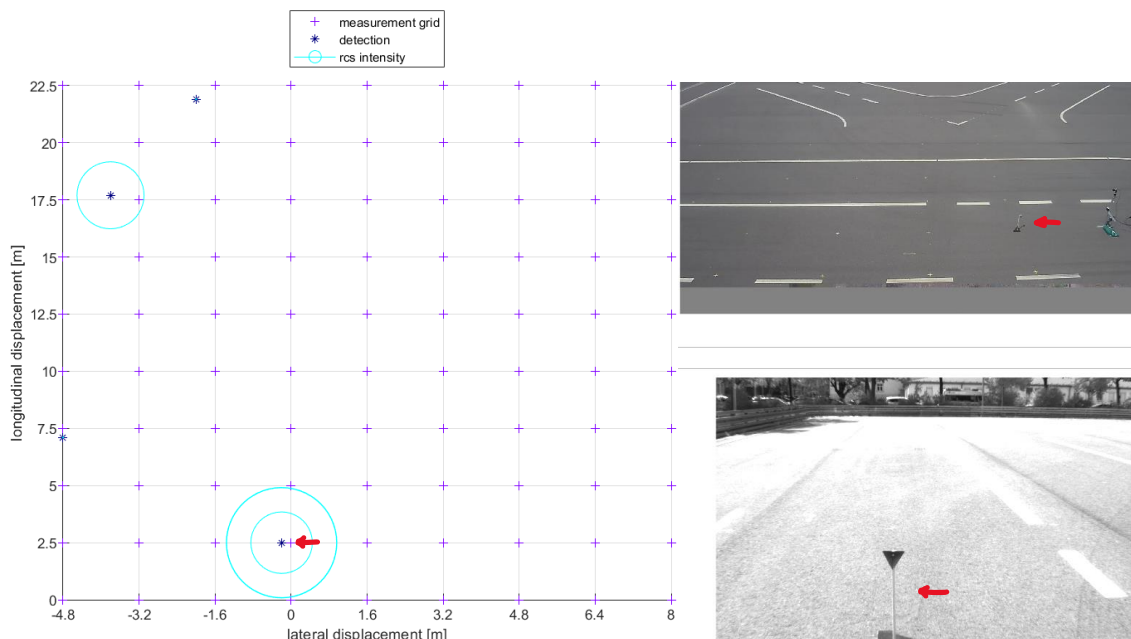


Fig. 54 - Display of the function with detections

Cluster mode function for the results display

(See Appendix).

Final function for the results display

This script can be found in the folder with the following path:

DanielDiaz_FinalThesis\conti_radar_SRR\scripts\fx_evalResults_polygon

In the final function for the results display I wanted to implement it as shown below:

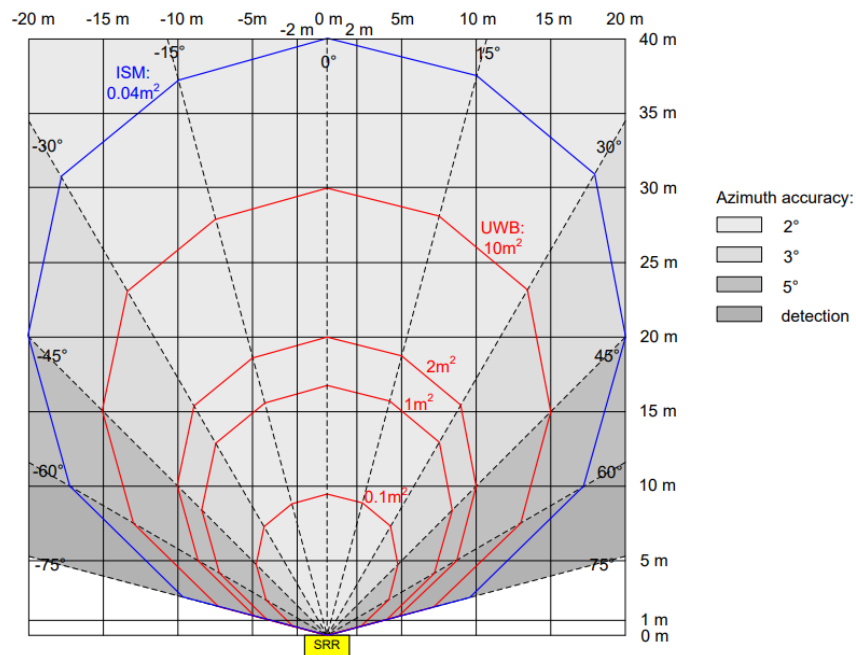


Fig. 55 - Field of View from SRR 20X with ISM band

The radar has an F.o.V. (field of view) of up to $\pm 75^\circ$ at medium distances. The intervals between the lines marking the angles correspond to an azimuth accuracy. Between 75° and 60° degrees we have a detection zone. Between 60° and 45° we have a zone with 5° of azimuth accuracy. Between 45° and 30° the zone has 3° of azimuth accuracy. Finally, between 30° and 0° the zone has 2° of azimuth precision.

On the other hand, we have the polygons. The blue polygon corresponds to an area of 0.04 m^2 of ISM band. The four red polygons correspond to UWB zones of 10 m^2 , 2 m^2 , 1 m^2 and 0.01 m^2 , respectively.

Ultra-wideband (UWB) is a radio-based communication technology for short-range use and fast and stable transmission of data. Thanks to its unrivalled precision, transmission speed, and reliability, UWB is often the technology of choice for indoor localization of moving assets in complex and space-sensitive environments.

The implementation of this function can be seen in the PLOT command block of the script, specifically in %ISM polygons, %lines and, in addition, new legends have been created as can be seen in %label & legend.

Below we will show the implementations of the new function, to see the whole function, see Appendix or file in the folder.

```
function fx_evalResults_polygon(in,img,vout)

.....

% detections
line(hax1,-in.Track_LatDispl.Data,
in.Track_LongDispl.Data,'LineStyle','none','Marker','*','Color',[0 0
.5]);

%rcs
for i = 1:length(in.Track_RCSValue.Data)
    line(hax1,-in.Track_LatDispl.Data(i),in.Track_LongDispl.Data(i),
    ...

'marker','o','MarkerSize',(in.Track_RCSValue.Data(i)+51),'Color','c');
end

% ISM polygons
pts1 = [0 0 0;9.8 2.626 0;17.321 10 0;20 20 0;17.84 30.9 0;10 37.321
0;0 40 0; ...
-10 37.321 0;-17.84 30.9 0;-20 20 0;-17.321 10 0;-9.8 2.626 0];
p1 = antenna.Polygon('Vertices', ...
pts1);
plot(p1,"Parent",hax1,'Color','b');

pts2 = pts1*0.75;
p2 = antenna.Polygon('Vertices', ...
pts2);
plot(p2,"Parent",hax1,'Color','r');

pts3 = pts1*0.5;
p3 = antenna.Polygon('Vertices', ...
pts3);
plot(p3,"Parent",hax1,'Color','r');

pts4 = pts1*0.422;
p4 = antenna.Polygon('Vertices', ...
pts4);
plot(p4,"Parent",hax1,'Color','r');

pts5 = pts1*0.2375;
p5 = antenna.Polygon('Vertices', ...
pts5);
plot(p5,"Parent",hax1,'Color','r');

% lines
deg = [15];
x = 0:1:25;
y = (sind(deg)/cosd(deg))*x;
plot(hax1,x,y,'LineStyle','--','Color','k');
hold on;
deg = [30];
x = 0:1:25;
y = (sind(deg)/cosd(deg))*x;
plot(hax1,x,y,'LineStyle','--','Color','k');
hold on;
deg = [45];
x = 0:1:25;
y = (sind(deg)/cosd(deg))*x;
```

```

plot(hax1,x,y,'LineStyle','--','Color','k');
hold on;
deg = [60];
x = 0:1:25;
y = (sind(deg)/cosd(deg))*x;
plot(hax1,x,y,'LineStyle','--','Color','k')
hold on;
deg = [75];
x = 0:1:15;
y = (sind(deg)/cosd(deg))*x;
plot(hax1,x,y,'LineStyle','--','Color','k')
hold on;

x = [0 0];
y = [0 56];
plot(hax1,x,y,'LineStyle','--','Color','k')
hold on;

deg = [15];
x = 0:1:56;
y = -(sind(deg)/cosd(deg))*x;
plot(hax1,y,x,'LineStyle','--','Color','k');
hold on;
deg = [30];
x = 0:1:43.3;
y = -(sind(deg)/cosd(deg))*x;
plot(hax1,y,x,'LineStyle','--','Color','k');
hold on;
deg = [45];
x = 0:1:25;
y = -(sind(deg)/cosd(deg))*x;
plot(hax1,y,x,'LineStyle','--','Color','k');
hold on;
deg = [60];
x = 0:1:14.44;
y = -(sind(deg)/cosd(deg))*x;
plot(hax1,y,x,'LineStyle','--','Color','k')
hold on
deg = [75];
x = 0:1:6.7;
y = -(sind(deg)/cosd(deg))*x;
plot(hax1,y,x,'LineStyle','--','Color','k')
hold on

% label & legend
xlabel(hax1,'lateral displacement [m]');
ylabel(hax1,'longitudinal displacement [m]');
legend(hax1,'measurement grid','detection','rcs
intensity','Location','northoutside');
text(hax1,0,9.5,"0.1 m^2","Color','r');
text(hax1,0,16.88,"1 m^2","Color','r');
text(hax1,0,20,"2 m^2","Color','r');
text(hax1,0,30,"UWB: 10 m^2","Color','r');
text(hax1,0,40,"ISM: 0.04 m^2","Color','b');
text(hax1,12,4,"75°","Color','k');
text(hax1,-12,4,"75°","Color','k');
text(hax1,18,11,"60°","Color','k');
text(hax1,-18,11,"60°","Color','k');

```

```

text(hax1,21,22,"45°","Color','k');
text(hax1,-21,22,"45°","Color','k');
text(hax1,18,33,"30°","Color','k');
text(hax1,-18,32,"30°","Color','k');
text(hax1,10,40,"15°","Color','k');
text(hax1,-10,40,"15°","Color','k');
text(hax1,0.5,41,"0°","Color','k');
grid(hax1,'on');
imshow(img,'Parent',hax2);
imshow(vout(:,:,1),'Parent',hax3);

```

end

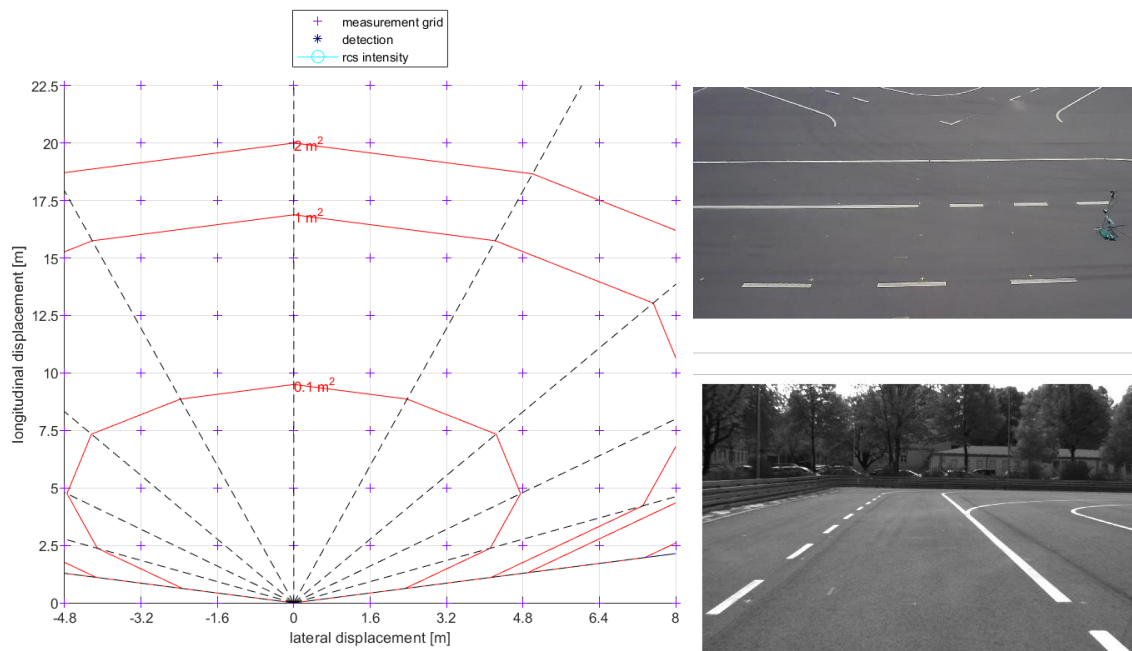


Fig. 56 - Display of the final function without detections

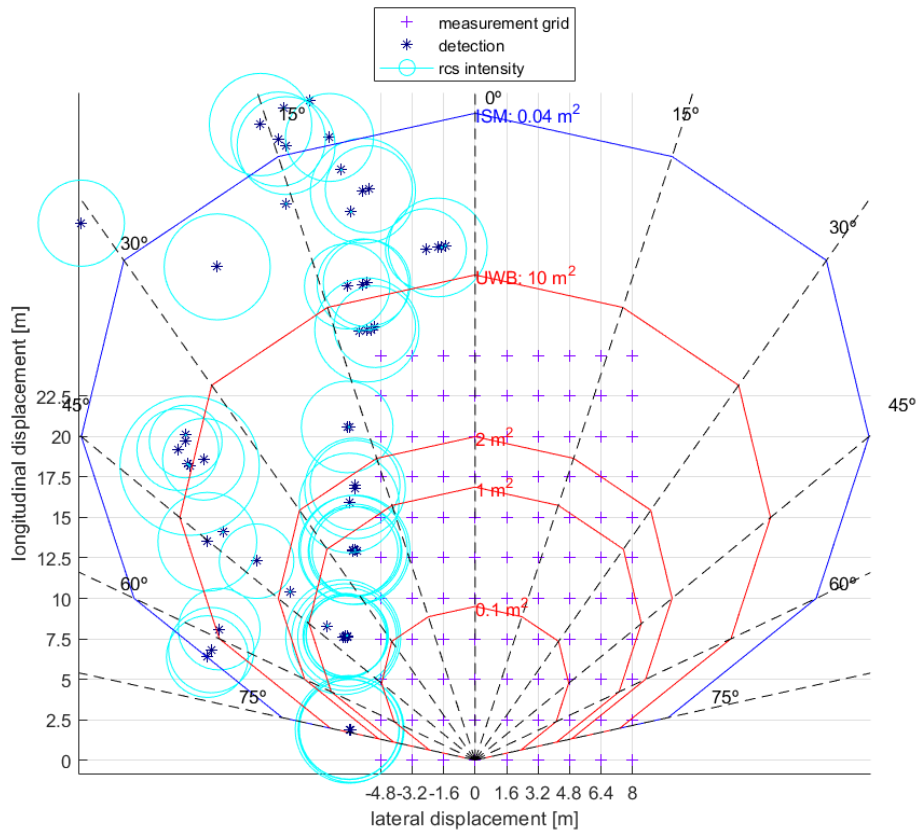


Fig. 57 – Overview of the display of the final function with detections

Once we have the final results display function, we can start with the measurements.

5 STUDY CASES

In this section we will look at the different case studies and the different measurements carried out on the test track.

5.1 FAMILIARIZATION

The measurements in this section can be found in the folder at the following path:

DanielDiaz_FinalThesis\conti_radar_SRR\records\2022-04-19_FamiliarizationMeasurements

Before starting with the useful measurements, we had to familiarise ourselves with the radar, how it works, the Simulink models, how to make a display, how to make a data log, in short how to make the whole setup work correctly.

For this we took a series of measurements of which we were seeing the display of results with the first way of displaying results that we created (see section 4.4.3).

STATIC MEASUREMENTS WITH A TRIPLE MIRROR

The object used for the first familiarisation measures was a triple mirror.



Fig. 58 – Triple Mirror being detected on the grid

The triple mirror is an ideal object to be detected by radar, as it reflects all the signals hitting it in the same direction towards the same point, like a concave mirror.

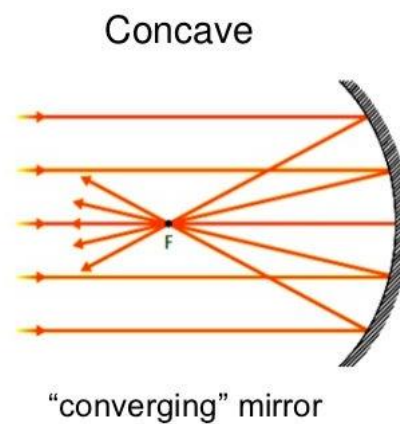


Fig. 59 – Reflections of electromagnetic waves impacting a concave mirror

The following images show a few tests carried out for the detection of the triple mirror with radar. In the graphics we could already start to see some reflections, which will be discussed later.

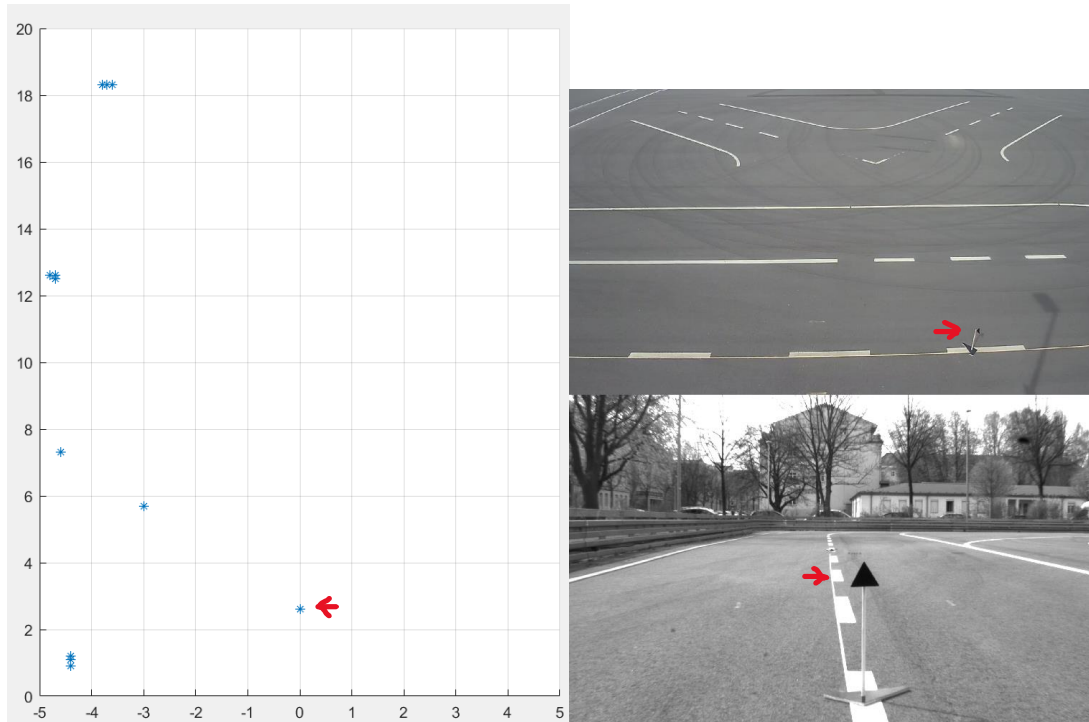


Fig. 60 – Triple mirror detected in X-Y (0, 2.5) m position of the grid

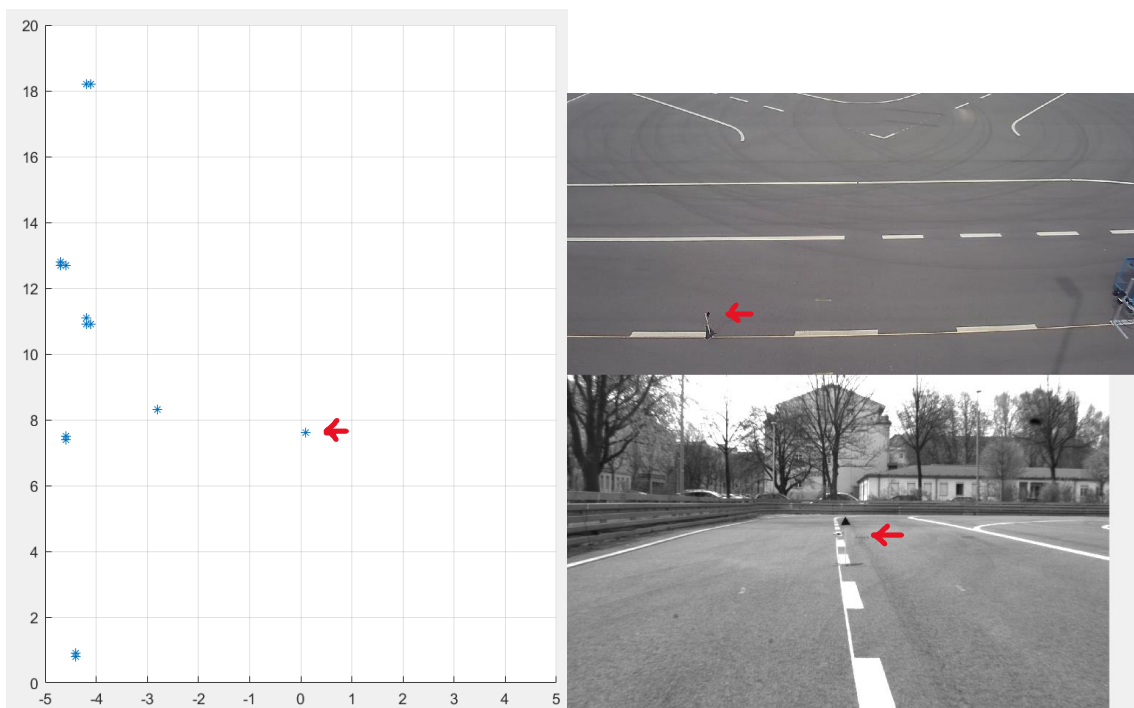


Fig. 61 – Triple mirror detected in X-Y (0, 7.5) m position of the grid

To see more familiarization with static measurements, see Appendix.

DYNAMIC TESTING WITH A BIKE

For a good familiarisation with the radar, it was also important to make some dynamic measurements, to see what the radar sees, how it detects and to learn how to save a dynamic measurement. The object for these dynamic measurements is a bike.

The first measurement with the bicycle describes a vertical trajectory on the $x=0$ m axis in the direction of the radar as follows. Also, this measurement can be found in the folder at the following path:

DanielDiaz_FinalThesis\conti_radar_SRR\records\2022-04-19_FamiliarizationMeasurements\SRR-Data_2022-04-19_123556_BikeStraightFwd

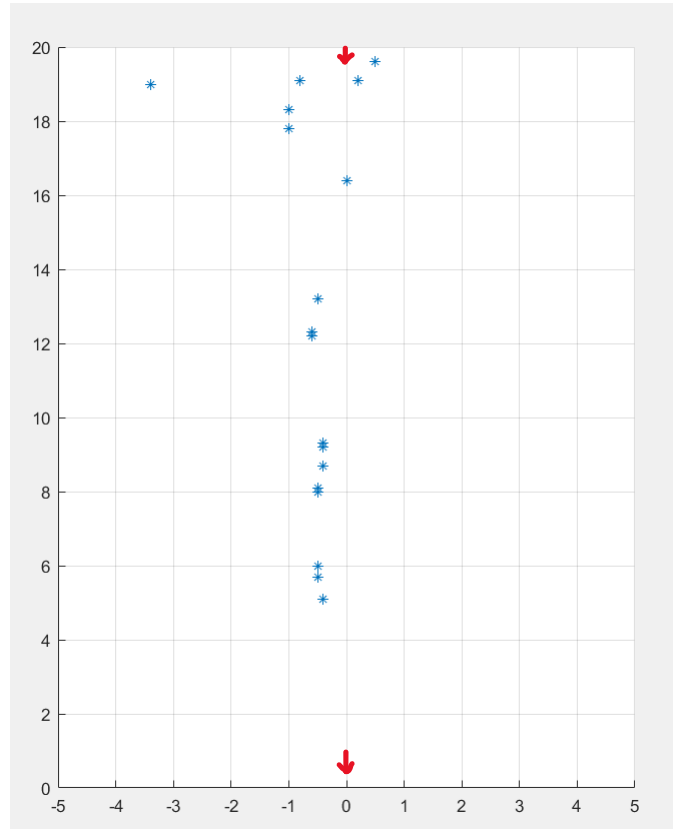


Fig. 62 - Bike describing a vertical path on the $x = 0$ m axis in the direction of the radar

To see more familiarization with dynamic measurements, see Appendix.

It should be emphasised that these measures were carried out for the sole purpose of familiarisation with the radar and setup, and have no value or purpose other than that.

5.2 STATIC MEASUREMENTS

Once you are familiar with the radar and the setup, and have developed a final function for displaying the results, you can start with the measurements.

The first measurements of the work are static measurements, for this we will place each object to be detected in all the positions of the grid, in order to be able to compare and analyse the results between the different objects.

The objects used for these measurements are a triple mirror, a pedestrian and finally a dummy.

The static measurements of the work can be found in the folder at the following path:

DanielDiaz_FinalThesis\conti_radar_SRR\records\StaticMeasurements

5.2.1 TRIPLE MIRROR

All the static measurements of the triple mirror can be found in the folder at the following path:

DanielDiaz_FinalThesis\conti_radar_SRR\records\StaticMeasurements\2022-05-23_TripleMirror

You can see a screenshot of all the static measurements at each grid position (see Fig. 28) with the triple mirror in the Appendix.

5.2.2 PEDESTRIAN

All the static measurements of the pedestrian can be found in the folder at the following path:

DanielDiaz_FinalThesis\conti_radar_SRR\records\StaticMeasurements\2022-05-03_StaticMeasurements_Pedestrian

You can see a screenshot of all the static measurements at each grid position (see Fig. 28) with the pedestrian in the Appendix.

5.2.3 DUMMY

All the static measurements of the dummy can be found in the folder at the following path:

DanielDiaz_FinalThesis\conti_radar_SRR\records\StaticMeasurements\2022-05-26_Dummy_Static

You can see a screenshot of all the static measurements at each grid position (see Fig. 28) with the dummy in the Appendix.

5.3 DYNAMIC MEASUREMENTS

The dynamic measurements of the work can be found in the folder at the following path:

DanielDiaz_FinalThesis\conti_radar_SRR\records\DynamicMeasurements

In this section, dynamic measurements will be carried out with 2 targets: a pedestrian and a bike.

The trajectories of the objects on the grid are described in the following image:

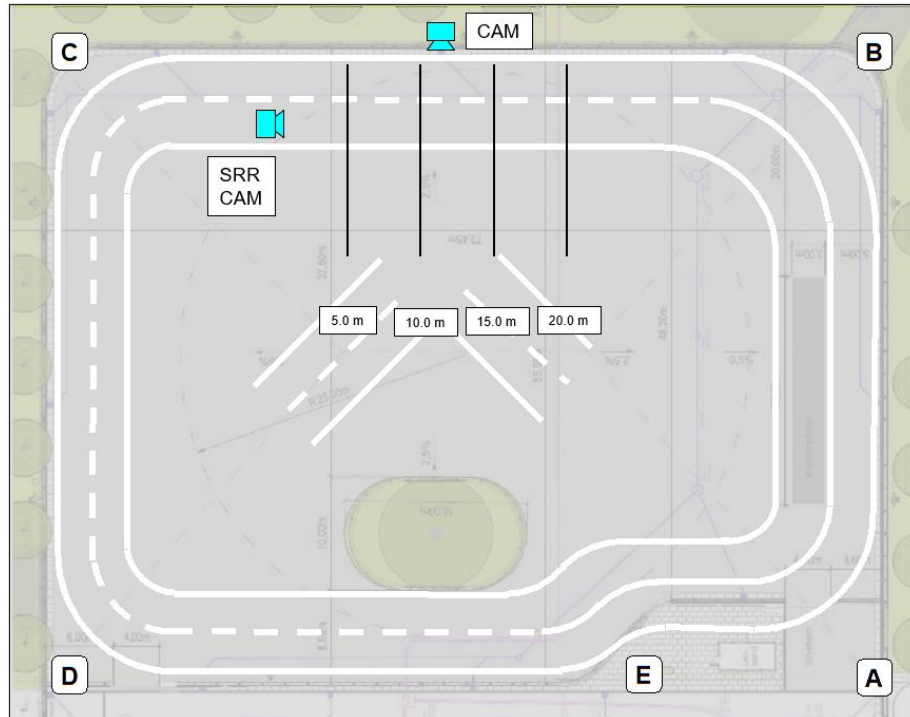


Fig. 63 - Grid trajectories of objects in dynamic measurements

Objects shall describe paths perpendicular to the radar at distances of 5, 10, 15 and 20 m, starting from the side of the guardrail.

5.3.1 PEDESTRIAN

All the dynamic measurements of the pedestrian can be found in the folder at the following path:

DanielDiaz_FinalThesis\conti_radar_SRR\records\DynamicMeasurements\Pedestrian

You can see a screenshot of all the dynamic measurements of each trajectory at the different set radar distances (see Fig. 63) with the pedestrian in the Appendix.

5.3.2 BICYCLE

All the dynamic measurements of the bike can be found in the folder at the following path:

DanielDiaz_FinalThesis\conti_radar_SRR\records\DynamicMeasurements\Bike

You can see a screenshot of all the dynamic measurements of each trajectory at the different set radar distances (see Fig. 63) with the bike in the Appendix.

5.3.3 EXTRA MEASUREMENTS

All the dynamic extra measurements can be found in the folder at the following path:

DanielDiaz_FinalThesis\conti_radar_SRR\records\DynamicMeasurements\ExtraMeasurements

All these extra measures have been carried out with cycling as a target. These measurements are about trajectories parallel to the radar and changes of trajectory in the middle of the trajectory.

You can see a screenshot of all the extra dynamic measurements with the bike in the Appendix.

6 ANALYSIS OF MEASUREMENTS AND RESULTS

In this section, an analysis of the measures will be carried out and conclusions will be drawn.

6.1 STATIC MEASUREMENTS

6.1.1 REFLECTIONS PROBLEMS

First of all, it should be noted that all measurements show the reflections of the guardrail, as it is a metal object of considerable size and highly reflective. When objects are placed close to the guardrail, on the x-axis = -4.8 m, many reflections are generated around the object and the guardrail as the signal bounces between them. This means that on the x-axis = -4.8 m of the grid the object is not detected accurately and many times it is detected out of accuracy (independently of its material) or we are simply not able to be able to position the object only by looking at the result display, without the help of external cameras.

Also, during the review of the measurement results I noticed that there was a reflection that was repeated in many measurements. This reflection always appeared around the X-Y (6.4, 2.5) m point.

The reflection appears in the following positions X-Y:

TRIPLE MIRROR: (7 / 56 measurements)

- ✓ (4.8, 2.5) m – (see Fig. 17 in Appendix)
- ✓ (-3.2, 5) m - (see Fig. 19 in Appendix)
- ✓ (0, 5) m - (see Fig. 21 in Appendix)
- ✓ (4.8, 5) m - (see Fig. 24 in Appendix)
- ✓ (1.6, 7.5) m - (see Fig. 29 in Appendix)
- ✓ (0, 10) m - (see Fig. 35 in Appendix)
- ✓ (1.6, 10) m - (see Fig. 36 in Appendix)

PEDESTRIAN: (36 / 56 measurements)

- ✓ From (-4.8,2.5) m – (see Fig. 68 in Appendix) to (-4.8, 5) m - (see Fig. 75 in Appendix)
- ✓ (-1.6, 5) m - (see Fig. 77 in Appendix)
- ✓ From (-3.2, 7.5) m - (see Fig. 83 in Appendix) to (4.8, 15) m - (see Fig. 109 in Appendix)

DUMMY: (0 / 56 measurements)

- It does not appear in any measure.

This allows us to draw some conclusions and/or hypotheses.

Firstly, we have the dummy that does not show this common reflection. It is an object that produces very few reflections. This is because it is made of a plastic material that is very poorly conductive and, therefore, is a minimally reflective material. We can also observe that its detections show a not very strong signal and this is due to the fact that the material absorbs part of the received signal and the return signal is weaker than the incoming signal. The RCS intensity is similar to that of the Triple Mirror, being a much bigger object. Sometimes, the RCS intensity is so weak that the dummy is not detected by the radar at some grid positions, e.g. (1.6, 2.5) m - Fig. 128, (3.2, 2.5) m - Fig. 129, (4.8, 2.5) m - Fig. 130, (-4.8, 7.5) m - Fig. 138.

The triple mirror produces very few reflections despite being made of a highly reflective metallic material, this is due to its shape, explained above (see Fig. 59). In the measurements of this object, the common reflection appears in 7 out of 56 measurements, i.e., 12.5%.

On the other hand, the pedestrian is the object that produces the most reflections. In the measurements, the common reflection appears in 36 out of 56 measurements, i.e. 64.28%. This may be because a pedestrian can carry highly reflective metallic objects such as a watch, a mobile phone, etc., also a pedestrian has many rounded shapes, remembering that round shapes are the most reflective. It is also worth noting that on the day of the measurements with the pedestrian the trolley was moved to the right (see Fig. 68 in Appendix) because the Wi-Fi signal that day was very weak and we wanted to gain a few metres to minimally boost the signal. This change of position of the trolley could create an interference in the radar signal and intervene in the production of that signal.

To test whether the change of position of the trolley created interference in the radar detection zone and affected the production of this reflection, we made a series of measurements to test this hypothesis. Of these measurements only the relevant ones will be shown, i.e. the ones where the reflection appears, to see all measurements, see Appendix.

Default position of the trolley and no object in the grid:

These measurements can be found in the folder at the following path:

DanielDiaz_FinalThesis\conti_radar_SRR\records\StaticMeasurements\2022-06-02_CommonReflectionTests

Positioning the trolley in its default position and without any objects on the rack, the radar shows no reflection in the whole grid and no common reflection is shown, only some ghost objects are shown.

Triple mirror position on the grid X-Y: (-3.2, 5) m

With the Triple mirror placed in this position, we also see that no reflection is shown in the whole grid and no common reflection is shown, only some ghost objects are shown.

Triple mirror position on the grid X-Y: (0, 5) m

With the Triple mirror placed in this position, we also see that no reflection is shown in the whole grid and no common reflection is shown, only some ghost objects are shown.

Triple mirror position on the grid X-Y: (3.2, 5) m

With the Triple mirror placed in this position, we also see that no reflection is shown in the whole grid and no common reflection is shown, only some ghost objects are shown.

Pedestrian position on the grid X-Y: (-3.2, 5) m

With the pedestrian placed in that position, we see that some reflection is shown in the grid and some ghost objects, but no common reflection is shown.

Pedestrian position on the grid X-Y: (0, 5) m

With the pedestrian placed in that position, we see that some reflection is shown in the grid and some ghost objects, but no common reflection is shown.

Pedestrian position on the grid X-Y: (3.2, 5) m

With the pedestrian placed in that position, we see that some reflection is shown in the grid and some ghost objects, but no common reflection is shown.

Once this series of measurements has been made, we can say that the common reflection does not depend on the object or its position, since with the trolley in its default position this reflection has not appeared in any of the measurements.

The following is to carry out the same measurements changing the position of the trolley, displaced 5 meters to the right (as in the static measurements of the pedestrian) in order to check if it is the position of the trolley that has a direct influence on the generation of the reflection.

TROLLEY POSITION SHIFTED 5 M TO THE RIGHT

No object in the grid:

In this case, no reflection is shown in the entire grid, nor does the common reflection appear, only some ghost objects.

Triple mirror position on the grid X-Y: (-3.2, 5) m

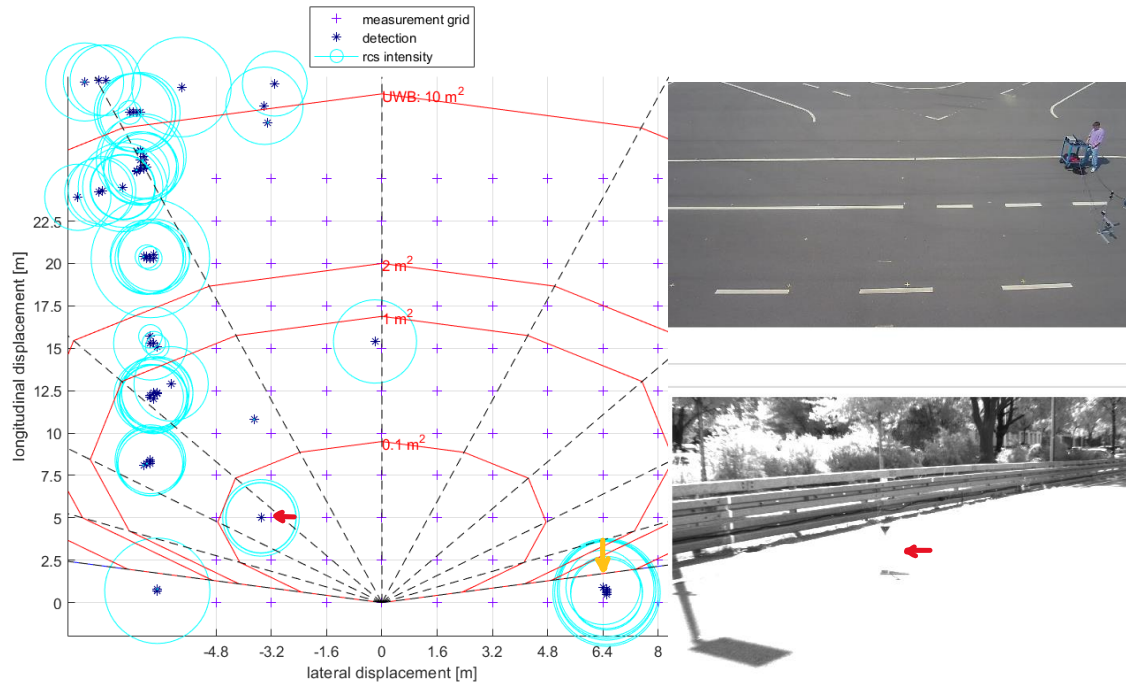


Fig. 64 – Trolley position shifted 5 m right and Triple mirror position on the grid X-Y (-3.2, 5) m

In this case, with the Triple mirror in that position on the grid and the trolley moved 5 meters to the right, the common reflection appears, and it's marked with a yellow arrow in Fig. X.

Triple mirror position on the grid X-Y: (0, 5) m

In this case, with the Triple mirror in that position on the grid and the trolley moved 5 meters to the right, the common reflection does not appear.

Triple mirror position on the grid X-Y: (3.2, 5) m

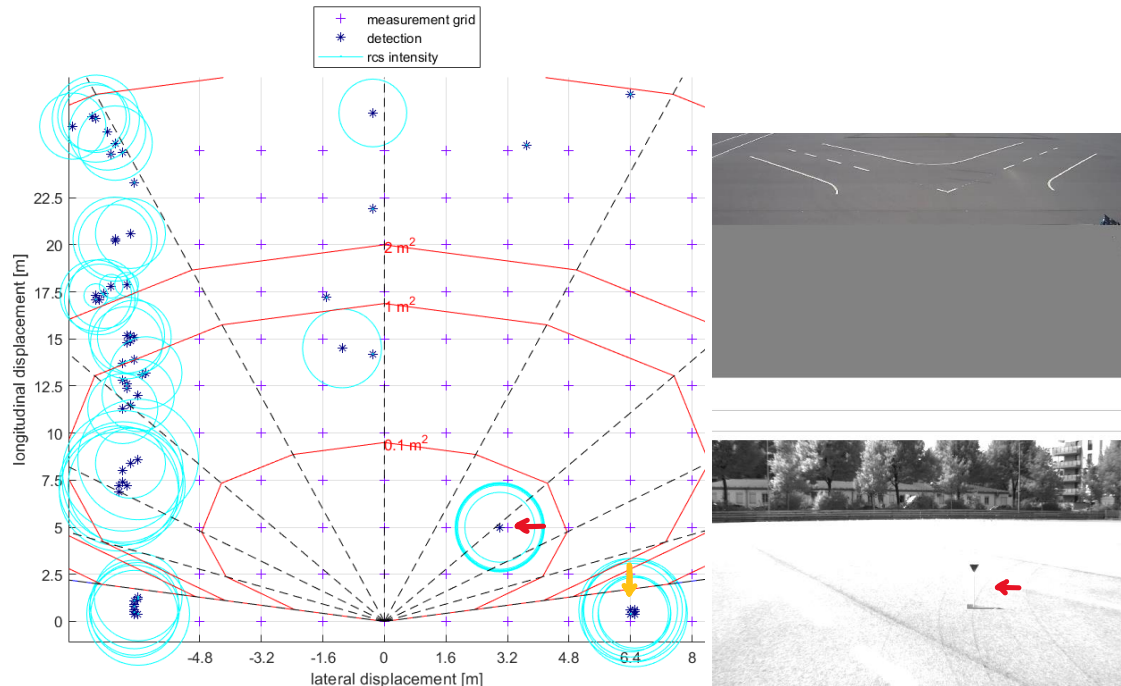


Fig. 65 – Trolley position shifted 5 m right and Triple mirror position on the grid X-Y (3.2, 5) m

In this case, with the Triple mirror in that position on the grid and the trolley moved 5 meters to the right, the common reflection appears, and it's marked with a yellow arrow in Fig. X.

Pedestrian position on the grid X-Y: (-3.2, 5) m

In this case, with the pedestrian in that position on the grid and the trolley moved 5 meters to the right, the common reflection does not appear.

Pedestrian position on the grid X-Y: (0, 5) m

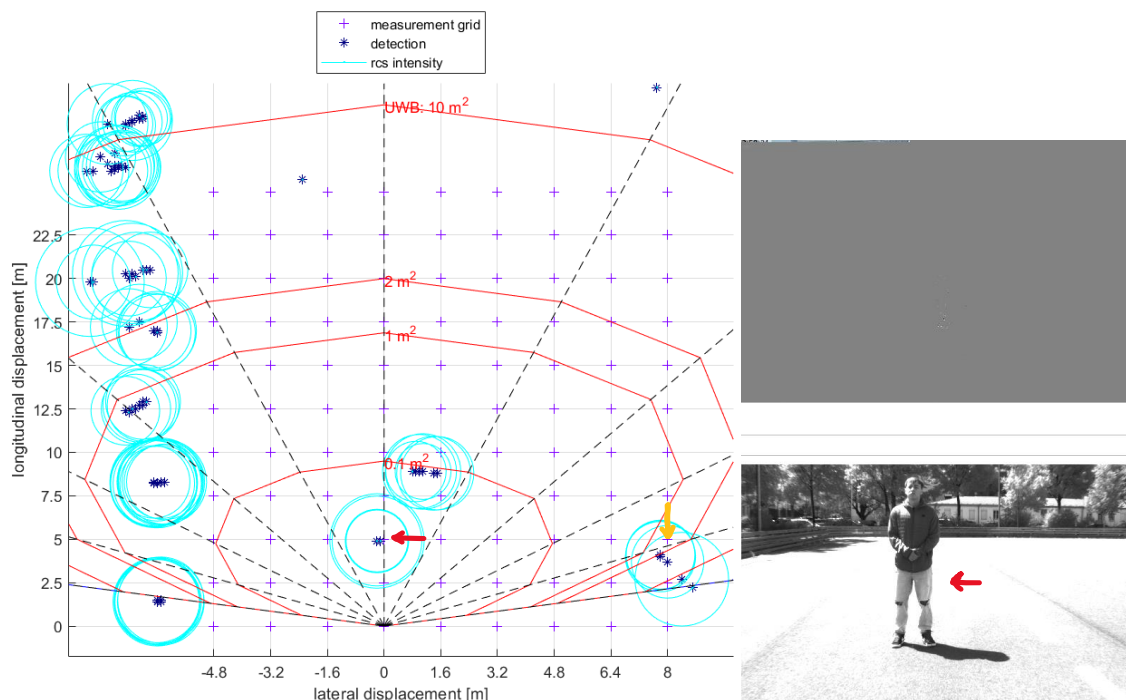


Fig. 66 – Trolley position shifted 5 m right and Pedestrian position on the grid X-Y (0, 5) m

In this case, with the pedestrian in that position on the grid and the trolley moved 5 meters to the right, the common reflection appears, and it's marked with a yellow arrow in Fig. X.

Pedestrian position on the grid X-Y: (3.2, 5) m

In this case, with the pedestrian in that position on the grid and the trolley displaced 5 m to the right, the common reflection does not appear.

After making these measurements we can hypothesize that the position of the trolley affects and creates interference in the radar detection zone and influences the generation of common reflection.

However, we don't know if it is the only element that influences the generation of the reflection, since it does not appear with an empty grid. Perhaps the guardrail plays a role as well, or the reflection is a combination of both.

To finish drawing a firm conclusion about the reflection, we decided to apply the mirror effect and move the setup to the other side of the grid, being as follows:

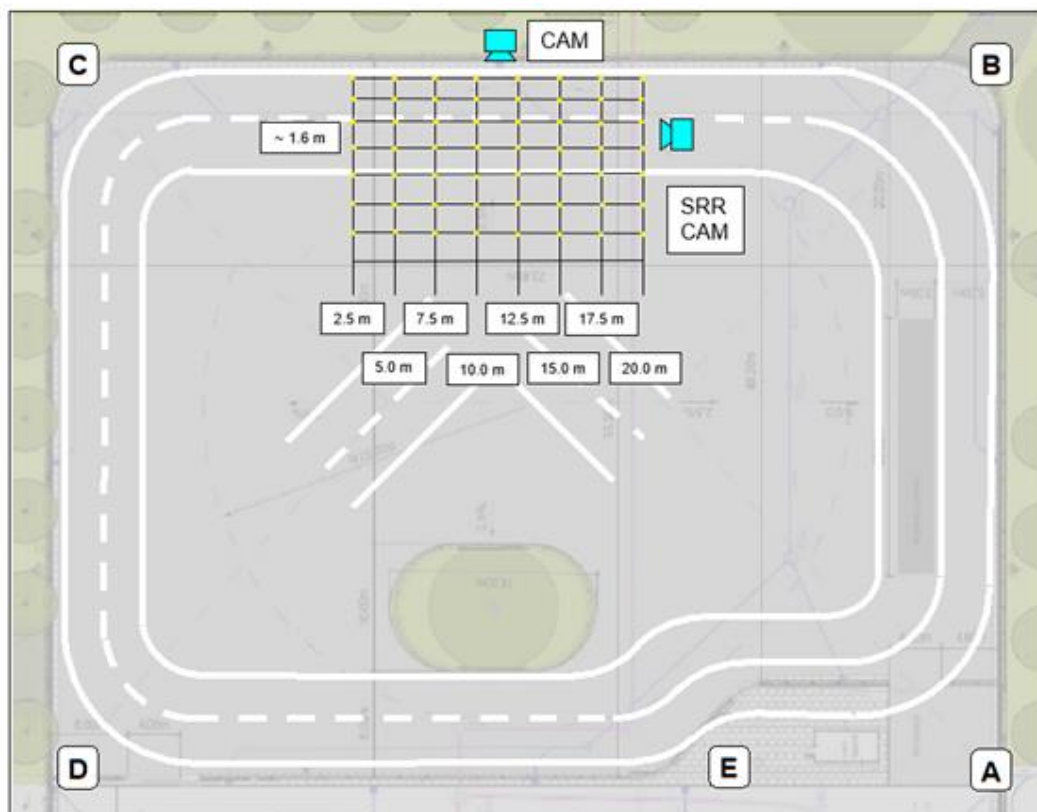


Fig. 67 - Setup moved to the other side of the grid making the mirror effect

In this way we will carry out the same measurements that have been carried out previously to see if the reflection is shown and where. As in the previous measures, only the relevant ones, i.e., where the reflection appears, will be shown. To see all measurements, see Appendix.

TROLLEY POSITION CHANGED TO THE OTHER SIDE OF THE GRID

No object in the grid:

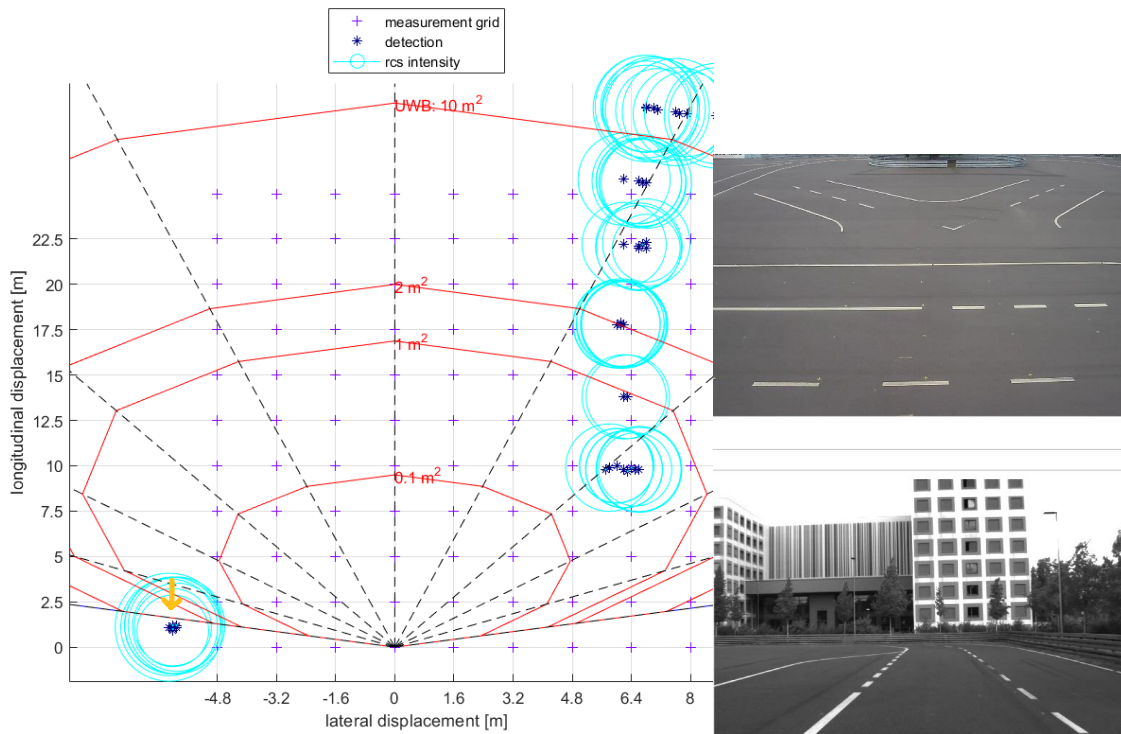


Fig. 68 - Trolley position changed to the other side of the grid and no object in the grid

In this first measurement, with the trolley in default position, the common reflection already appears making the mirror effect, and it's marked with a yellow arrow in Fig. 68.

Triple mirror position on the grid X-Y: (3.2, 5) m

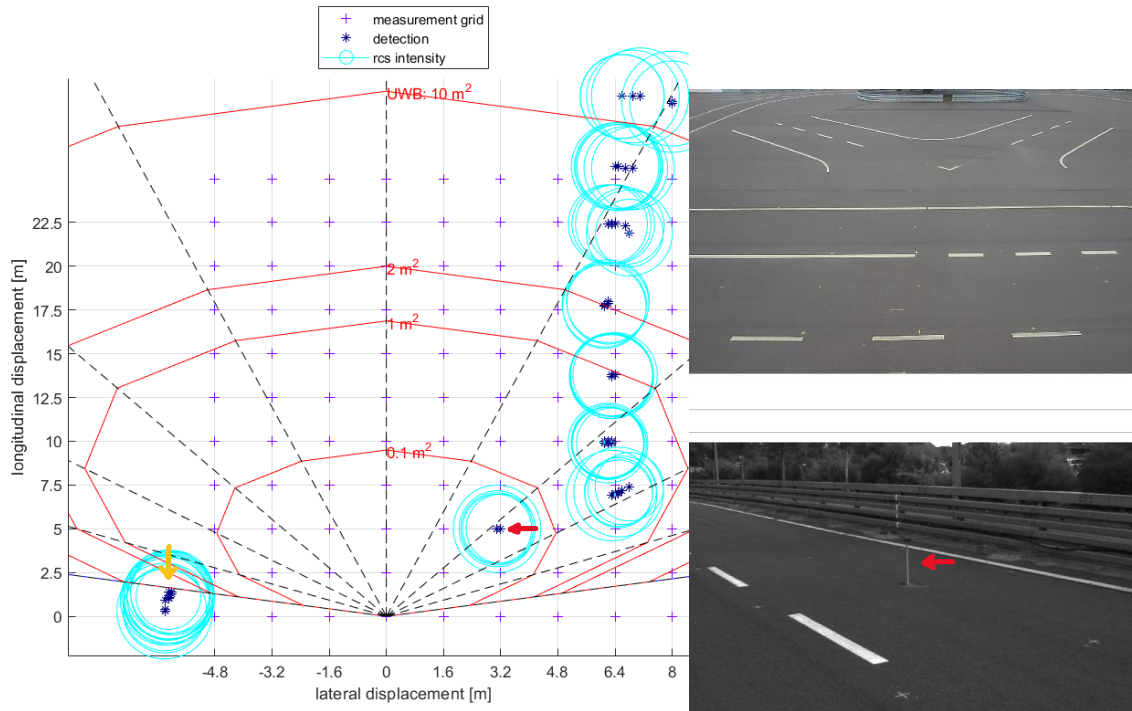


Fig. 69 - Trolley position changed to the other side of the grid and Triple mirror position on the grid X-Y (3.2, 5) m

In this case, with the Triple mirror in that position on the grid, the common reflection appears making the mirror effect, and it's marked with a yellow arrow in Fig. 69.

Triple mirror position on the grid X-Y: (0, 5) m

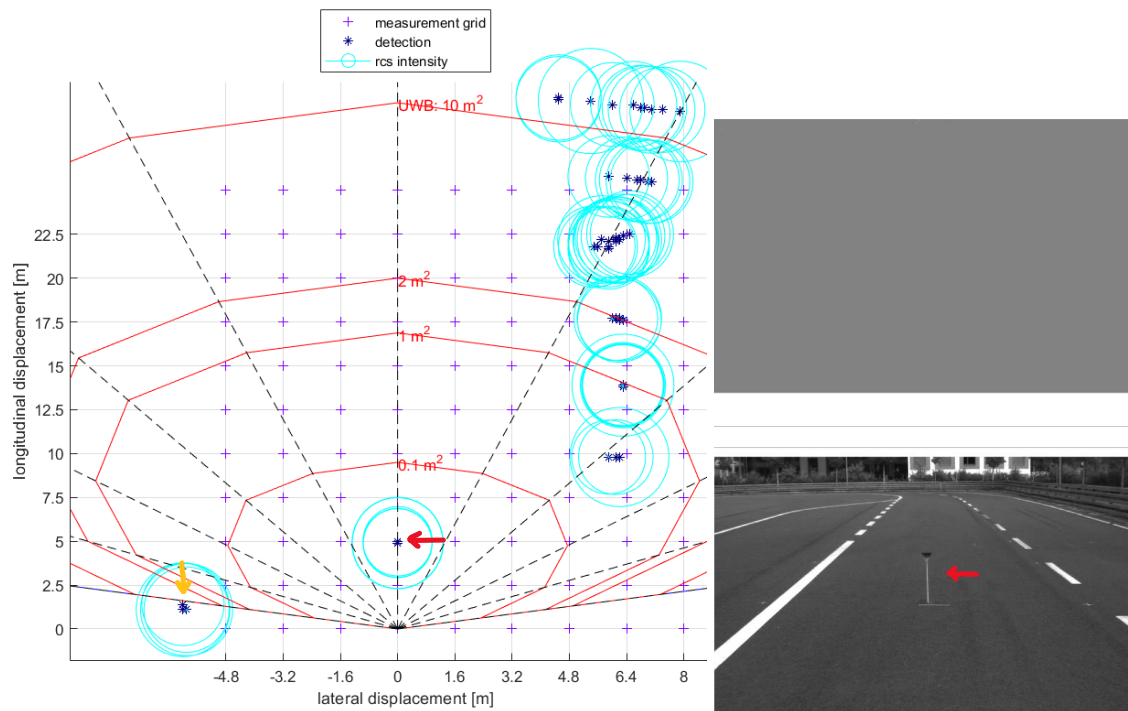


Fig. 70 - Trolley position changed to the other side of the grid and Triple mirror position on the grid X-Y (0, 5) m

In this case, with the Triple mirror in that position on the grid, the common reflection appears making the mirror effect, and it's marked with a yellow arrow in Fig. 70.

Triple mirror position on the grid X-Y: (-3.2, 5) m

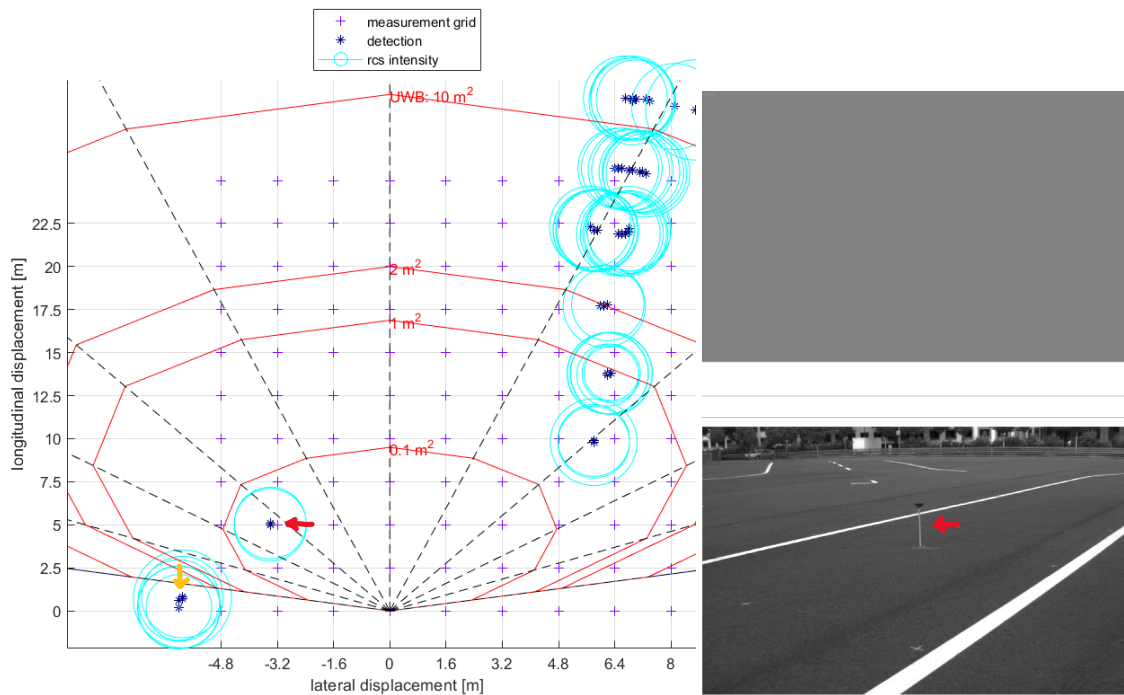


Fig. 71 - Trolley position changed to the other side of the grid and Triple mirror position on the grid X-Y (-3.2, 5) m

In this case, with the Triple mirror in that position on the grid, the common reflection appears making the mirror effect, and it's marked with a yellow arrow in Fig. 71.

Pedestrian position on the grid X-Y: (3.2, 5) m

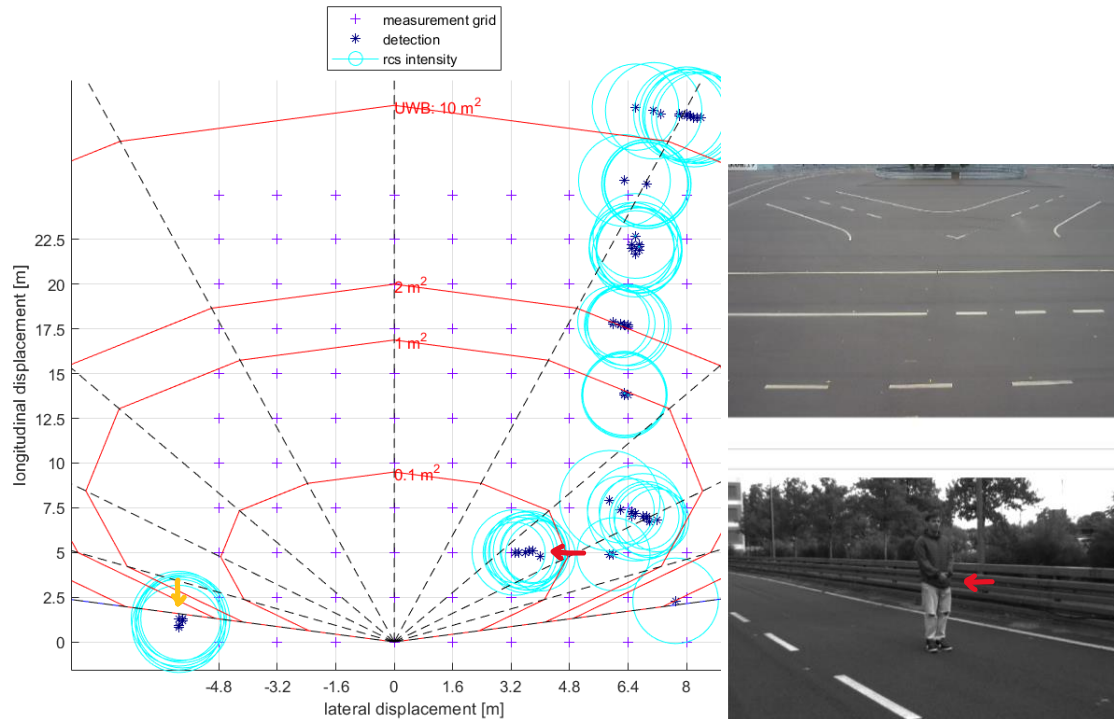


Fig. 72 - Trolley position changed to the other side of the grid and pedestrian position on the grid X-Y (3.2, 5) m

In this case, with the pedestrian in that position on the grid, the common reflection appears making the mirror effect, and it's marked with a yellow arrow in Fig. 72.

Pedestrian position on the grid X-Y: (0, 5) m

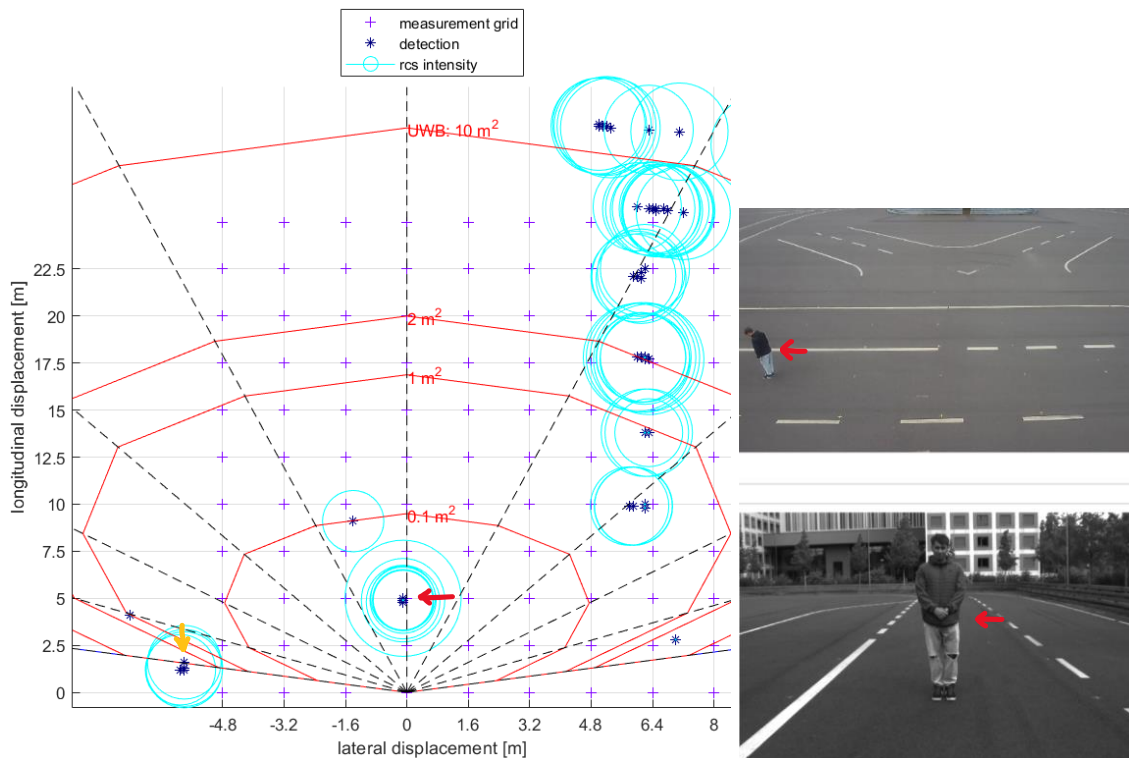


Fig. 73 - Trolley position changed to the other side of the grid and pedestrian position on the grid X-Y (0, 5) m

In this case, with the pedestrian in that position on the grid, the common reflection appears making the mirror effect, and it's marked with a yellow arrow in Fig. 73.

Pedestrian position on the grid X-Y: (-3.2, 5) m

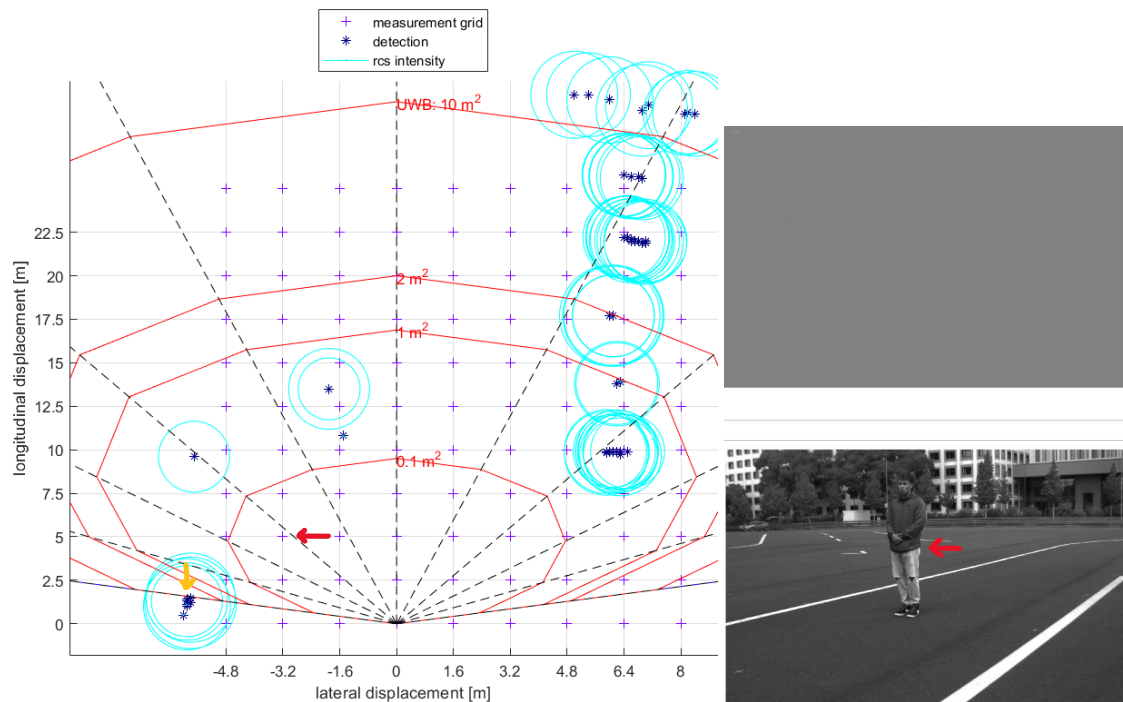


Fig. 74 - Trolley position changed to the other side of the grid and pedestrian position on the grid X-Y (-3.2, 5) m

In this case, with the pedestrian in that position on the grid, the radar doesn't detect the pedestrian but the common reflection appears making the mirror effect, and it's marked with a yellow arrow in Fig. 74.

After making these measurements and analysing them, we have seen that the reflection appears in each and every one of the measurements, even with the trolley in default position, therefore we can affirm that the reflection does not only depend on the position of the trolley.

Consequently, the hypothesis that the reflection is a combination of the trolley, its position and the guardrail, begins to gain strength and importance.

In order to confirm the hypothesis and be more certain, we will also carry out the measurements with the trolley displaced 5 m to the left in this case, as it is the other side.

TROLLEY POSITION CHANGED TO THE OTHER SIDE OF THE GRID AND SHIFTED 5 M TO THE LEFT

No object in the grid:

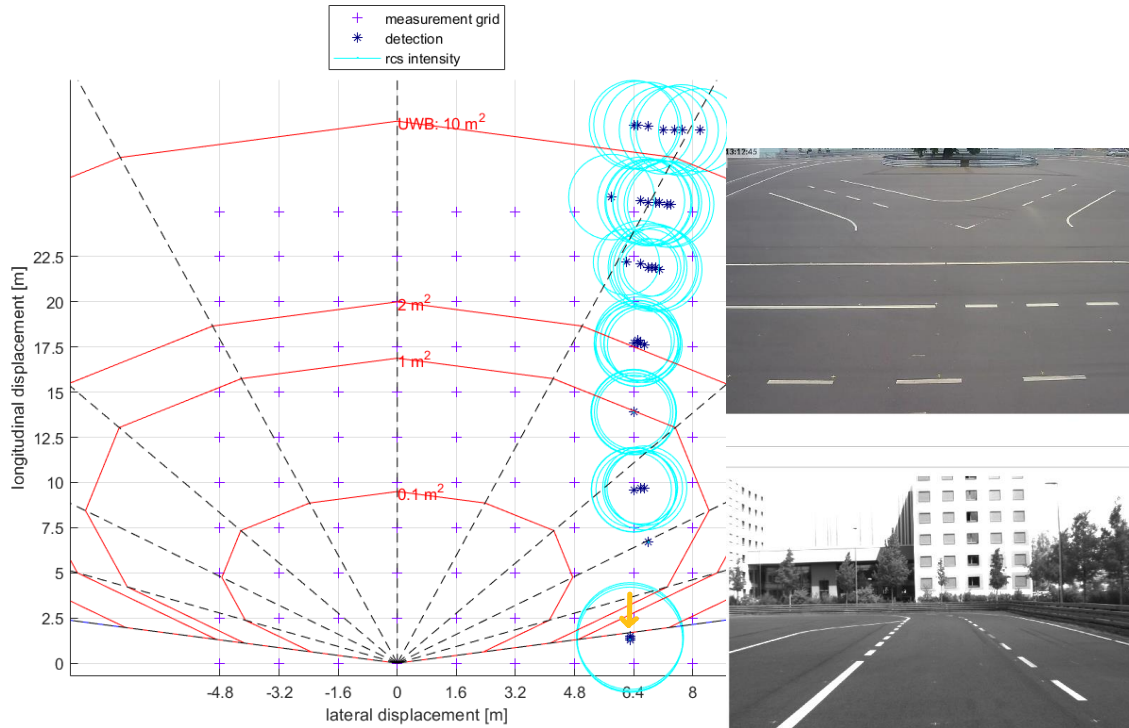


Fig. 75 - Trolley position changed to the other side of the grid and shifted 5 m to the left and no object in the grid

In this case, without any object in the grid, the reflection appears on the side of the guardrail (marked with yellow arrow in Fig. 75), symmetrically to how it appeared in the measurements with the trolley in default position.

Triple mirror position on the grid X-Y: (3.2, 5) m

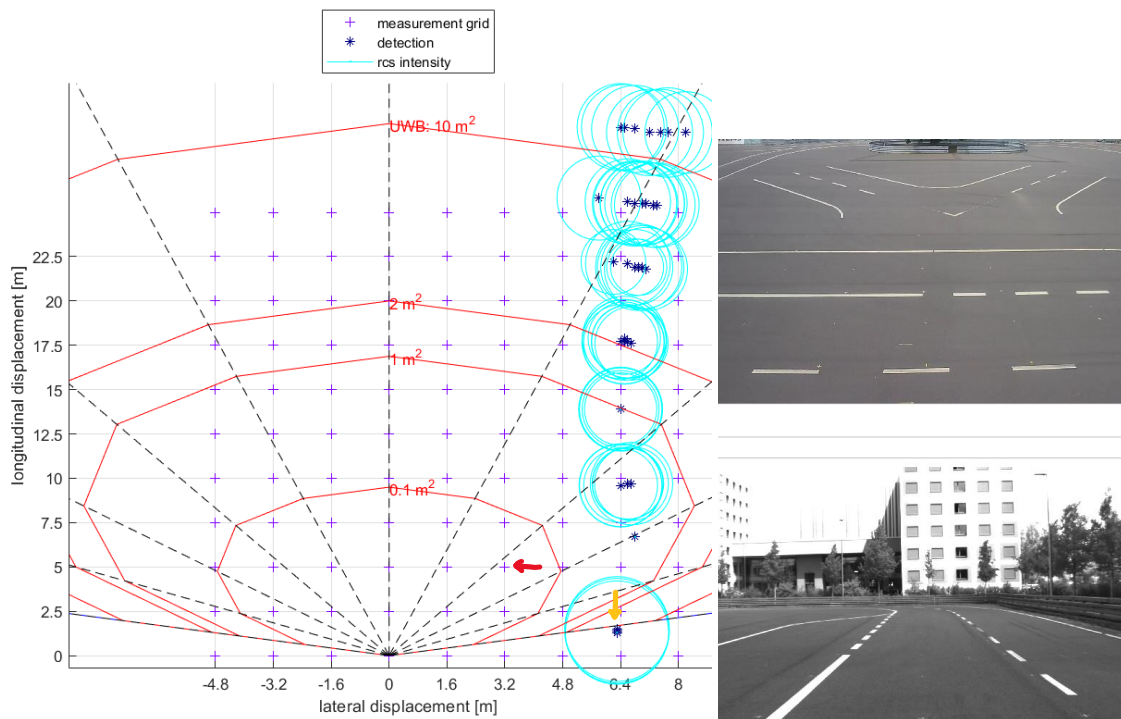


Fig. 76 - Trolley position changed to the other side of the grid and shifted 5 m to the left and Triple mirror position on the grid X-Y (3.2, 5) m

In this case, with the Triple mirror in that grid position, the radar doesn't detect the triple mirror but the reflection also appears on the side of the guardrail (marked with yellow arrow in Fig. 76), symmetrically as it appeared in the measurement with the trolley in default position.

Triple mirror position on the grid X-Y: (0, 5) m

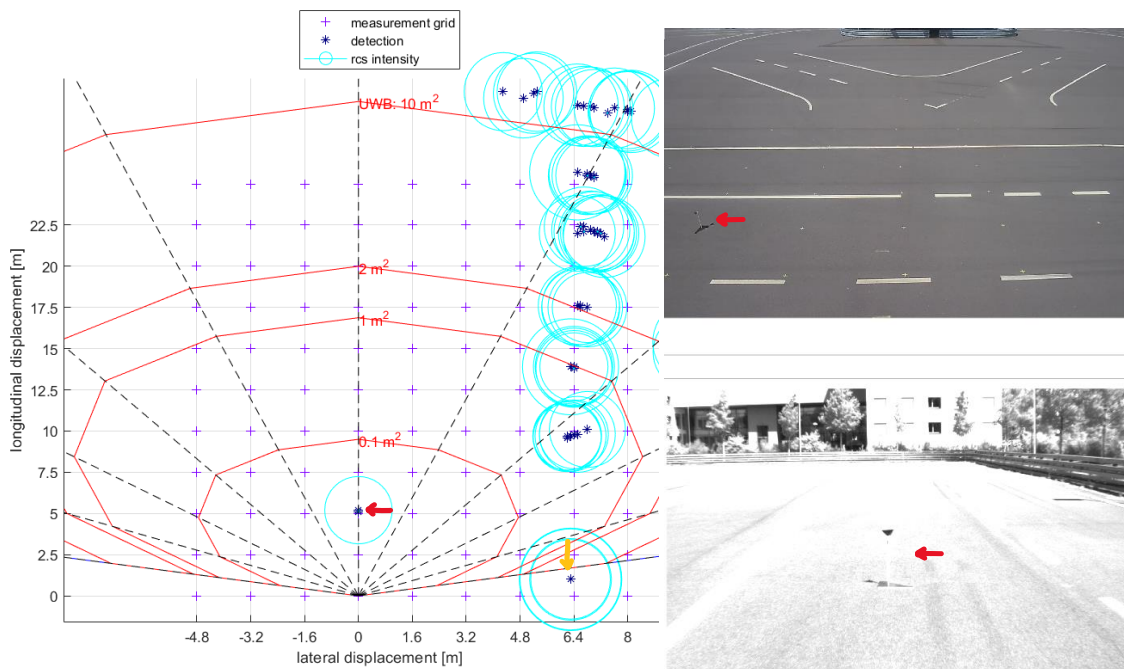


Fig. 77 - Trolley position changed to the other side of the grid and shifted 5 m to the left and Triple mirror position on the grid X-Y (0, 5) m

In this case, with the Triple mirror in that grid position, the reflection also appears on the side of the guardrail (marked with yellow arrow in Fig. 77), symmetrically as it appeared in the measurement with the trolley in default position.

Triple mirror position on the grid X-Y: (-3.2, 5) m

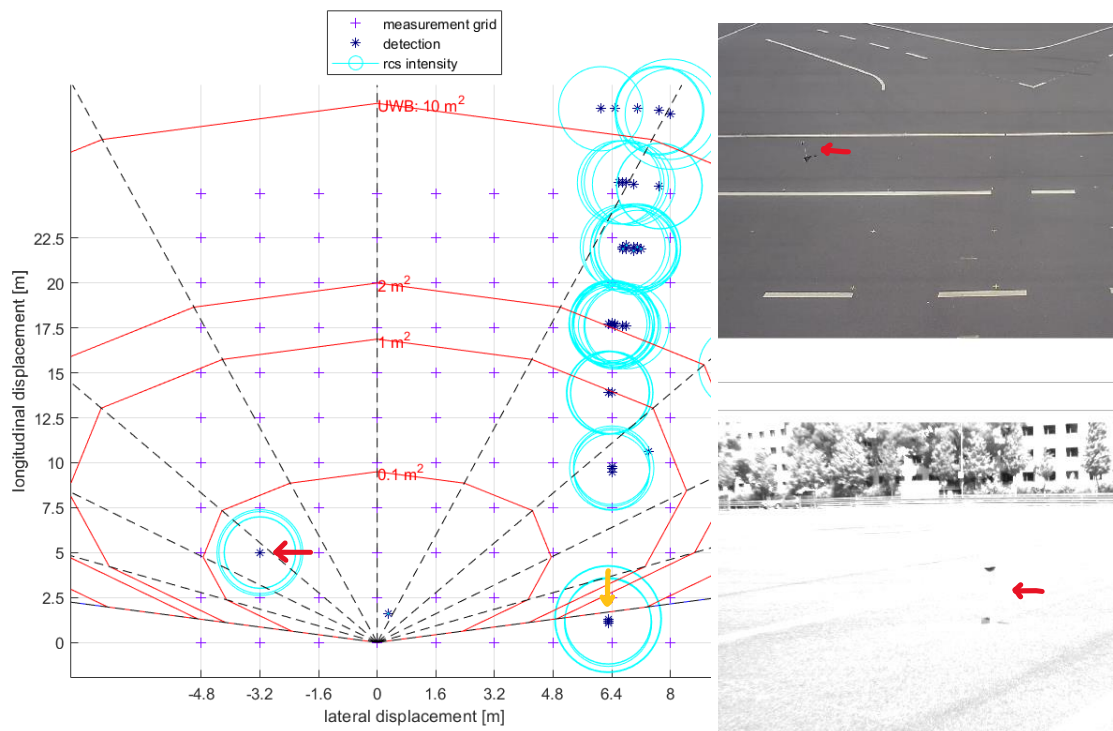


Fig. 78 - Trolley position changed to the other side of the grid and shifted 5 m to the left and Triple mirror position on the grid X-Y (-3.2, 5) m

In this case, with the Triple mirror in that grid position, the reflection also appears on the side of the guardrail (marked with yellow arrow in Fig. 78), symmetrically as it appeared in the measurement with the trolley in default position.

Pedestrian position on the grid X-Y: (3.2, 5) m

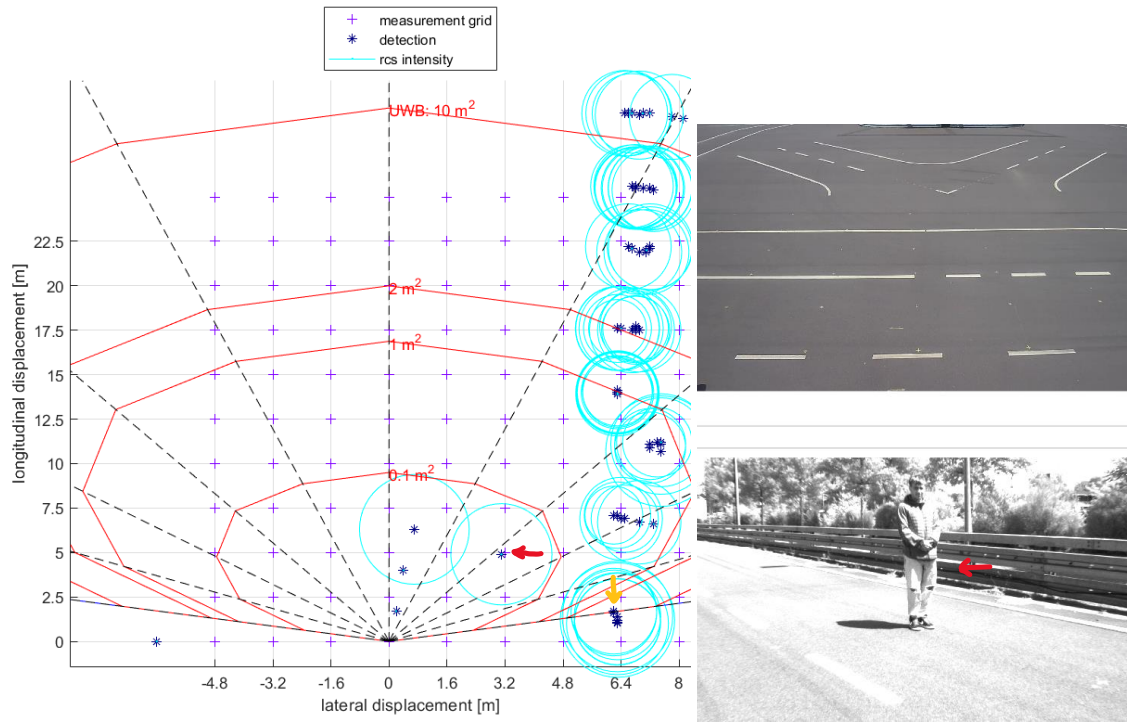


Fig. 79 - Trolley position changed to the other side of the grid and shifted 5 m to the left and pedestrian position on the grid X-Y (3.2, 5) m

In this case, with the Triple mirror in that grid position, the reflection also appears on the side of the guardrail (marked with yellow arrow in Fig. 79), symmetrically as it appeared in the measurement with the trolley in default position.

Pedestrian position on the grid X-Y: (0, 5) m

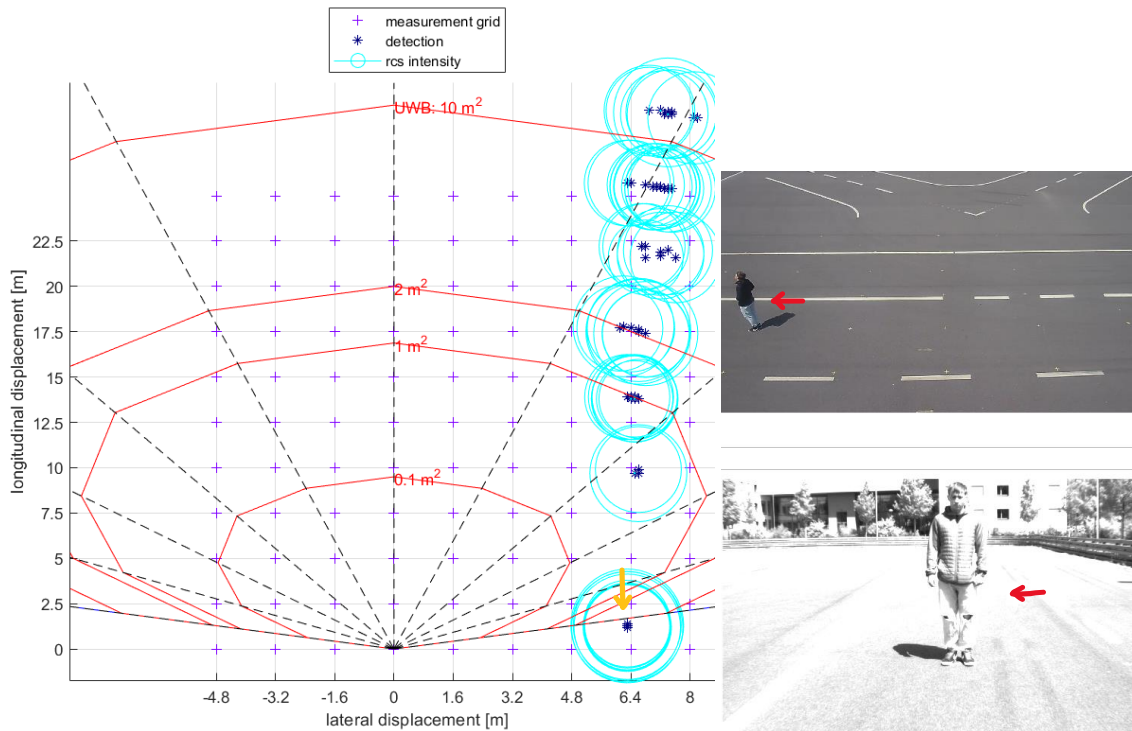


Fig. 80 - Trolley position changed to the other side of the grid and shifted 5 m to the left and pedestrian position on the grid X-Y (0, 5) m

In this case, with the Triple mirror in that grid position, the radar doesn't detect the pedestrian but the reflection also appears on the side of the guardrail (marked with yellow arrow in Fig. 80), symmetrically as it appeared in the measurement with the trolley in default position.

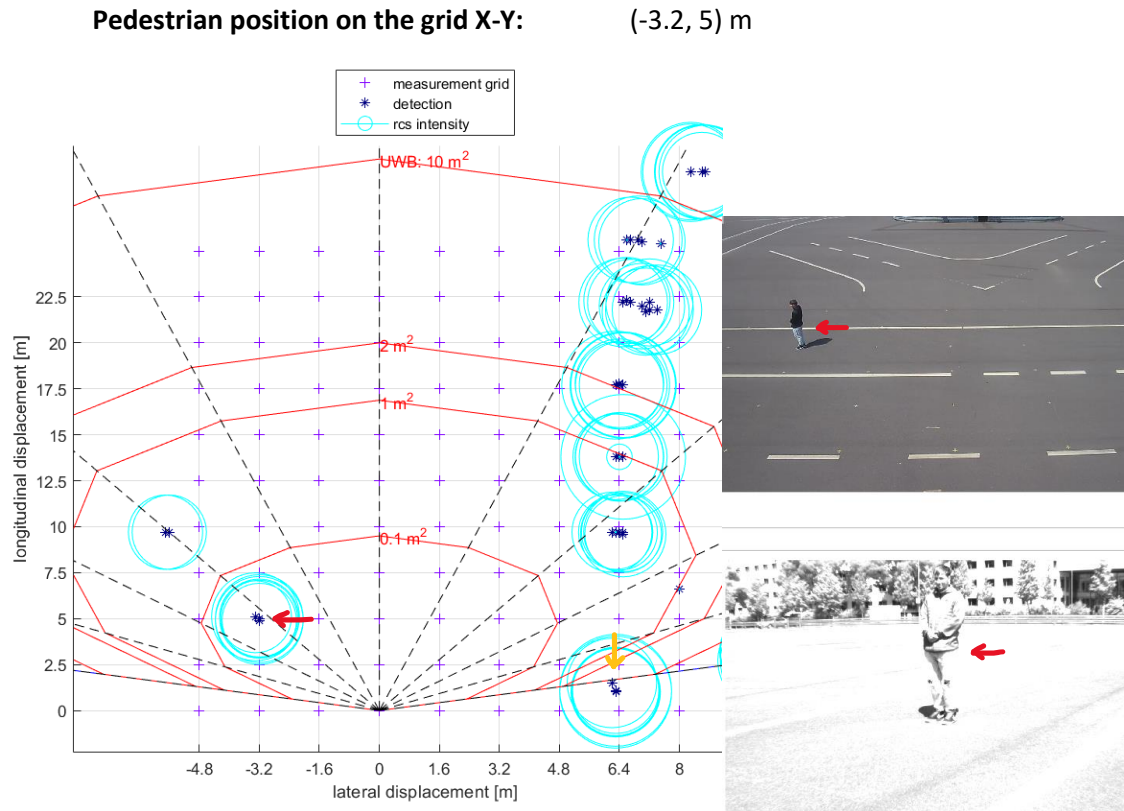


Fig. 81 - Trolley position changed to the other side of the grid and shifted 5 m to the left and pedestrian position on the grid X-Y (-3.2, 5) m

In this case, with the Triple mirror in that grid position, the reflection also appears on the side of the guardrail (marked with yellow arrow in Fig. 81), symmetrically as it appeared in the measurement with the trolley in default position.

After making these measurements and having made several hypotheses, we can draw a conclusion with some firmness.

The reflection depends on the combination of:

- ✓ the position of the trolley, because in the static measurements with the pedestrian, the position of the trolley was out of its default position (displaced 5 m to the right) and the reflection appeared in almost 70% of the measurements.
- ✓ the trolley, because the reflection appears in all measurements with the setup on the other side of the grid and the trolley in its default position.
- ✓ the guardrail, because it is a large object and is present very close to the grid, and extends to its entire length. We know that it is made up of a conductive metallic material, therefore highly reflective.

The signal that comes out of the radar bounces throughout the length of the guardrail and generates infinite reflections. Some of these signals can bounce off the trolley and generate a reflection like the one we have been dealing with. It should be noted that the trolley is an element of considerable size and is made of a metallic material.

However, this hypothesis may be the closest to reality, but it is somewhat difficult to confirm and know with certainty, since the signals emitted by the radar, and the signals that could bounce off the different objects, are imperceptible to the human eye and we do not know how it moves through space.

6.1.2 DATA FILTER

Once the problems of static measurements have been analysed, we must analyse the data, that is, we must assess what data interests us and what data does not, to know what to show and what not in the results display. For this we want to create a data filter.

To exemplify the creation of the filter we will use the following static measurement with Triple mirror:

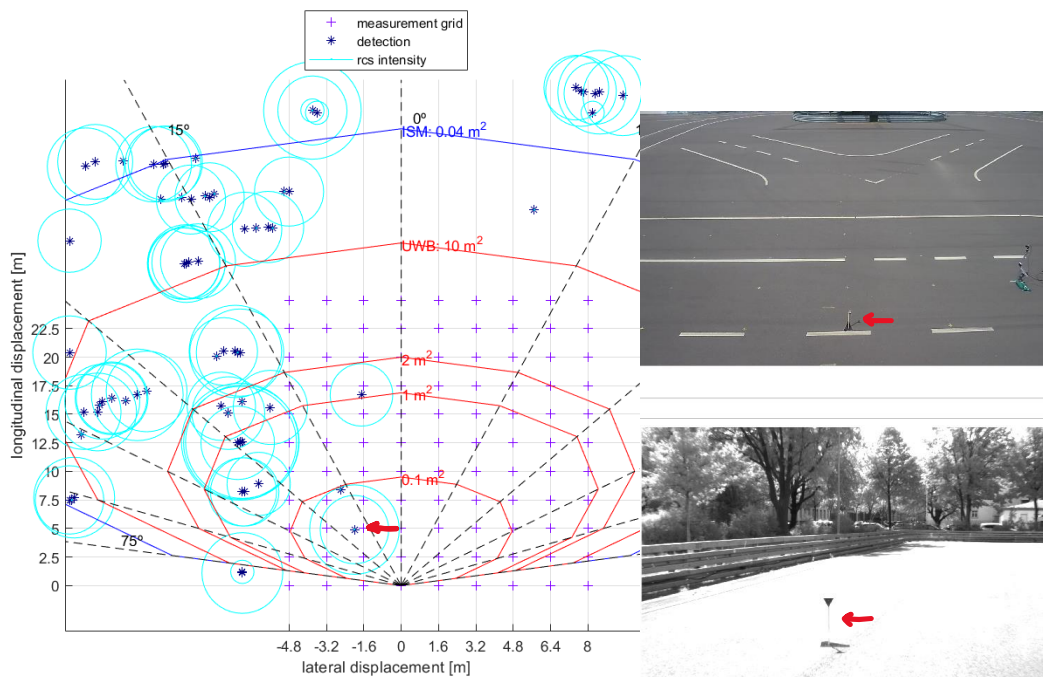


Fig. 82 - Example static measurement, Triple mirror position in the grid X-Y (-1.6, 5) m

This measurement corresponds to the static measurement with Triple mirror in the X-Y position (-1.6, 5) m of the grid.

FILTER BY RCS

As we can see in Fig. 82, the graph shows many detections that do not interest us, many reflections of weak RCS intensity, and some ghost objects that directly lack RCS intensity (see Fig. 83).

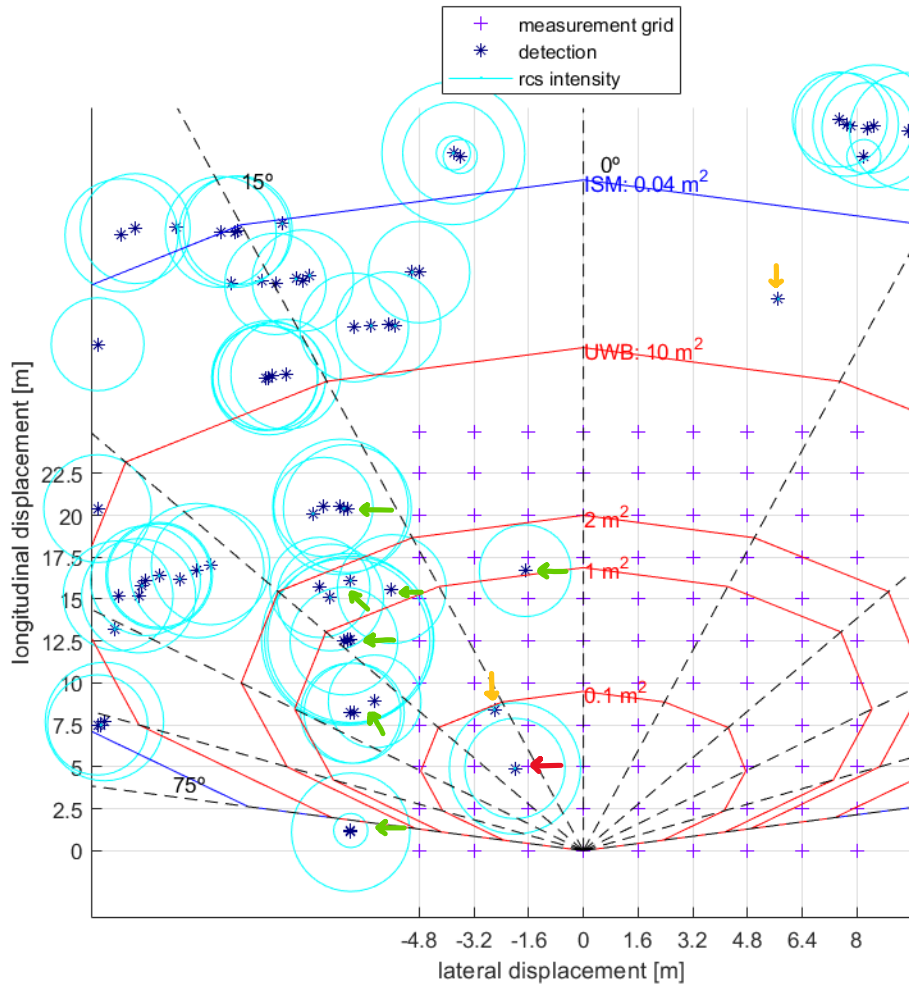
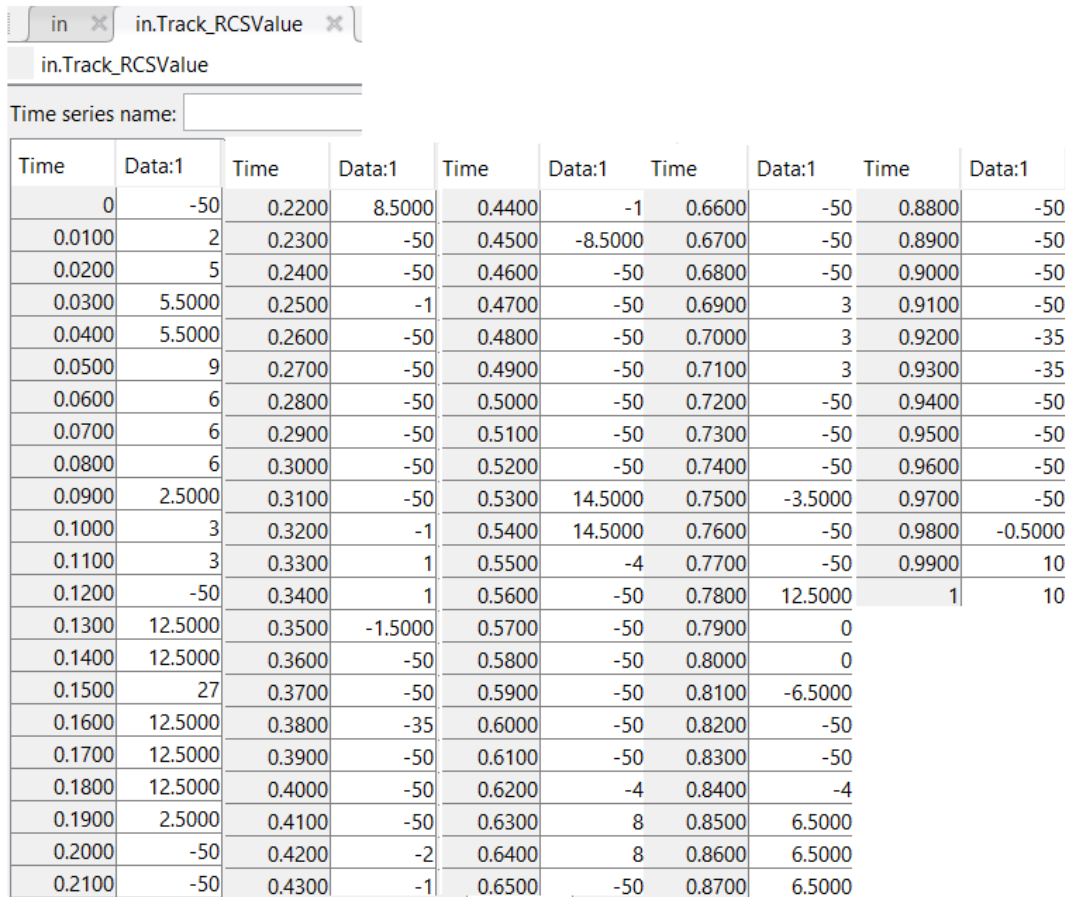


Fig. 83 – Ghost objects (yellow arrows) and some reflections (green arrows) in the measurement

The objective is to create a filter to remove all these data marked with yellow and green arrows (see Fig. 83) as they are data of no interest that disturb the detection of the real object.

To create a filter by RCS intensity value we must understand the values between which this intensity moves and for that we must see what data the variable contains. The variable we are interested in has the name of **in.Track_RCSValue** and it is a subvariable of the variable **in**.



Time	Data:1	Time	Data:1	Time	Data:1	Time	Data:1	Time	Data:1
0	-50	0.2200	8.5000	0.4400	-1	0.6600	-50	0.8800	-50
0.0100	2	0.2300	-50	0.4500	-8.5000	0.6700	-50	0.8900	-50
0.0200	5	0.2400	-50	0.4600	-50	0.6800	-50	0.9000	-50
0.0300	5.5000	0.2500	-1	0.4700	-50	0.6900	3	0.9100	-50
0.0400	5.5000	0.2600	-50	0.4800	-50	0.7000	3	0.9200	-35
0.0500	9	0.2700	-50	0.4900	-50	0.7100	3	0.9300	-35
0.0600	6	0.2800	-50	0.5000	-50	0.7200	-50	0.9400	-50
0.0700	6	0.2900	-50	0.5100	-50	0.7300	-50	0.9500	-50
0.0800	6	0.3000	-50	0.5200	-50	0.7400	-50	0.9600	-50
0.0900	2.5000	0.3100	-50	0.5300	14.5000	0.7500	-3.5000	0.9700	-50
0.1000	3	0.3200	-1	0.5400	14.5000	0.7600	-50	0.9800	-0.5000
0.1100	3	0.3300	1	0.5500	-4	0.7700	-50	0.9900	10
0.1200	-50	0.3400	1	0.5600	-50	0.7800	12.5000	1	10
0.1300	12.5000	0.3500	-1.5000	0.5700	-50	0.7900	0		
0.1400	12.5000	0.3600	-50	0.5800	-50	0.8000	0		
0.1500	27	0.3700	-50	0.5900	-50	0.8100	-6.5000		
0.1600	12.5000	0.3800	-35	0.6000	-50	0.8200	-50		
0.1700	12.5000	0.3900	-50	0.6100	-50	0.8300	-50		
0.1800	12.5000	0.4000	-50	0.6200	-4	0.8400	-4		
0.1900	2.5000	0.4100	-50	0.6300	8	0.8500	6.5000		
0.2000	-50	0.4200	-2	0.6400	8	0.8600	6.5000		
0.2100	-50	0.4300	-1	0.6500	-50	0.8700	6.5000		

Fig. 84 - Content of subvariable *in.Track_RCSValue* during 1 s of measurement

As we can see in Fig. 84, the data values are between -50 and 30. From this information we can start the filter using the RCS threshold.

We find the RCS filter created implemented in the final result display function, the last function of section 4.4.3, and we'll see it below.

The function with this filter can be found in the folder in the following path:

DanielDiaz_FinalThesis\conti_radar_SRR\scripts\fx_evalResults_filtered

This function is an enhancement to the final results display function in section 4.4.3, so only the implementations will be shown. To see the full function, see Appendix or file in the folder.

```
function fx_evalResults_filtered(in,img,vout)
```

```

%% INIT
% filter parameters / thresholds
% RCS value range: -50 ... +30
rcs_thresh = 0;

...

%% PLOT
...
% detections
xDir=-1; %xDir is a X directional vector

```



```

line(hax1,xDir*in.Track_LatDispl.Data(in.Track_RCSValue.Data >=
rcs_thresh), ...
    in.Track_LongDispl.Data(in.Track_RCSValue.Data >= rcs_thresh), ...
    'LineStyle','none', ...
    'Marker','*','Color',[0 0 .5]);

% rcs
for i = 1:length(in.Track_RCSValue.Data)
    if in.Track_RCSValue.Data(i) >= rcs_thresh

line(hax1,xDir*in.Track_LatDispl.Data(i),in.Track_LongDispl.Data(i),
...
'marker','o','MarkerSize',(in.Track_RCSValue.Data(i)+51),'Color','c');
    end
end
...

```

As we saw at the beginning of the function, we add a value to the RCS threshold, a value that we will use to filter the data. The objective of the filter is that the display only shows the data that contains a value equal to or greater than the one given to the threshold.

The implementation of the command lines can be seen in the %detections and %rcs command blocks, where it is requested that only variables with a value equal to or greater than the threshold be marked.

The value given to the threshold can be varied to find an average value suitable for all the measurements, since by setting a very high value sometimes the object disappears, and by setting a very low value many data appear that we do not know. they interest Performing various tests, the value of threshold must be comprised between the interval of 0 to 10.

Next, we will see what the filter shows by setting an RCS threshold value of 0 and also with a value of 10.

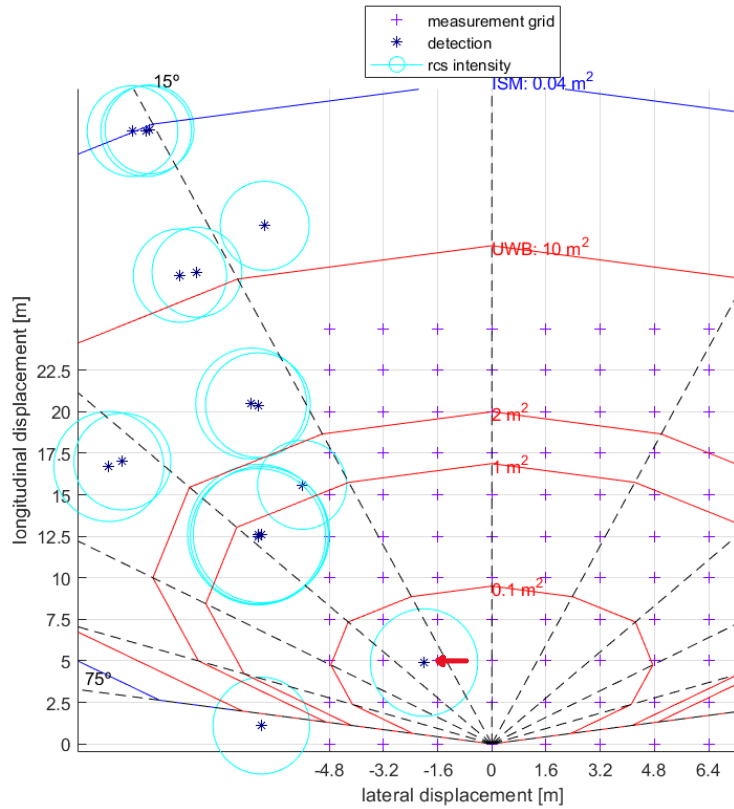


Fig. 85 - Filter applied with an RCS threshold value of 0

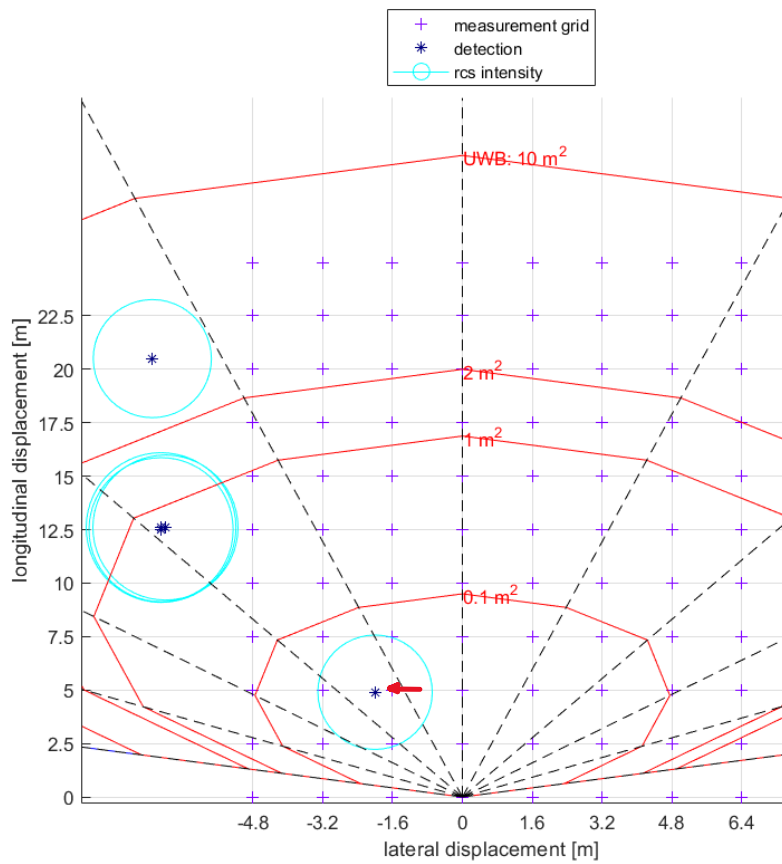


Fig. 86 - Filter applied with an RCS threshold value of 10

Below there's a comparison of the display without filter and with filter of RCS threshold value equal to 0 and a filter of RCS threshold value equal to 10.

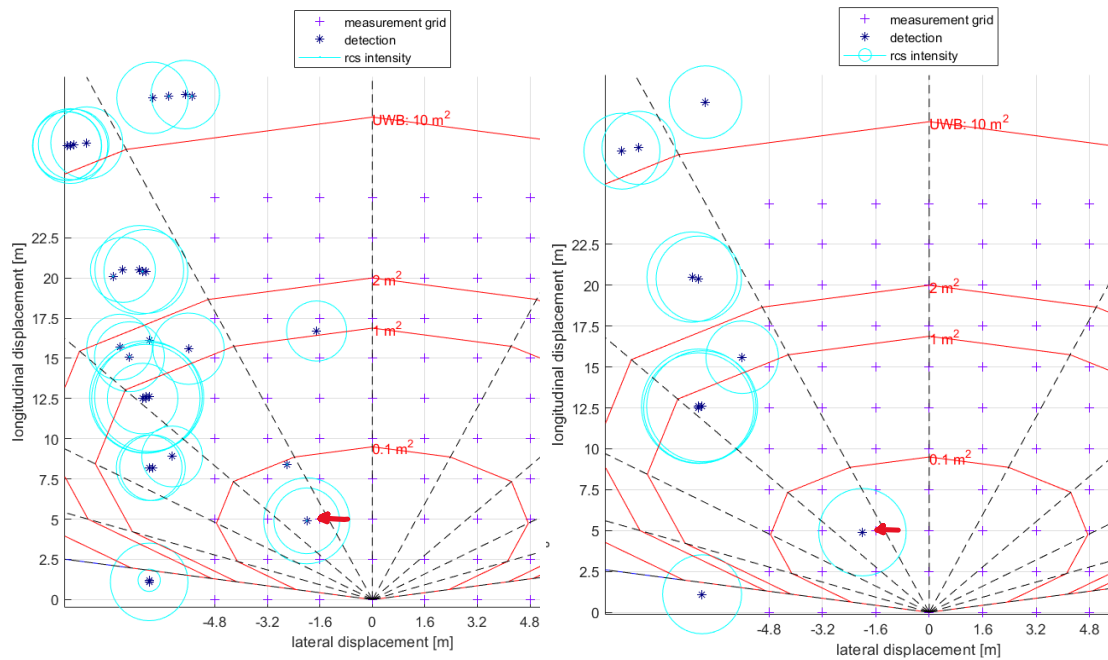


Fig. 87 - Comparison of the display without filter (left) and with filter (right) of RCS threshold value = 0

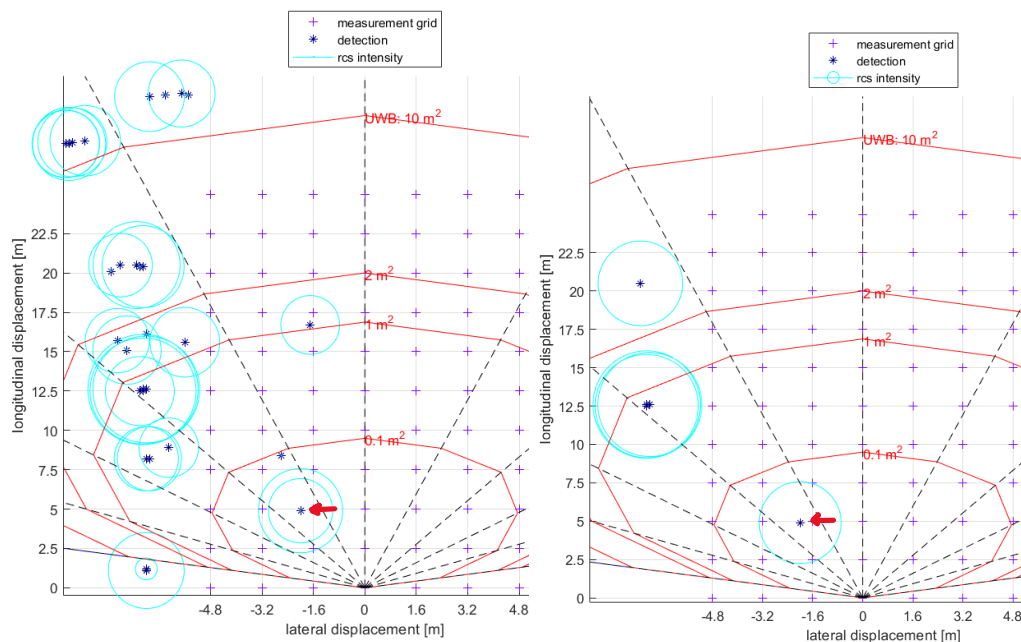


Fig. 88 - Comparison of the display without filter (left) and with filter (right) of RCS threshold value = 10

As we can see, the filter works correctly and eliminates the ghost objects and is able to leave the object as the only detection of the grid that was the objective, both for a threshold value of 0 and 10.

Achieving this is very important because for a real situation in which the radar of a car has to detect an object, it is essential that the radar is capable of filtering the data so that it only detects what it is interested in, which are the real objects that could pose a danger or an obstacle.

The next step is to filter by region, remember that the radar range is approximately 250 meters and there is a lot of data that may appear outside the area of interest. For this we will use the ISM and UWB polygons.

FILTER BY REGION

The objective of this filter is that the result display function only shows the data within the polygon that we decide. In this case, the polygon chosen for the filter is the UWB polygon: 10 m², since it covers the entire grid but not as excessively as the ISM polygon: 0.04 m².

The function with this filter can be found in the folder in the following path:

DanielDiaz_FinalThesis\conti_radar_SRR\scripts\fx_evalResults_finalfilter

This function is an enhancement of the final results display function in section 4.4.3, so only implementations will be displayed next to the previous filter by rcs. For the full function, please refer to the Appendix or the folder file.

```
function fx_evalResults_finalfilter(in,img,vout)
...
%% INIT
% filter parameters / thresholds
% RCS value range: -50 ... +30
rcs_thresh = 0;

...

%% PLOT
...
% detections
xDir=-1;
% line(hax1,xDir*in.Track_LatDispl.Data(in.Track_RCSValue.Data >=
rcs_thresh), ...
%   in.Track_LongDispl.Data(in.Track_RCSValue.Data >= rcs_thresh), ...
%   'LineStyle','none', ...
%   'Marker','*','Color',[0 0 .5]);

% ISM polygons
pts1 = [0 0 0;9.8 2.626 0;17.321 10 0;20 20 0;17.84 30.9 0;10 37.321 0;0
40 0; ...
-10 37.321 0;-17.84 30.9 0;-20 20 0;-17.321 10 0;-9.8 2.626 0;0 0 0];
pts2 = pts1*0.75;

xv = pts2(:,1);
yv = pts2(:,2);
xq = xDir*in.Track_LatDispl.Data(in.Track_RCSValue.Data >= rcs_thresh);
% fitting rcs values are needed
yourNewRCS = in.Track_RCSValue.Data(in.Track_RCSValue.Data >=
rcs_thresh);
yq = in.Track_LongDispl.Data(in.Track_RCSValue.Data >= rcs_thresh);
```

```
[inpol] = inpolygon(xq,yq,xv,yv);
% detections plot
line(hax1,xq(inpol),yq(inpol), ...
      'LineStyle','none', ...
      'Marker','*','Color',[0 0 .5]);

% rcs plot
% data of inpolygon function
for i = 1:length(yourNewRCS)
    line(hax1,xq(inpol),yq(inpol), ...

        'LineStyle','none','marker','o','MarkerSize',((yourNewRCS(i)+51)/2),'Color','c');
end

...
```

To create this filter, many commands from the previous function had to be changed and new variables created, see command blocks % detections, % ISM polygons, % fitting rcs values are needed, % detections plot and % rcs plot% data of inpolygon function.

The display of results with the application of the combination of both filters is as follows:

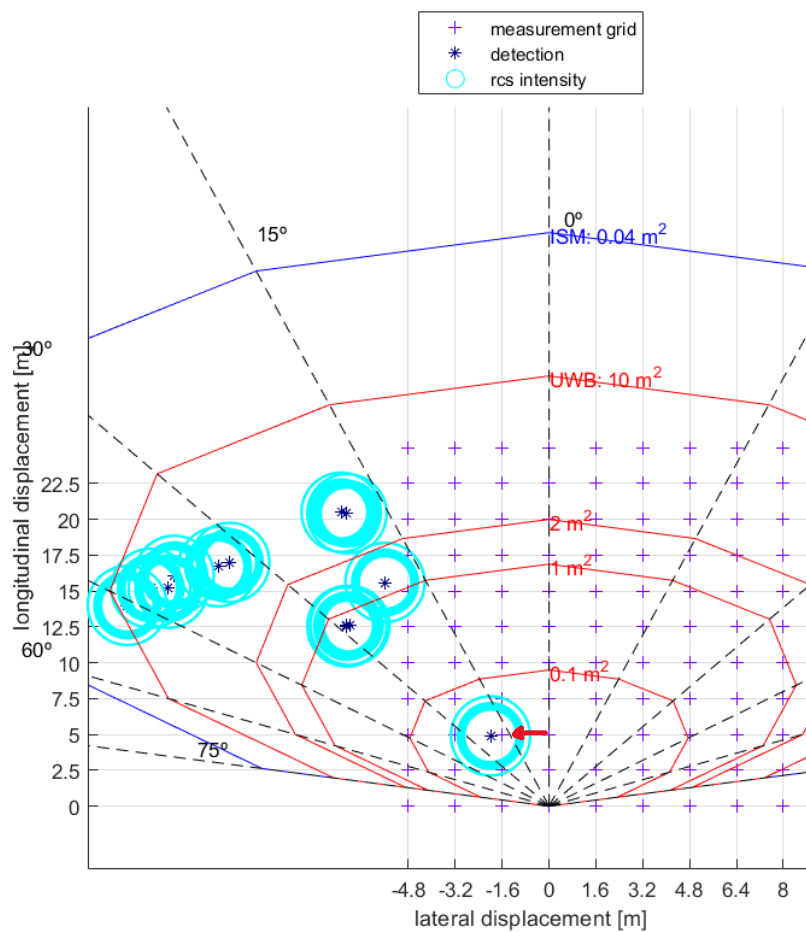


Fig. 89 - Display of results with the application of the combination of both filters, filter by RCS and by polygon 10 m2

Next, we will show a comparison between the measure without filter and with the application of the combination of both filters:

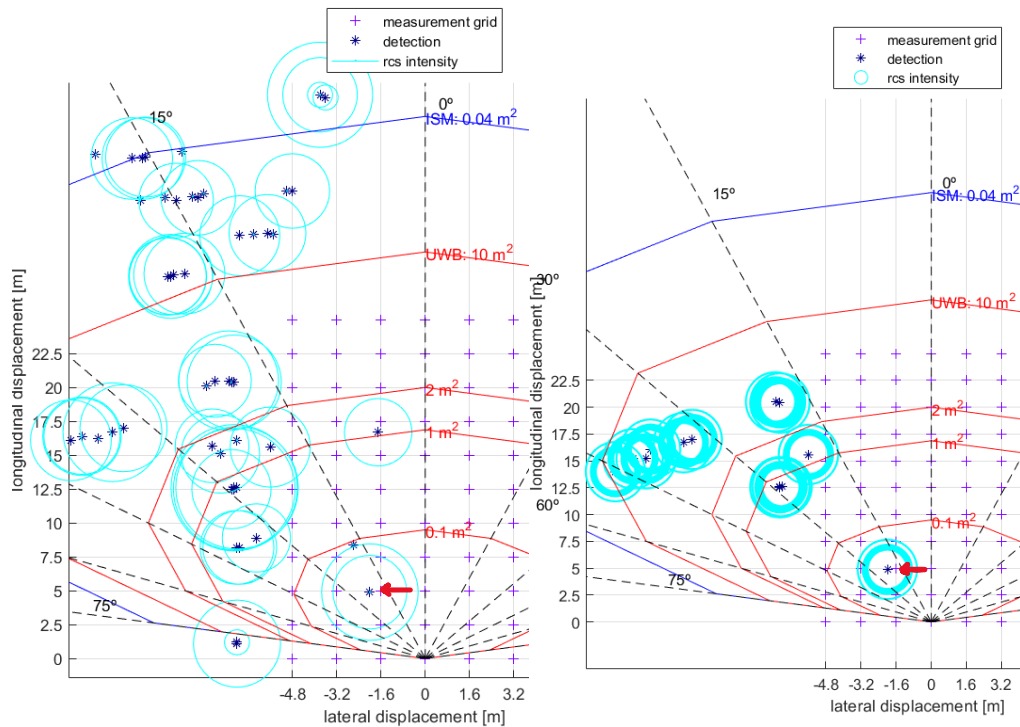


Fig. 90 - Comparison of the display without filter (left) and with the application of the combination of both filters (right)

In this way we can already say that we have fulfilled the objective of creating a good data filter for the radar to keep only data of interest.

6.2 DYNAMIC MEASUREMENTS

Dynamic measurements present the same problems as static measurements, many reflections and ghost objects, that is, data of no interest. The goal with dynamic measures is the same as with static measures, to be able to create a filter to remove this data of no interest. Let's see what happens when we apply the same filter as to the static measures.

To exemplify it we will use the following dynamic measure:

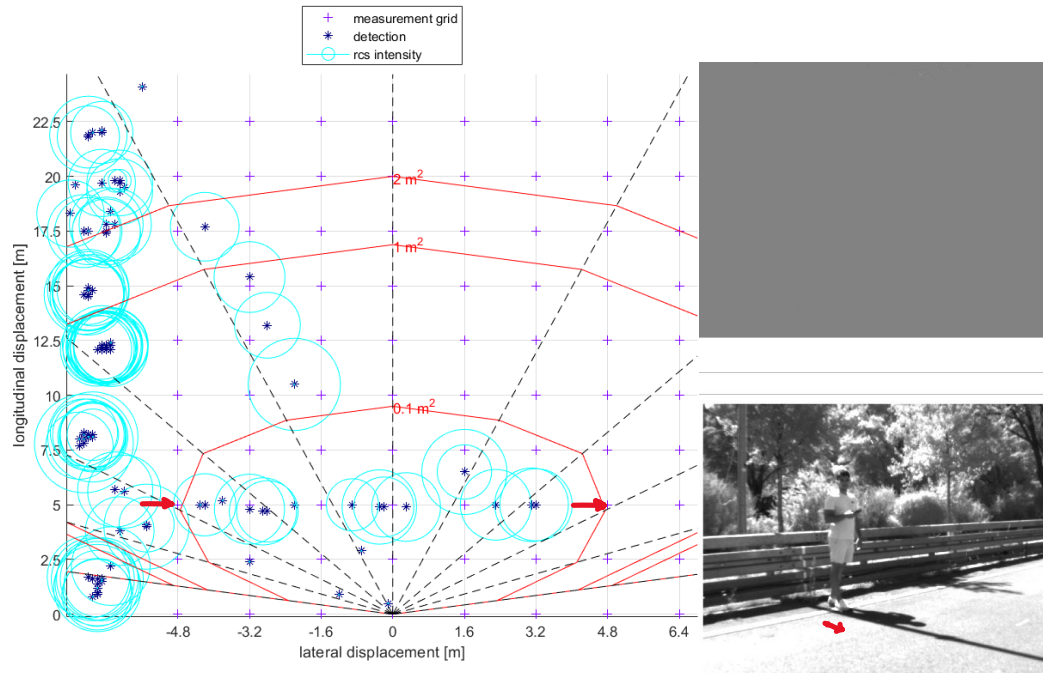


Fig. 91 - Pedestrian describing perpendicular trajectory to the radar at 5 m

The following image shows this same measurement with the filter applied (rcs_threshold = 0):

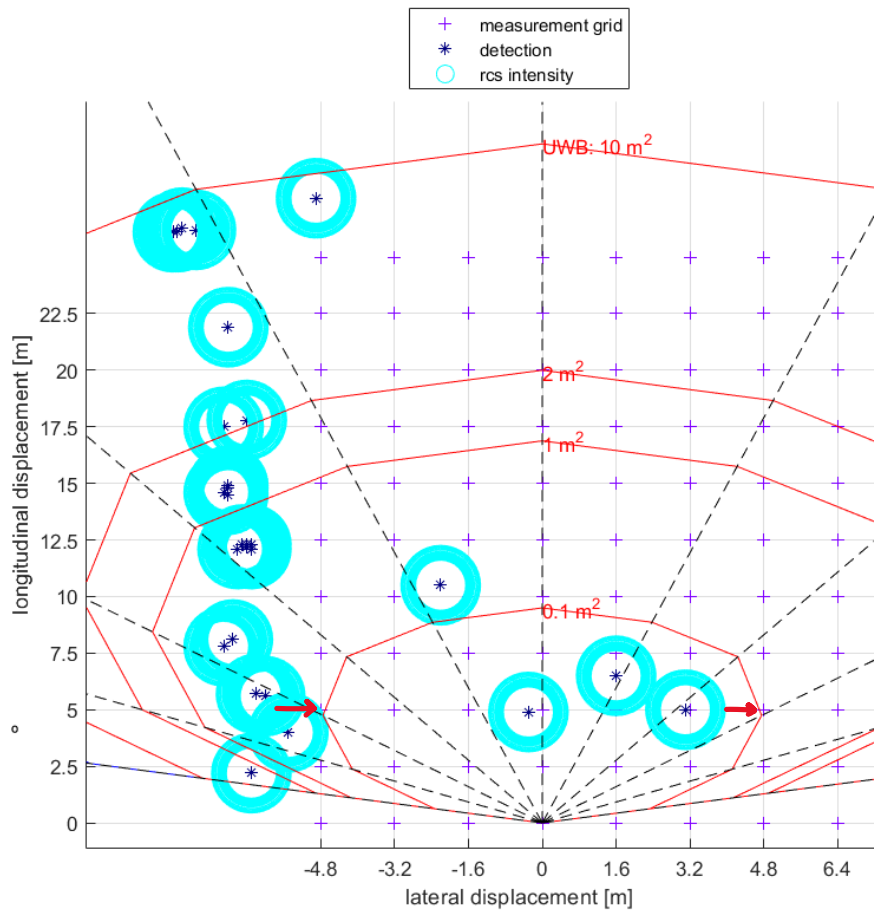


Fig. 92 - Dynamic measurement with filter applied

Let's make a comparison between the measurement without filter and the measurement with filter.

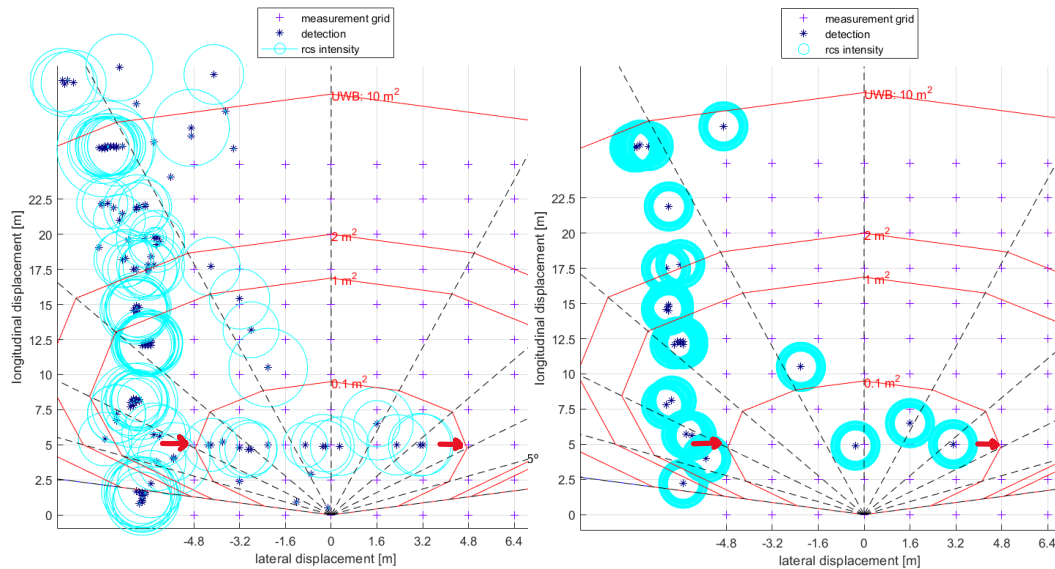


Fig. 93 - Comparison between the measurement without filter (left) and the measurement with filter (right)

As we can see, the filter fulfils its function and eliminates a lot of data of no interest, and also eliminates data outside the area of interest.

However, part of the object's path is lost and not detected. This is due to the fact that in a dynamic measurement the RCS intensity with which one works is less than in a static measurement, since the object is moving and not fixed. When the object is fixed, the radar receives more information about its position, since more signals are received from the same position. When the object is moving, the radar receives fewer signals from its position and therefore the radar shows less signal strength.

For the dynamic measurement filter we must adjust the value of the RCS threshold for a lower value. The lower the value of the RCS threshold, the more data of lower RCS intensity it will show on the display.

We have seen that for static measurements the ideal range of the RCS threshold value varies between 0 and 10. Let's see what is the effective and ideal range for dynamic measurements.

To begin with, we will change the value of the RCS threshold to -5.

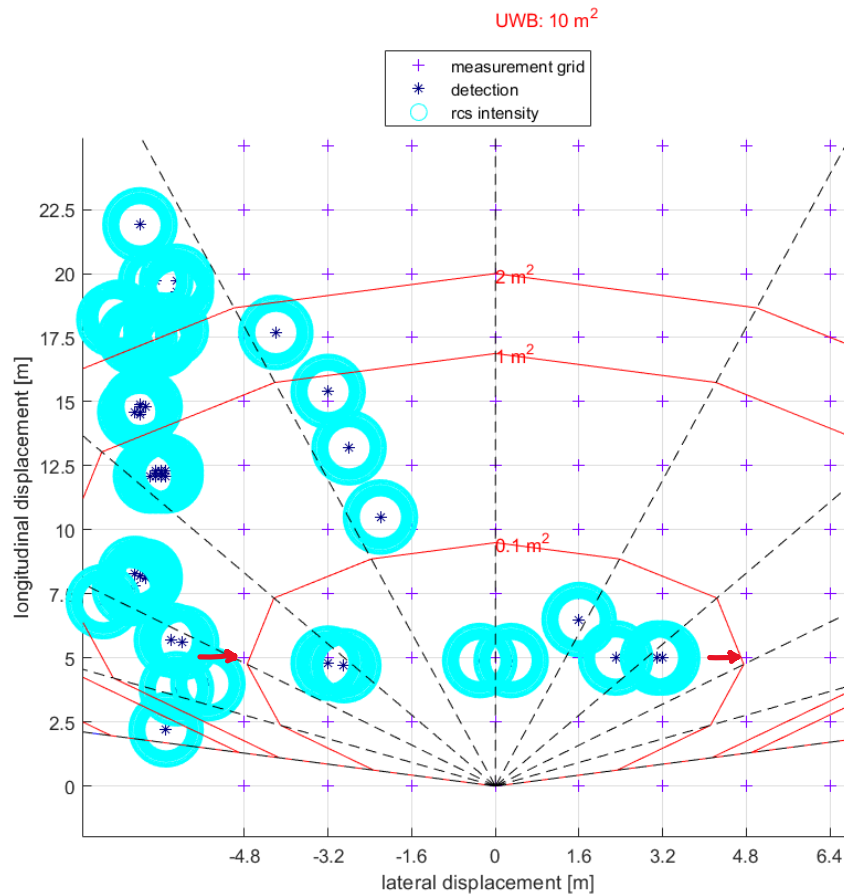


Fig. 94 - Dynamic measurement with filter applied with RCS threshold = -5

For this value of RCS threshold, the display shows more path and also more reflections.

Let's see what happens with a value of -10.

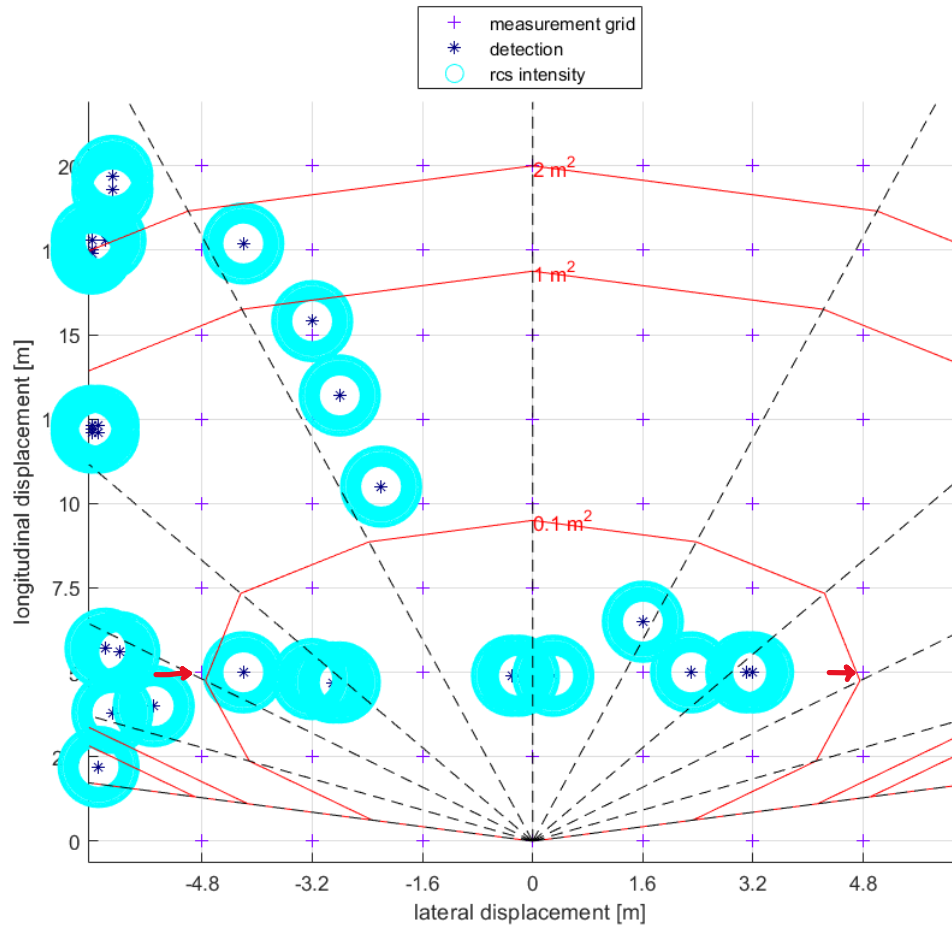


Fig. 95 - Dynamic measurement with filter applied with RCS threshold = -10

For this value of RCS threshold, the display shows more trajectory than with value -5, and does not show more reflections, that is, it increases the description of the trajectory but maintains the same reflections.

Let's see if we can finish describing a more complete trajectory with a value of -15.

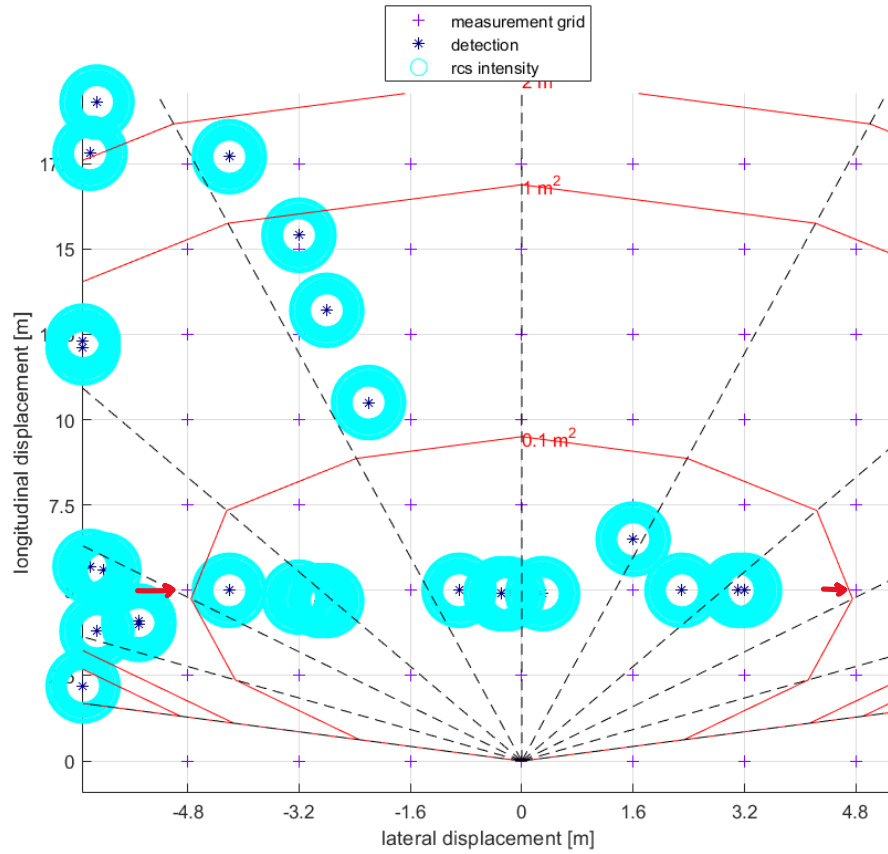


Fig. 96 - Dynamic measurement with filter applied with RCS threshold = -15

With this value we continue to gain trajectory description and keep the same reflections. Let's keep testing with a value of -20.

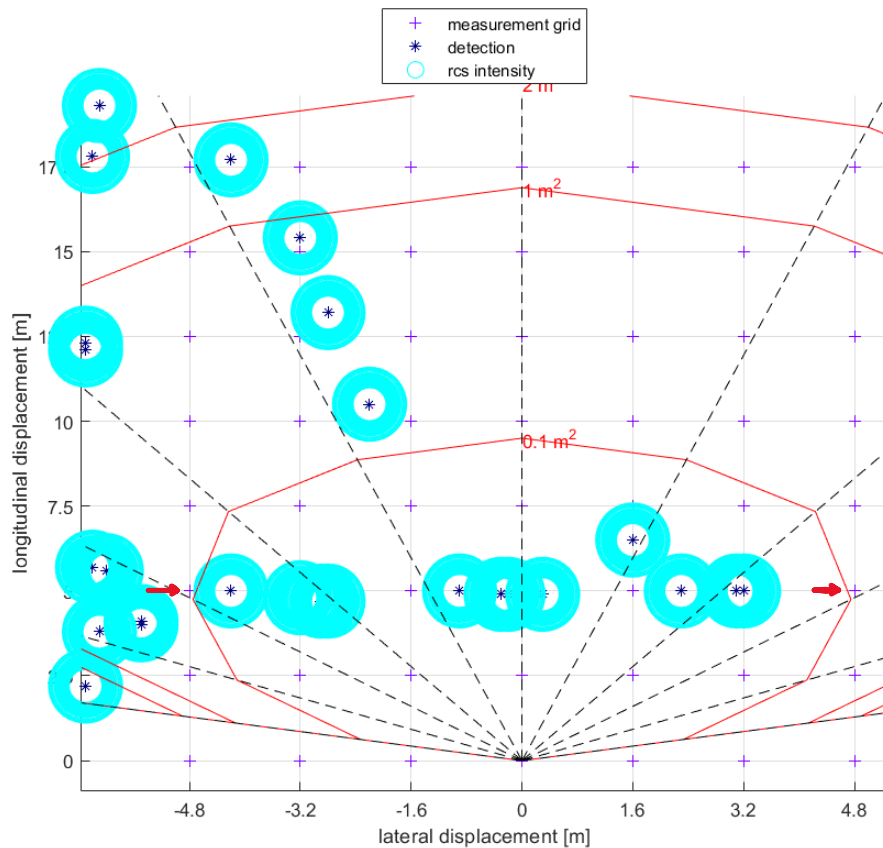


Fig. 97 - Dynamic measurement with filter applied with RCS threshold = -20

With this value we have stopped gaining trajectory description, so we can already draw a conclusion from the value range of the RCS threshold for dynamic measurements. The ideal range for dynamic measurements should be between -20 and -10, giving an average value of -15.

Something that we can highlight is that we can know the difference in the RCS intensity value between a dynamic and a static measurement, it is a difference of 20 threshold, -15 average for dynamic and 5 average for static.

Another thing that should be noted is that the radar is more reliable for static measurements than for dynamic measurements, since in static measurements it receives much more signal intensity. Therefore, the filter is also more reliable for static measurements.

7 IMPACT OF THE TECHNOLOGY

In this section I will give my view on the impact that radar sensors may have on future technology.

First of all, it should be noted that radar sensors are a technology that is still under development and there is still a lot of room for improvement.

However, a good radar, with good programming, with good data processing (filters, classification, etc.) can be a more than useful tool for implementation in today's vehicles,

and I would even dare to say mandatory. This would mean a reduction in the number of accidents on the road in the event of any kind of driver inattention, if the driver falls asleep, if the driver is drunk, etc. In other words, this is a great tool in the field of advanced driver assistance systems (ADAS). Nowadays, this is something that is already being implemented in many vehicles nowadays, brands are getting reliable radars for this purpose.

However, radar sensors are not sufficient for autonomous driving, we are talking about the future, something that has not yet been achieved with firm reliability. In order to achieve autonomous driving, in my opinion, it is essential to combine several technologies, such as radar sensors with an intelligent camera. A good programming of this combination of technologies would allow us to know what is going on at all times. On the one hand, the camera provides you with object classification, different visual routes for the vehicle, traffic sign reading, etc. On the other hand, the radar is capable of positioning these objects in space, measuring distances, etc.

Programming both technologies well and being able to combine them would be a big step towards the goal of autonomy. Even so, I think it would still be difficult to achieve firm reliability.

8 CONCLUSIONS

The development of this thesis on this subject has brought me many things. It is a work in which I have put a lot of enthusiasm, a lot of enthusiasm, a lot of hours and a lot of effort. All of this has been noticeable and has resulted in a great piece of work. Undoubtedly the most professional work I have ever carried out. Every step forward has been carefully analysed, consulted and thought through, and none of the work has been done just for the sake of it.

First of all, the objective of introducing the subject of radar sensors has been achieved, we are talking about a present and future technology in the automotive sector, a very useful tool.

On the other hand, we have worked day by day with Simulink and Matlab, these programs are very important and very useful in the world of engineering, I have realised that with them you can do an infinite number of things. Before starting my thesis, my familiarity and knowledge with these programmes was more than basic, and I can say that after a year I have been working with them.

Choosing a topic for the thesis that would be useful for my future was another of the main objectives.

On the other hand, developing the thesis in another country has made me acquire technical and subject-specific vocabulary in another language, in this case in English.

I have no doubt that the learning obtained will be very useful for my future.

9 REFERENCES

WEB PAGES:

1. Roberto Rodríguez. (2016, May 20). *Ralph: sistema radar de detección de obstáculos*. <https://elb105.com/ralph-sistema-radar-de-deteccion-de-obstaculos/>
2. TecnoCarreteras. (2013, February 5). *ClearWay, un sistema radar para detección de obstáculos en la carretera*. <https://www.tecnocarreteras.es/quienes-somos/>
3. SICK. (2022). *Sensores de radar RMS3xx - Tecnología de radar para detección de objetos rápida en entornos difíciles*. <https://www.sick.com/es/es/soluciones-de-medicion-y-deteccion/sensores-de-radar/rms3xx/c/g448551>
4. Nicolas Scheiner, F. K. N. A. J. D. & B. S. (2021, November 16). *Object detection for automotive radar point clouds – a comparison*. <https://aiperspectives.springeropen.com/articles/10.1186/s42467-021-00012-z>
5. INFINEON. (2022). *Radar sensors for automotive*. <https://www.infineon.com/cms/en/product/sensor/radar-sensors/radar-sensors-for-automotive/>
6. Anonymous. (2020, April 10). *Help Me understand Radar Reflection*. <https://www.rdforum.org/threads/98822/>
7. Different authors. (n.d.). *Sample records for radar reflection*. Retrieved July 6, 2022, from <https://www.science.gov/topicpages/r/radar+reflection>
8. InnoSenT. (2022). *RADAR TECHNOLOGY*. <https://www.innosent.de/en/radar/>
9. Roderick Burnett. (2020, March 24). *Understanding How Ultrasonic Sensors Work*. <https://www.maxbotix.com/articles/how-ultrasonic-sensors-work.htm>
10. Cabe Atwell. (2021, March 1). *What is a radar sensor?* <https://www.fierceelectronics.com/sensors/what-a-radar-sensor#:~:text=Radar%20sensors%20are%20conversion%20devices,motion%20characteristics%2C%20and%20motion%20trajectory>
11. Wikipedia. (2022, January 30). *Object detection*. https://en.wikipedia.org/wiki/Object_detection
12. Zhou, Y.; Yue, Y.M. Radar Depth and Velocity Estimation. Encyclopedia. Available online: <https://encyclopedia.pub/entry/23779>
13. Christiana Honsberg, S. B. (n.d.). *Ángulo acimut*. Retrieved July 6, 2022, from <https://www.pveducation.org/es/fotovoltaica/2-propiedades-de-la-luz-del-sol/%C3%A1ngulo-acimut>
14. Wikipedia. (2022, June 14). *Efecto Doppler*. https://es.wikipedia.org/wiki/Efecto_Doppler
15. The Electrical Engineering Handbook (Different authors). (n.d.). *Tracking Radar*. Retrieved July 6, 2022, from <https://www.sciencedirect.com/topics/engineering/tracking-radar>
16. Christian Wolff. (n.d.). *Radar basics*. Retrieved July 6, 2022, from <https://www.radartutorial.eu/01.basics/Physical%20fundamentals%20of%20the%20radar%20principle.en.html>
17. tutorialspoint. (n.d.). *Radar Systems - Range Equation*. Retrieved July 6, 2022, from

https://www.tutorialspoint.com/radar_systems/radar_systems_range_equation.htm#

18. copradar. (n.d.). *Radar Range Equation*. Retrieved July 6, 2022, from <https://copradar.com/rdrange/>
19. Radar and ARPA Manual. (2014). *Radar Equation*. <https://www.sciencedirect.com/topics/engineering/radar-equation>
20. techopedia. (2022). *Industrial, Scientific and Medical Radio Band (ISM Band)*. <https://www.techopedia.com/definition/27785/industrial-scientific-and-medical-radio-band-ism-band>
21. kinexon. (2022). *UWB Technology*. <https://kinexon.com/uwb-technology/>

ARTICLES:

22. Chipengo, U. (2019). Full physics simulation of terrain-adaptive 77 GHz automotive radar for early pedestrian detection. *Microwave and Optical Technology Letters*, 61(5), 1375–1380. <https://doi.org/10.1002/MOP.31714>
23. Eltrass, A., & Khalil, M. (2018). *Automotive radar system for multiple-vehicle detection and tracking in urban environments; Automotive radar system for multiple-vehicle detection and tracking in urban environments*. <https://doi.org/10.1049/iet-its.2017.0370>
24. Scheiner, N., Kraus, F., Appenrodt, N., Dickmann, J., & Sick, B. (n.d.). *AI Perspectives Object detection for automotive radar point clouds-a comparison*. <https://doi.org/10.1186/s42467-021-00012-z>
25. Chipengo, U. (2019). *Full physics simulation of terrain-adaptive 77 GHz automotive radar for early pedestrian detection*. <https://doi.org/10.1002/mop.31714>
26. Manjunath, A., Liu, Y., Henriques, B., & Engstle, A. (2018). *Radar Based Object Detection and Tracking for Autonomous Driving; Radar Based Object Detection and Tracking for Autonomous Driving*. <https://doi.org/10.1109/ICMIM.2018.8443497>
27. Valerian Paulet, M., Salceanu, A., & Maria Neacsu, O. (2016). *Ultrasonic radar; Ultrasonic radar*. 20–22. <https://doi.org/10.1109/ICEPE.2016.7781400>
28. Marghany, M. (2020). Quantum of radar theory. *Synthetic Aperture Radar Imaging Mechanism for Oil Spills*, 111–125. <https://doi.org/10.1016/B978-0-12-818111-9.00007-0>
29. LACOMME, P., HARDANGE, J.-P., MARCHAIS, J.-C., & NORMANT, E. (2001). DESIGN OVERVIEW. *Air and Spaceborne Radar Systems*, 371–402. <https://doi.org/10.1016/B978-189112113-5.50022-X>
30. Bole, A., Wall, A., & Norris, A. (2014). The Radar System – Technical Principles. *Radar and ARPA Manual*, 29–137. <https://doi.org/10.1016/B978-0-08-097752-2.00002-7>
31. Bole, A., Wall, A., & Norris, A. (2014). Target Detection. *Radar and ARPA Manual*, 139–213. <https://doi.org/10.1016/B978-0-08-097752-2.00003-9>

32. LACOMME, P., HARDANGE, J.-P., MARCHAIS, J.-C., & NORMANT, E. (2001). PROPAGATION. *Air and Spaceborne Radar Systems*, 35–46. <https://doi.org/10.1016/B978-189112113-5.50006-1>
33. Doviak, R. J., & Zrnić, D. S. (1993). Radar and Its Environment. *Doppler Radar and Weather Observations*, 30–63. <https://doi.org/10.1016/B978-0-12-221422-6.50008-5>
34. Skolnik, M. I. (2002). Radar. *Reference Data for Engineers*, 36-1-36–22. <https://doi.org/10.1016/B978-075067291-7/50038-8>
35. LACOMME, P., HARDANGE, J.-P., MARCHAIS, J.-C., & NORMANT, E. (2001). OTHER OBSERVATION RADARS. *Air and Spaceborne Radar Systems*, 337–343. <https://doi.org/10.1016/B978-189112113-5.50020-6>
36. LACOMME, P., HARDANGE, J.-P., MARCHAIS, J.-C., & NORMANT, E. (2001). OPERATIONAL ASPECTS. *Air and Spaceborne Radar Systems*, 445–448. <https://doi.org/10.1016/B978-189112113-5.50026-7>
37. *Radar Equation - an overview | ScienceDirect Topics*. (n.d.). Retrieved June 30, 2022, from <https://www.sciencedirect.com/topics/engineering/radar-equation>
38. Li, H. J., & Kiang, Y. W. (2005). Radar and Inverse Scattering. *The Electrical Engineering Handbook*, 671–690. <https://doi.org/10.1016/B978-012170960-0/50047-5>
39. Y. Yang, S. -p. Xiao and W. -m. Zhang, "Effect of specular reflection on radar detection," *2016 CIE International Conference on Radar (RADAR)*, 2016, pp. 1-5, <https://doi.org/10.1109/RADAR.2016.8059375>.
40. Scheiner, N., Kraus, F., Appenrodt, N. *et al.* Object detection for automotive radar point clouds – a comparison. *AI Perspect* **3**, 6 (2021). <https://doi.org/10.1186/s42467-021-00012-z>
41. A. Manjunath, Y. Liu, B. Henriques and A. Engstle, "Radar Based Object Detection and Tracking for Autonomous Driving," *2018 IEEE MTT-S International Conference on Microwaves for Intelligent Mobility (ICMIM)*, 2018, pp. 1-4, <https://doi.org/10.1109/ICMIM.2018.8443497>.
42. Mahdi Chamseddine, J. R. D. S. O. W. (2021). *Ghost Target Detection in 3D Radar Data using Point Cloud based Deep Neural Network*. 1–6.



10 ACKNOWLEDGEMENTS

I would like to thank the entire HTW University Dresden (Germany) for their impressive facilities, and the material I have been provided with in order to be able to carry out this thesis. Especially, I would like to thank Prof. Trautmann for his involvement in my learning and in this work, always willing to help and to provide knowledge. I would also like to thank Franziskus Mendt for his help in the day-to-day and field work, his help with everything related to the Matlab program has been an essential personal contribution, and has been a great learning experience for me.